PI3K/AKT AND GSK3β CONTROL MOUSE ES CELL SELF-RENEWAL BY A NOVEL MECHANISM CONVERGING ON C-MYC

by

MATTHEW E. BECHARD

(Under the Direction of Stephen Dalton)

ABSTRACT

Self-renewal of murine embryonic stem cells (mESCs) is controlled through the activity of leukemia inhibitory factor (LIF) by a mechanism requiring the activation of STAT3. Also critical for mESC self-renewal is the phosphotidylinositol 3-kinase (PI3K) pathway which signals through Akt and under self-renewing conditions is proposed to inhibit glycogen synthase kinase 3β (Gsk3β) through the phosphorylation of serine 9 (S9). Several key studies have demonstrated that inhibition of Gsk3β activity is required to maintain mESCs in a pluripotent, self-renewing state. Recently, it was demonstrated that the proto-oncogene c-*MYC*, a direct target of LIF/STAT3 signaling, is essential for maintenance of mESC self-renewal. Mouse ESC differentiation relies upon the threonine 58 (T58) dependent phosphorylation and degradation of c-myc. T58 dependent degradation correlates with the activation of Gsk3β, a kinase known to promote c-myc instability through T58-dependent phosphorylation. We demonstrate that Gsk3β, normally inactive and cytoplasmic during self-renewal, accumulates in the nucleus an active form during early mESC differentiation. The activation and nuclear accumulation of Gsk3β was shown to trigger the differentiation of mESCs by promoting the T58 dependent phosphorylation and degradation of c-myc. We show that PI3K/Akt signaling, in addition to its suppression of Gsk3β activity, prevents Gsk3β from accessing nuclear substrates like c-myc by promoting its efficient nuclear export. This novel mode of Gsk3β regulation was shown to occur via the PI3K/Akt-dependent binding of the Gsk3β binding protein Frat, which we define as responsible for mediating the nuclear export of Frat. These observations define a novel mechanism explaining how PI3K/Akt signaling and GSK3β control mESC self-renewal through the regulation of c-myc.

INDEX WORDS: Embryonic stem cells, Self-renewal, Gsk3β, PI3K/Akt, Frat, nuclear export, nuclear accumulation.

PI3K/AKT AND GSK3β CONTROL MOUSE ES CELL SELF-RENEWAL BY A NOVEL MECHANISM CONVERGING ON C-MYC

by

MATTHEW E. BECHARD

B.S. University of Florida, 2001

M.S. University of Florida, 2003

A Dissertation Submitted to the Graduate Faculty of The University of Georgia in Partial Fulfillment of the Requirements for the Degree

DOCTOR OF PHILOSPHY

ATHENS, GEORGIA

2010

PI3K/AKT AND GSK3β CONTROL MOUSE ES CELL SELF-RENEWAL BY A NOVEL MECHANISM CONVERGING ON C-MYC

by

MATTHEW E. BECHARD

Major Professor:	Stephen Dalton
Committee:	Mary Bedell
	Michael Terns
	Lance Wells

Electronic Version Approved:

Maureen Grasso
Dean of the Graduate School
The University of Georgia
May 2010

DEDICATION

This dissertation is dedicated to my wife Laura Bechard and my new son Jacob Bechard. The undying support from my wife and the unconditional love from my son provided me with the drive to complete this degree.

ACKNOWLEDGEMENTS

I would first like to thank Dr. Stephen Dalton. Originally, I contacted Steve after completing my master's degree looking for a job as a technician. Somehow he convinced me to pursue a PhD instead and start my graduate career all over again. After coming to the end of these 6 years I have to say he was right and it was the best decision I ever made. Steve is a great adviser and a brilliant scientist, who over the years has demanded my absolute best all the time with no apologies. This has made me into a better scientist and gave me the training necessary to bring my career to heights I never thought possible. Working for Steve has been a joy and I will be forever grateful for all that he has provided for me. To the members of my committee, Dr. Michael Terns, Dr. Lance Wells and Dr. Mary Bedell your advice and helpful discussions over the years have been invaluable to my training as a scientist.

To the current members of the Dalton Lab, Keri, Laura, Ian, Dave, Mike, Amar, Tim and Ann you all in some way have contributed to this work and to my training as a scientist and for that I thank you. I have to offer special acknowledgements to Mike, Dave, Amar, Tim and Ian you guys are a ridiculous, merciless and unapologetic group of brilliant scientists who have made this lab an awesomely fun place to work both personally and professionally. I don't think I will ever find another lab to work in that has been as good as this one and for that you will all be sorely missed. I will especially remember our lunch times. What started out as a couple of us hanging out at lunch has somehow attained legendary status throughout the building. Our lunch time discussions have provided me with hours and hours of entertainment over the years that has kept me

sane during stressful times. Dave, I would be remiss if I didn't offer my undying gratitude for all of your invaluable contributes to this work. Our discussions over my experiments, critiques of my results and my scientific writing over the past five years have been invaluable to my training as a scientist.

To all of the friends I have made over my 6 years here living in Athens, I thank all of you for the support you gave me, and the fun times we had. Especially Kelly and Sarah, you guys are the best friends I have ever had and are like family to me, your support has been invaluable. To Kelly, the hours and hours of video games we played over the years has been an essential distraction that helped keep me sane.

To my wife Laura Bechard, I will always remember my PhD as the time I met the love of my life and started my own family. Without the support you have given me over the years none of this would have been possible. For that I can never really thank you enough.

Last but not least I have to thank my family for their unconditional support and love; I am truly blessed to have you all in my life. Especially my parents, Kathryn and Ed Bechard, words can't describe how much I appreciate all that you have done for me. I would not have gotten as far as I have in my life without you.

TABLE OF CONTENTS

Page

LIST OF TABLES

Page

LIST OF FIGURES

Page

CHAPTER 1

Literature Review and Introduction

Murine Embryonic Development

Murine embryogenesis begins with a series of cleavage events, the first being the generation of two cell stage embryos from the fertilized egg (Fig 1.1). During the 2-cell stage, maternal mRNA, used by the zygote, is degraded and the embryonic genome activated (35, 74). By 2 days post coitum (dpc) the zygote consists of 8 cells and is referred to as a morula (35, 74). Up to and including the 4-cell stage embryos, the individual cells (blastomeres) are totipotent, meaning they have the capacity to form a viable mouse (57). Beyond the 8-cell stage the individual blastomeres start to develop toward more specific lineages, losing totipotent capacity (Fig. 1.1) (57, 74).

The first identifiable differentiation event during mouse embryogenesis occurs at the 16-cell stage where the outer layer of cells form the trophectoderm (Fig. 1.1) (74). Trophectoderm will eventually give rise to extraembryonic tissue forming the bulk of the placenta. Over the next series of divisions, a cavitation event occurs as the inner layer of blastomeres compact and flatten against each other forming an inner cell mass (ICM) surrounded by a fluid-filled cavity called a blastocoele (Fig. 1.1) (74). At this stage of development the embryo is referred to as a blastocyst stage embryo. Cells of the ICM are pluripotent and can hence give rise to all the embryonic

germ layers of the mouse. Pluripotent cells of the ICM have been isolated and cultured *in vitro*, forming murine embryonic stem cells (mESCs) (33, 66).

Just prior to implantation at 4.0 dpc, cells of the ICM undergo another differentiation event forming two distinct layers, the primitive endoderm and the epiblast (or primitive ectoderm) (Fig 1.1) (74). The primitive endoderm will give rise to extraembryonic lineages that support the epiblast. Cells that remain in contact with the trophectoderm form parietal endoderm, while cells in contact with the epiblast form visceral endoderm (74). Cells of the epiblast however, retain their pluripotent capacity giving rise to all three embryonic germ layers mesoderm, endoderm and ectoderm (42, 74). Differentiation to the three embryonic germ layers, giving rise to the adult mouse, initiates during gastrulation. Previously, the ICM was the only source of pluripotent cells that had been described. Two groups however, have since reported that pluripotent stem cells can be isolated from the epiblast of post-implantation stage mouse embryos. These are referred to as epiblast stem cells (EpiSCs) (16, 109).

Pluripotent Embryonic Stem Cells

Murine embryonic stem cells (mESCs) were first isolated from the ICM of a pre-implantation blastocyst stage mouse embryo and grown *in vitro* over 20 years ago by Evans and Kaufman (1981) and Martin (1981) (Fig. 1.2) (33, 66). Cultured mESCs have the unique capacity to proliferate, or self-renew, indefinitely without undergoing replicative senescence (21). Mouse ESCs were shown to retain the pluripotent capacity of the ICM by their ability to differentiate into all three germ layers both *in vitro* and *in vivo* when injected into athymic mice (Fig. 1.2) (21). When re-injected back into a

blastocyst stage mouse embryo mESCs were shown to contribute to all three germ layers as well as the germline, further establishing their pluripotent capacity (14). This established the two properties that define cells as pluripotent embryonic stem cells: The ability to self-renew indefinitely *in vitro* while maintaining the ability to differentiate into all three germ layers during *in vivo* embryonic development.

Since their isolation, much research has been directed toward determining the essential factors necessary to maintain the pluripotent, self-renewing state of mESCs. Traditionally, mESCs are maintained *in vitro* as adherent colonies on a monolayer of mouse embryonic fibroblasts (MEFs) in fetal bovine serum (FBS) based culture media. Subsequently, it was discovered that serum based media conditioned by buffalo rat liver (BRL) cells could replace MEFs in maintaining mESCs *in vitro* (100). The use of BRL cells led to the discovery of a secreted soluble differentiation inhibiting factor (DIA) that was required to maintain mESCs in the absence of MEFs (99, 121). Further characterization of the DIA revealed it to be strikingly similar in both structure and function to leukemia inhibitor factor (LIF), a cytokine involved in activating the JAK/STAT pathway (99, 121). Growth of mESCs in the presence of LIF was shown to replace the DIA as an absolute requirement for the maintenance of the undifferentiated, pluripotent mESC state (99, 121).

Following removal of LIF, mESCs spontaneously differentiate into derivatives of all three embryonic germ layers (Fig 1.2). Methods involving the removal of LIF and the addition of specification factors have also been developed to direct the differentiation of mESC toward specific lineages such as cardiomyocytes, smooth muscle, hematopoietic cells, and neurons (Fig. 1.2) (98). Typically however, mESCs most efficiently undergo

spontaneous differentiation as aggregates in suspension known as embryoid bodies (EBs). EBs, despite lacking spatial information, will develop primitive endoderm, primitive ectoderm and their derivatives in a manner similar to a developing ICM (30, 98).

Like hESCs and mESCs, EpiSCs have unlimited *in vitro* self-renewing capacity, while maintaining their pluripotency (16, 109). Maintenance of EpiSCs does not require LIF but, like hESCs, require Activin/Nodal signaling (16, 109). The similarity of EpiSCs to hESCs has helped elucidate key differences between mouse and human ESCs, increasing our overall understanding of ESC biology.

Transcriptional Regulation of Pluripotency

Maintaining mESCs is dependent on a number of intrinsic factors, the most important are the transcription factors Oct4, Nanog and Sox2 (4, 20, 71, 76). Oct4, encoded by the *Pou5f1* gene, is a POU domain transcription factor initially expressed in all blastomeres of a developing embryo (88). Expression of Oct4 is restricted to the pluripotent cells of the ICM and is down-regulated upon differentiation (88). Deletion of Oct4 from developing embryos causes embryonic lethality due to failure to form ICM (76). Expression of Oct4 above or below endogenous levels results in differentiation, demonstrating the importance of its regulation in maintenance of ESC pluripotency (79, 82). The undifferentiated embryonic stem cell transcription factor 1 (Utf1), an ESC specific co-activator, was also shown to have an ESC specific enhancer activated by Oct4 and Sox2 (77). Sox2, a HMG-domain containing transcription factor, has been demonstrated to play an important role in maintaining an undifferentiated ESC state (4,

61). Oct4 in conjunction with Sox2 has been shown to cooperatively regulate Utf1, and a number of ESC specific genes including *Fgf4*, *Fbxo15*, and *Nanog* while also positively self-regulating their own genes (91). Nanog is a homeodomain transcription factor that first appears in the mouse embryo prior to blastocyst and ICM formation, persists until implantation and is restricted to pluripotent cells (20). While lack of Nanog expression *in vivo* and *in vitro* causes differentiation of pluripotent ESCs toward extraembryonic lineages, its over-expression has been demonstrated to maintain their pluripotency in the absence of LIF (20, 71). Nanog, Oct4, and Sox2 have been shown to co-occupy a large group of developmentally important genes (12). This has led to the hypothesis that Oct4, Sox2 and Nanog form a transcriptional network important in maintaining ESC pluripotency.

The roles Oct4, Sox2 and Nanog have in maintaining ESC pluripotency involve both the activation of ESC specific genes and the repression of genes important for differentiation. A large portion of genes repressed by Oct4, Sox2 and Nanog in pluripotent cells are also targets of the polycomb group (PcG) proteins (13). PcG proteins are transcriptional repressors that have recently been shown to have a role in repressing genes that promote ESC differentiation (13). Together this indicates that Oct4, Sox2 and Nanog along with epigenetic PcG-mediated processes maintain ESC pluripotency by activating genes important for self-renewal, and repress those important for differentiation. Despite evidence describing the involvement of intrinsic factors like Oct4, Sox2 and Nanog in ESC pluripotency, little is known in regards to how they connect to important extrinsic factors. LIF, along with factors present in serum like bone morphogenic proteins (BMPs), are important extrinsic factors shown to have a role in

regulating a number of biochemical pathways important for ESC self-renewal (81, 121, 126). Further research into connections between important extrinsic and intrinsic factors should shed light on how they work together to maintain ESC pluripotency, increasing our overall understanding of ESC biology.

Induced Pluripotent Stem Cells

The reprogramming of terminally differentiated cells to a pluripotent stem cell state was first demonstrated by Takahashi and Yamanaka in 2006. The reprogramming was accomplished by retrovirally introducing the transcription factors Oct4, Sox2, Kruppel-like factor 4 (Klf4) and c-myc into embryonic and adult fibroblast cells (108). Despite the inability to produce chimeric mice, this first generation of induced pluripotent stem cells (iPSCs) shared many characteristics associated with ESCs like morphology, expression of ESC specific markers and proliferative capacity (108). Following this seminal work, several groups improved upon this by selecting for Nanog expressing cells following retroviral introduction of Oct4, Sox2, Klf4 and c-myc, generating germline competent iPSCs (84, 119). In addition to their germ-line competency the gene expression and methylation pattern of this generation of iPSCs, unlike their predecessors, were nearly identical to that of mESCs (70, 84, 119). More importantly, this generation of iPSCs completely satisfied the two defining properties of pluripotent ESCs, the ability to self-renewal indefinitely while maintaining their pluripotent capacity. Due to their obvious therapeutic applications, many researchers have now generated iPSCs from a variety of cell types using non-retroviral methods, making iPSCs a more compatible source for cell-replacement therapies (83, 85, 101).

Signaling Pathways that Regulate mESC Self-renewal

LIF/STAT3. LIF, a member of the interleukin 5-type cytokine family, activates the JAK/STAT3 (Janus kinase/signal transducer and activator of transcription) pathway by binding to the LIF receptor β (LIFRβ), triggering its dimerization with the glycoprotein-130 receptor (gp130) (32, 78). The dimerization of LIFRβ to gp130 activates the tyrosine kinase JAK (Janus Kinase) which phosphorylates the receptor complex allowing recruitment of STAT3 (Fig. 1.3) (32, 78). Recruited STAT3 is then phosphorylated by JAK leading to its dimerization and nuclear translocation where it regulates target genes important for mESC self-renewal (Fig. 1.3) (78). Two lines of evidence demonstrate that activation of STAT3 is essential for mESC maintenance. First, ectopic expression of activated STAT3 maintains mESC self-renewal in the absence of LIF (67). Second, a dominant negative version of STAT3 promotes mESC differentiation despite the presence of LIF (78). However, until recently, the target genes regulated by LIF/STAT3 in mESCs have not been well characterized.

In several biological contexts, STAT3 directly activates the transcription of c-myc, a member of the *MYC* family of proto-oncogenes (60, 95). Classified as a helix-loop-helix/leucine zipper transcription factor, c-myc has well-documented roles in cancer, cell immortalization, proliferation, cell cycle control and blocking differentiation (18, 60, 73, 94). In the mouse embryo c-myc is widely expressed in highly proliferative cells, becoming more restricted as development progresses. The importance of c-myc in embryonic development is well-established as its deletion is embryonic lethal at 10.5 dpc (25). Phenotypically, these c-myc null embryos are abnormally small with enlarged hearts, a fluid filled pericardia and defects in the closure of the neural tube (25).

Due to its prominent role in cellular biology, the protein stability of c-myc and its regulation has been extensively studied. The stability of c-myc is regulated through two phosphorylation sites, serine 62 (S62) and threonine 58 (T58) (Fig. 1.4) (93). The kinases shown to phosphorylate c-myc on S62 and T58 are ERK (extracellular signal-regulated kinase) and glycogen synthase kinase (Gsk3β), respectively (Fig. 1.4) (93). During the highly proliferative phases of the cell cycle, c-myc is phosphorylated at S62 by ERK, resulting in its stabilization (Fig. 1.4) (93). However, during the low proliferative phases of the cycle Gsk3β is activated, promoting its destabilization by phosphorylating c-myc at T58 (Fig. 1.4) (93). Following the phosphorylation of T58, protein phosphatase 2A (PP2A) removes the S62 phosphate group, leaving the phospho-T58 form of c-myc. This highly unstable form of c-myc is then recognized by the ubiquitinylation pathway and quickly degraded (Fig. 1.4) (93).

Of significance to this project, all of the aforementioned functional characteristics of c-myc coincide with the basic characteristics of pluripotent ESCs. However, mouse ESCs lacking c-myc showed only marginal effects on *in vitro* expansion and differentiation (6). Although these results argue against an essential role for c-myc in mESC self-renewal, functional redundancy between c-myc and N-myc, another *MYC* family member, has been demonstrated (64). Moreover, c- and N-myc are co-expressed in pluripotent cells, explaining why there isn't a significant effect on self-renewal in c-myc$^{-/-}$ null mESCs (19, 55, 64). The importance of c-myc in embryonic development and its connection to the LIF/STAT3 pathway led to the hypothesis that c-myc is an important target of STAT3 in the maintenance of mESC self-renewal. Recent work from our laboratory has demonstrated that c-myc, highly expressed and stable in mESCs, is a

transcriptional target of STAT3 (19). Furthermore, upon LIF withdrawal during mESC differentiation c-myc undergoes significant degradation following its phosphorylation at threonine 58 (19). Expression of a highly stable mutant form of c-myc that evades Gsk3β-mediated degradation (c-myc^{T58A}) is sufficient to maintain mESC self-renewal in the absence of LIF (19). These studies clearly demonstrate that c-myc is a key target of the LIF/STAT3 pathway and is critical to the maintenance of mESC self-renewal.

PI3K pathway. The PI3K pathway has well-documented roles in a number of biological processes including proliferation, cell migration, tumorigenicity and cell survival (116). The PI3K family consists of several lipid kinases capable of phosphorylating phosphoinositides, producing second messengers such as phosphoinositide 3,4-bisphosphate (PIP_2) and phosphoinositide 3,4,5-triphosphate (PIP_3) (115, 116). Activation of PI3K signaling results in the production of PIP_3, which binds to and activates the pleckstrin homology domain-containing proline-directed kinase (PDK1) (Fig. 1.5) (116). Production of PIP_3 also recruits Akt to the membrane where PDK1, in combination with other kinases, catalyzes its phosphorylation mediated activation (Fig. 1.5). Akt then goes on to regulate a number of proteins important for multiple areas of cell biology including protein synthesis, apoptosis, glucose metabolism, and proliferation (15). Akt is best known however for its role in the inhibition of Gsk3β activity in response to insulin signaling.

A possible role for the PI3K pathway in mESCs was first postulated by a study demonstrating that deletion of PTEN, a negative regulator of the PI3K pathway, results in accelerated growth of mESCs (104). Moreover, of the three classes of PI3Ks, class I_A is activated by the LIF/STAT3 pathway via the gp130 receptor (11, 107). This has led

others to investigate the role PI3K signaling has in mESC self-renewal. One key study demonstrated that LIF can activate PI3K/Akt signaling, affecting downstream targets like Gsk3β (87). In addition, treatment of mESCs with the PI3K specific inhibitor LY294002 significantly decreased Nanog levels and reduced the ability of LIF to maintain mESCs (103). Furthermore, it was demonstrated that expression of a constitutively active form of Akt was sufficient to maintain mESC self-renewal in the absence of LIF (118). Together, these studies strongly indicate an important role for the PI3K/AKT pathway in regulating mESC maintenance.

BMPs. Mouse ESCs grown in the presence of LIF alone, without FBS, cannot maintain pluripotency, resulting in their differentiation toward neural lineages (80, 126). This led researchers to investigate other factors in FBS that could be important for the maintenance of mESC self-renewal. The led to the identification of BMPs, which in conjunction with LIF, were shown to contribute to the maintenance of mESC pluripotency (126). BMPs contribute to the maintenance of mESC pluripotency through the activation of the inhibitors of differentiation (Id) transcription factors via the SMAD pathway (126). Furthermore, enforced expression of Id transcription factors completely bypasses the need for BMPs (126). Additionally, BMPs were also shown to contribute to mESC maintenance by inhibition of the MAPK pathway (90). Similar to LIF, BMPs alone are not sufficient to maintain mESC self-renewal as in the presence of BMPs alone (absence of LIF) mESCs differentiate toward endoderm and mesoderm lineages (53). This led to the conclusion that mESCs are pre-disposed toward differentiation and the presence of BMPs and LIF together help maintain an undifferentiated mESC state by blocking differentiation.

Wnt/β-catenin. Originally described as the Wingless pathway in *Drosophila*, the canonical WNT pathway plays a key role in many areas of mammalian development including proliferation, differentiation, axial polarity and axonal guidance (41, 89). The canonical Wnt pathway is activated by the binding of Wnt molecules, a family of secreted glycoproteins, to the Frizzled receptor family. In the absence of Wnt signaling, a protein complex involving Gsk3β, Axin, and Adenomatous Polyposis Coli (APC) is formed (Fig. 1.6) (29, 36). The Axin/Gsk3β/APC protein complex binds to β-catenin, the primary target of the canonical Wnt pathway, promoting its Gsk3β mediated phosphorylation and proteolytic degradation (Fig. 1.6) (29, 36). However, in the presence of Wnt proteins, the Axin/Gsk3β/APC protein complex is disrupted via disheveled, preventing the degradation of β-catenin (Fig. 1.6). The resulting accumulation of stable β-catenin leads to its nuclear translocation where it binds to the T-cell factor/lymphoid-enhancer factor (Tcf/Lef) family of proteins, targeting a number of genes for activation including c-myc, brachyury, and cyclin D1 (89).

The canonical WNT pathway has a well-established role in regulating multiple aspects of murine embryonic development (62). Specifically, murine embryos lacking WNT3a undergo a significant increase in neuralization while failing to form a paraxial mesoderm layer (106, 128). Moreover, deletion of the WNT co-receptors Lrp5/6 impaired the ability of murine embryos to form mesoderm (56). Additional studies have also implicated Wnt signaling in directing germ layer differentiation in vitro as well. Expression of the WNT antagonist Sfrp2 in mESCs was also shown to promote neural differentiation (3). Furthermore, activation of the canonical WNT pathway in mESCs either by inactivating APC or expressing a dominant active form of β-catenin is sufficient

to inhibit neural differentiation (44). This led researchers to postulate a role for the canonical WNT pathway in promoting mESC self-renewal by blocking differentiation. In support of this, activation of the WNT pathway alone by addition of recombinant WNT3a or the Gsk3 inhibitor 6-bromoindirubin-3'-oxime (BIO) was shown to be sufficient to promote mESC self-renewal (92). However, Gsk3β is a downstream target of another pathway important for mESC self-renewal, the PI3K pathway. Therefore, inhibition of Gsk3β activity via BIO is not an accurate method to investigate the role of WNT signaling in mESC self-renewal. Contrary to this work it was subsequently demonstrated that recombinant WNT3a alone cannot in fact support long-term mESC self-renewal (81). It has, however, been shown that canonical WNT signaling, much like BMP signaling, works synergistically with LIF/STAT3 signaling to promote mESC self-renewal (81). More research into the role of canonical WNT pathway in mESC self-renewal and differentiation is needed.

Function and Regulation of Glycogen Synthase Kinase 3β.

Gsk3β. Glycogen Synthase Kinase3 (Gsk3), a serine/threonine kinase, in the mammalian system exists as two distinct isoforms, Gsk3α and Gsk3β, approximately 51 and 47 kDa respectively (123). Gsk3α and Gsk3β are highly similar in overall structure, sharing a 98% identity in their kinase domains and are co-expressed in most tissues (123). The two isoforms are however, not functionally redundant as Gsk3β null mice are embryonic lethal due to liver degeneration (49). The apparent specificity the beta isoform has over the alpha isoform in regards to liver function could explain why most researchers focus on this particular isoform when investigating the regulation and function of Gsk3β. Originally Gsk3β was identified and named for its role in the phosphorylation-mediated

regulation of glycogen synthase (124). In addition to metabolism, Gsk3β targets a number of other proteins involved in development, cell proliferation, and cell cycle including β-catenin, cyclin D1, NFκB, p53, and c-myc (29, 43). In addition, Gsk3β is involved in the progression of diseases such as diabetes, Alzheimer's disease and cancer (36). As such, investigating the function and regulation of Gsk3β activity in cell biology has become an important area of research.

One of the more intriguing aspects of Gsk3β is its preference for substrates that are pre-phosphorylated. Examination of several of the more well-established pre-phosphorylated Gsk3β substrates like glycogen synthase, c-myc, beta-catenin, and CREB revealed a consensus recognition motif, Ser/Thr-X-X-X-pSer/pThr (29). The pre-phosphorylated Ser/Thr, located 4 residues C-terminal to the target site in this motif, is commonly referred to as the P+4 site while the target Ser/Thr residue is referred to as the P+0. Resolution of the three-dimensional structure of Gsk3β revealed a binding of the P+4 phosphate group to a positively charged binding pocket in the kinase domain that's important for Gsk3β activity (24). This indicates that the binding of the P+4 phosphate group to these key residues may optimally align the catalytic site toward the P+0 target site, increasing the efficiency of phosphorylation (24). Although not an absolute requirement, this observation offers an explanation as to why the efficiency of Gsk3β phosphorylation of pre-phosphorylated substrates is an order of magnitude higher than those without the priming phosphate.

Regulation of Gsk3β activity. Regulation of Gsk3β activity is accomplished using a number of mechanisms involving phosphorylation, intracellular localization and complex formation. One well studied mechanism of regulating Gsk3β activity occurs through the

phosphorylation of a serine 9 residue (S9) near its N-terminus. This phosphorylation event causes the N-terminus of Gsk3β to act as a pseudosubstrate, folding over the active site allowing the phosphoserine group to occupy the previously mentioned positively charged binding pocket (29). The intramolecular binding of this primed pseudosubstrate occupies the catalytic groove of Gsk3β blocking its activity toward any other substrate (29). This mechanism of inhibition is however competitive as primed substrates, in high amounts, can outcompete the pseudosubstrate (37). One of the major kinases responsible for inhibition of Gsk3 via S9 phosphorylation was found to be Akt. Some of the other kinases demonstrated to regulate Gsk3β via S9 phosphorylation are $p90^{RSK}$, Protein Kinase C, Protein Kinase A and p70 S6 kinase (43). Akt however, through the PI3K pathway, has been demonstrated as responsible for the insulin mediated inhibition of Gsk3β (23). The PI3K/Akt mediated inhibition of Gsk3β has therefore been well-studied due to obvious implications and potential applications in regards to the treatment of diabetes.

More recently, regulation of Gsk3β activity has been shown to occur through protein complex formation. A prime example where the activity of Gsk3β is modulated due to protein complex formation occurs in the canonical Wnt pathway (29, 36). Under conditions in which the Wnt pathway is not active Gsk3β exists in a protein complex with Axin and Adenomatous Polyposis Coli (APC) (29, 36). While in this protein complex the activity of Gsk3β toward β-catenin is enhanced (45, 52, 59). However, upon activation of the Wnt pathway, the Gsk3β/Axin/APC complex is disrupted and Gsk3β binds to Frat (frequently rearranged in T-cell lymphomas) instead (29, 36). Recently, several studies involving surface scanning mutagenesis of Gsk3β and analysis of its

crystal structure have revealed partially overlapping binding regions for Axin and Frat (7, 34, 40). Therefore, the binding of Frat is likely to interfere with Axin binding, disrupting the Gsk3β/Axin/APC protein complex and the Gsk3β-dependent phosphorylation of β-catenin. In fact, a small Frat-derived peptide called Frat-tide is commonly used to specifically interfere with Gsk3β-Axin binding (110). Moreover, Frat binding to Gsk3β also results in an inhibition of Gsk3β activity toward some but not all substrates like, Axin and β-catenin (29, 110). Wnt-mediated inactivation of Gsk3β however, is not S9 phosphorylation dependent and is therefore thought to be independent of PI3K/insulin signaling (27, 29).

Regulation of Gsk3β subcellular localization. Another important aspect in the regulation and function of Gsk3β is its subcellular localization. Although Gsk3β is considered to be a cytosolic protein, it has both nuclear and cytoplasmic targets, requiring Gsk3β to localize to both compartments (43). Several studies have demonstrated a role for the nuclear accumulation of Gsk3β in many aspects of cell biology. One example occurs during the S-phase of the cell cycle where the activation and nuclear localization of Gsk3β is required for the phosphorylation mediated degradation of cyclin D1 (26). The stimulation of apoptotic signaling cascades was also shown to signal for the nuclear accumulation of Gsk3β (10). The regulation of the transcription factors p53 and c-myc have been shown to require the activation and nuclear localization of Gsk3β as well (51, 129). Despite the evidence that the nuclear accumulation of Gsk3β plays an important role in its function, surprisingly little is known about its nuclear import/export. A functional bipartite nuclear localization sequence (NLS) has been defined that is both necessary and sufficient to promote the nuclear localization of Gsk3β (69). In addition,

the nuclear export of Gsk3β was shown to occur in a Crm1-mediated fashion. Crm1 is an exportin protein that binds to proteins containing a nuclear export sequence (NES), transporting them out of the nucleus in an energy dependent manner. However, Gsk3β does not have a definable NES, suggesting that its nuclear export is dependent upon a binding partner. In support of this, the Gsk3β binding protein Frat was shown to mediate the export of Gsk3β under certain conditions (38). Altogether, this evidence opens the possibility that Gsk3β binding proteins regulate the nuclear accumulation of Gsk3β. Further clarification of how the nuclear import/export of Gsk3β is regulated will provide a better understanding of the role Gsk3β has in many important aspects of cellular biology.

Gsk3β and mESC self-renewal/differentiation. Recently, the role Gsk3β has in cellular biology has been expanded to include mESC self-renewal and differentiation. Several key studies have demonstrated that inhibition of Gsk3β is vital to maintaining mESC self-renewal. First, inhibition of Gsk3β can maintain mESC self-renewal in the absence of LIF for a short period of time (92). Second, inhibition of Gsk3β significantly improves the derivation frequency of mESCs from blastocysts (111). Third, the homozygous deletion of both isoforms of Gsk3β severely comprises the differentiation capability of mESCs (28). Finally, mESC self-renewal was maintained for long periods of time in the absence of all exogenous signals by combining Gsk3β inhibition with inhibition of ERK signaling (127). The combination of Gsk3β and ERK inhibition was also shown to aid in the generation of iPS cells from neural stem cells (96). In addition, the activation of Gsk3β has been linked to the progression of mESC differentiation. This was shown when the activation of Gsk3β, via inhibition of the PI3K/AKT pathway, caused the down

regulation of Nanog (103). In corroboration of this, re-inhibition of Gsk3β was shown to reverse the down regulation of Nanog (103). Moreover, our laboratory demonstrated a significant correlation between an activation of Gsk3β and the phosphorylation-mediated degradation of c-myc during mESC differentiation (19). This evidence is consistent with the previously described role Gsk3β has in regulating the stability of c-myc in other biological contexts (48, 51, 93). Altogether, this has led to the hypothesis that Gsk3β has a substantial role in regulating mESC self-renewal and differentiation by controlling the stability of c-myc (Fig. 1.7).

Conclusions

Investigating the function and interaction of signaling pathways in regulating mESC self-renewal and differentiation is an important area of research that will increase our overall understanding of ES cell biology. Current literature has defined the LIF/STAT3 pathway as important in maintaining mESC self-renewal (19). In addition, self-renewal has been demonstrated to depend on the active expression of stable c-myc, a target of the LIF/STAT3 pathway (19). The PI3K pathway through Akt is proposed to inhibit Gsk3β via S9 phosphorylation, also critical for mESC self-renewal (87, 103). Furthermore, activation of Gsk3β has been linked to the degradation of c-myc following the removal of LIF (19, 127). These observations point to a convergence of the LIF/STAT3 and PI3K/Akt pathways on the activation and regulation of c-myc. However, major questions still remain as to how PI3K/Akt, Gsk3β, and c-myc function together in regulating mESC self-renewal and differentiation. Although collapse of c-myc levels correlates to an activation of Gsk3β during early mESC differentiation, the significance in regards to regulating mESC differentiation remains undefined. Moreover,

despite the importance of the PI3K/Akt pathway to self-renewal, the mechanism by which the pathway acts is undefined. Together, these questions represent significant shortfalls in our understanding of self-renewal, pluripotency, and early cell fate decisions made by mESCs. This work addresses these significant gaps by demonstrating a role for PI3K/Akt signaling in regulating the stability of c-myc by controlling the activation and localization of Gsk3β. Overall these data establish a mechanism for how the PI3K/Akt/Gsk3β signaling axis is involved in regulating the self-renewal and differentiation of mESCs.

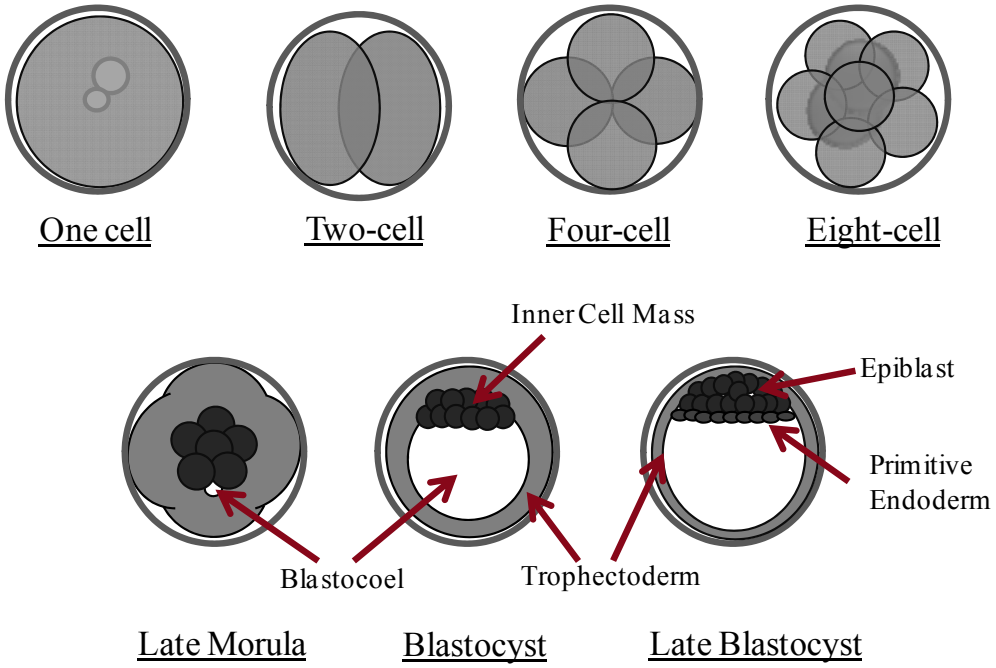

Figure 1.1. Early embryonic development. A diagram depicting the early stages of embryonic development through the blastocyst stage where pluripotent stem cells are isolated.

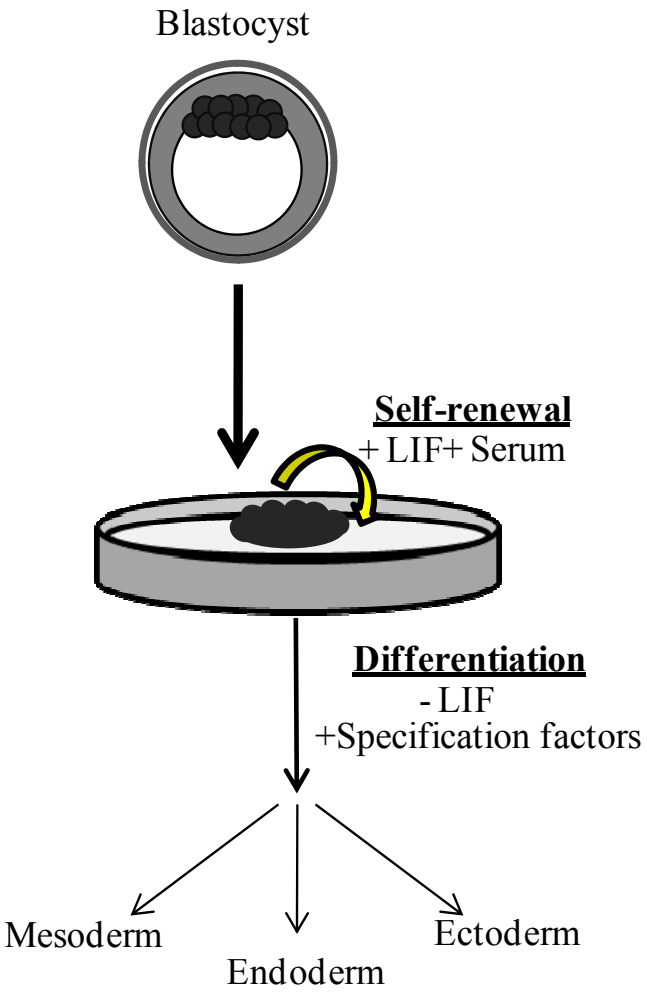

Figure 1.2. Murine embryonic stem cells. Cells isolated from the ICM of a blastocyst, in the presence of serum and LIF can self-renewal indefinitely. However, in the absence of LIF and in the presence of specification factors mESCs differentiate toward the three germ layers.

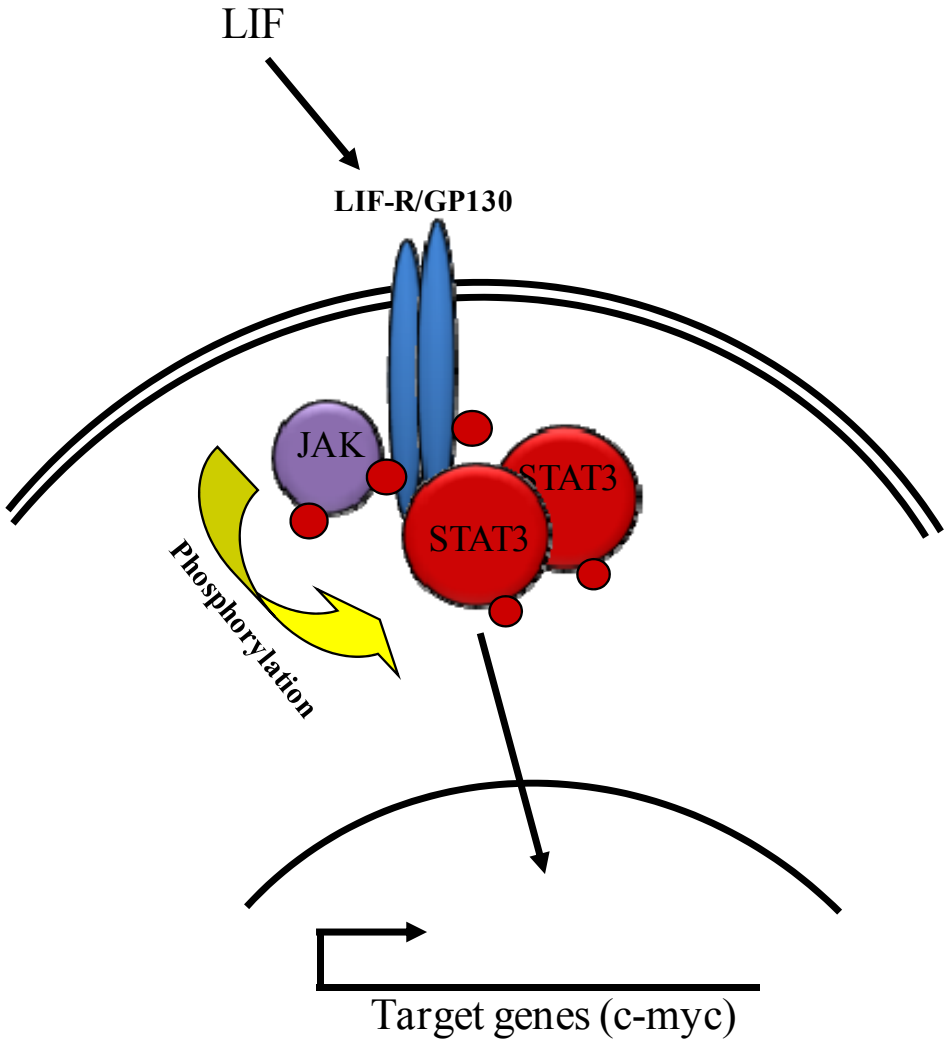

Figure 1.3. The JAK/STAT3 pathway. The JAK/STAT3 pathway, activated by LIF, has been shown to aid in maintaining self-renewal through the activation of a number of important genes, including c-myc. Red circles denote phosphorylation events.

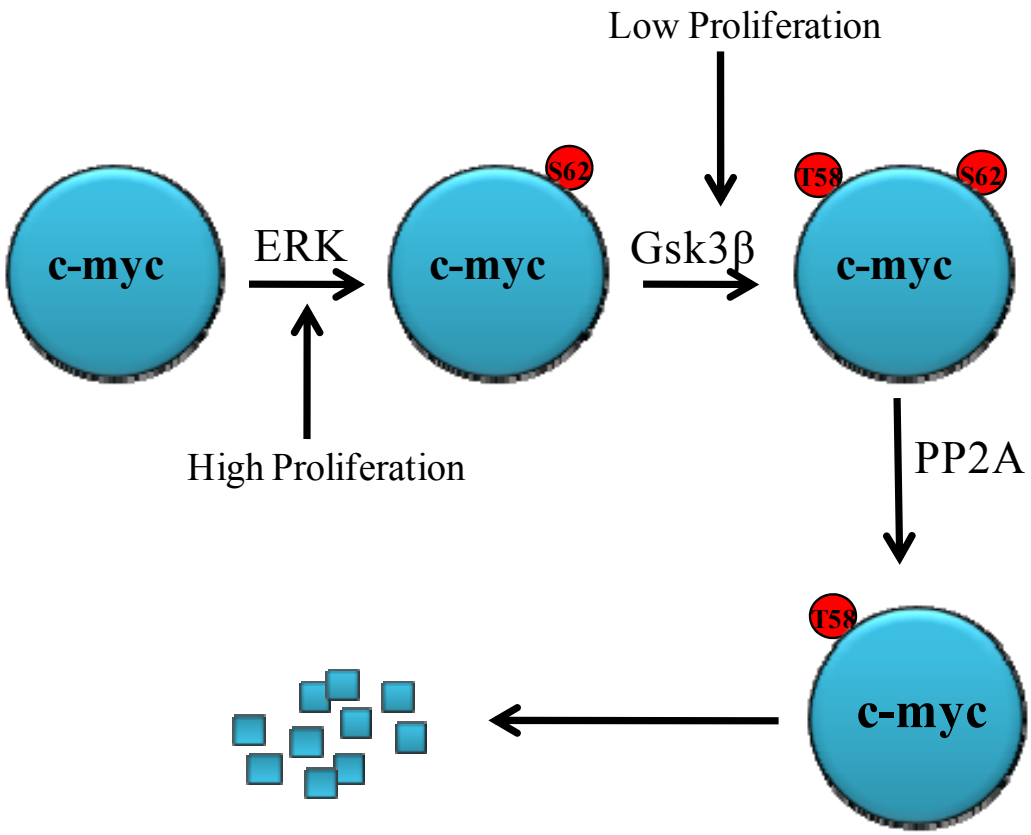

Figure 1.4. Regulation of c-myc stability. The above diagram depicts the life cycle of c-myc from its most stable, phospho-S62, form to its least stable, phospho-T58, form. Red circles denote phosphorylation events.

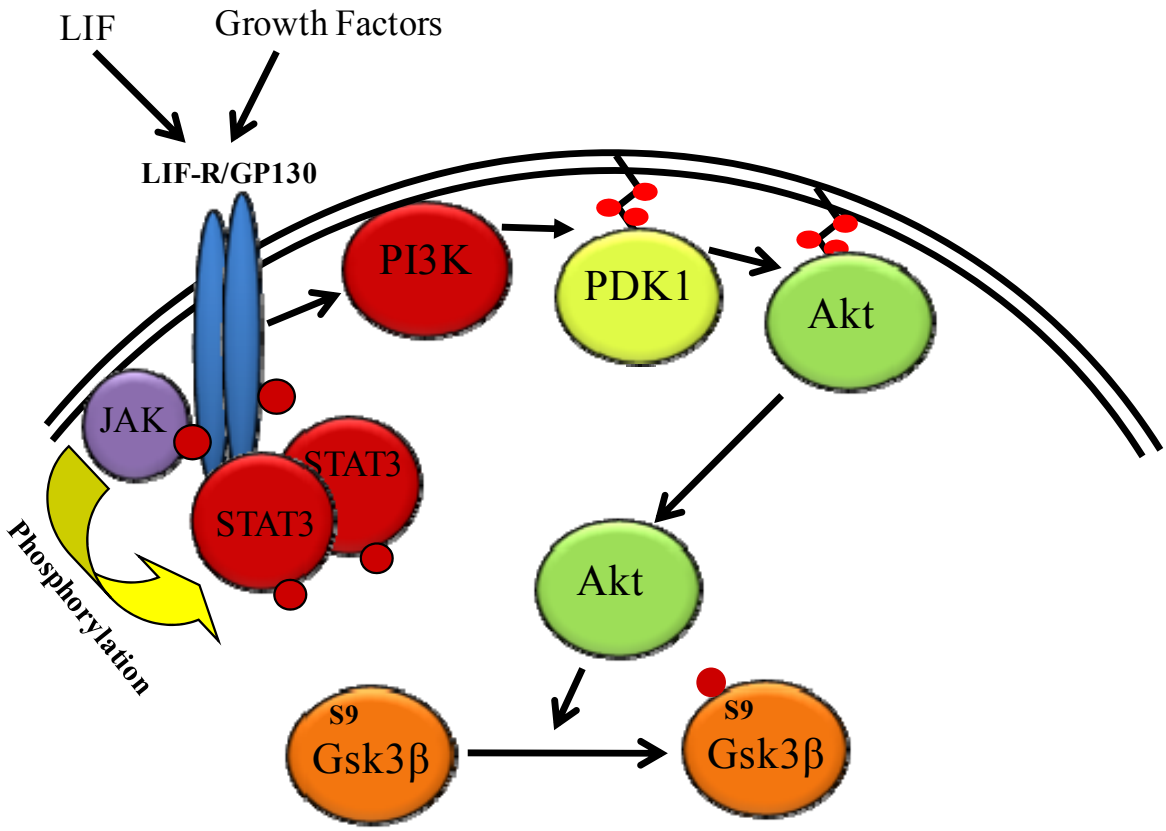

Figure 1.5. The PI3K/Akt pathway. The above diagram depicts the activation of Akt through the PI3K pathway and its effect on Gsk3β activity. Red circles denote phosphorylation events

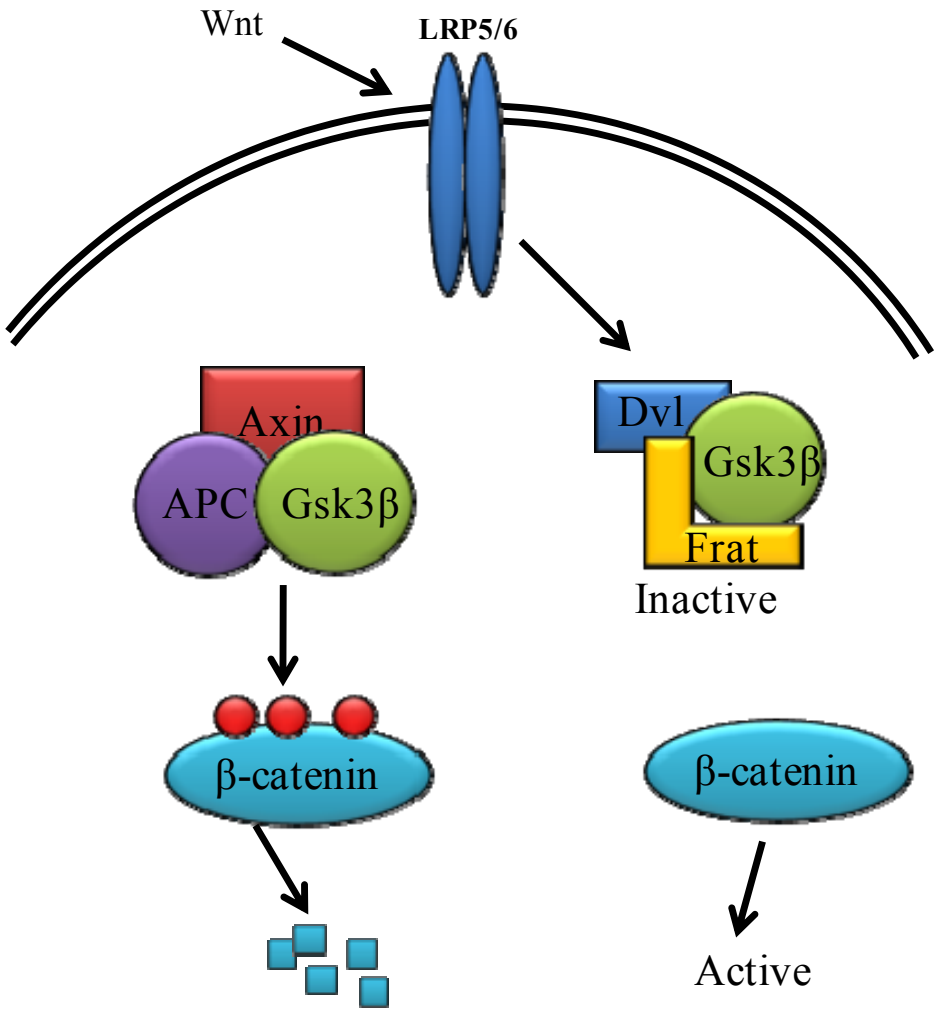

Figure 1.6. The canonical Wnt pathway. The above diagram depicts the role Gsk3β has in regulating the stability of β-catenin in the Wnt pathway. Red circles denote phosphorylation events.

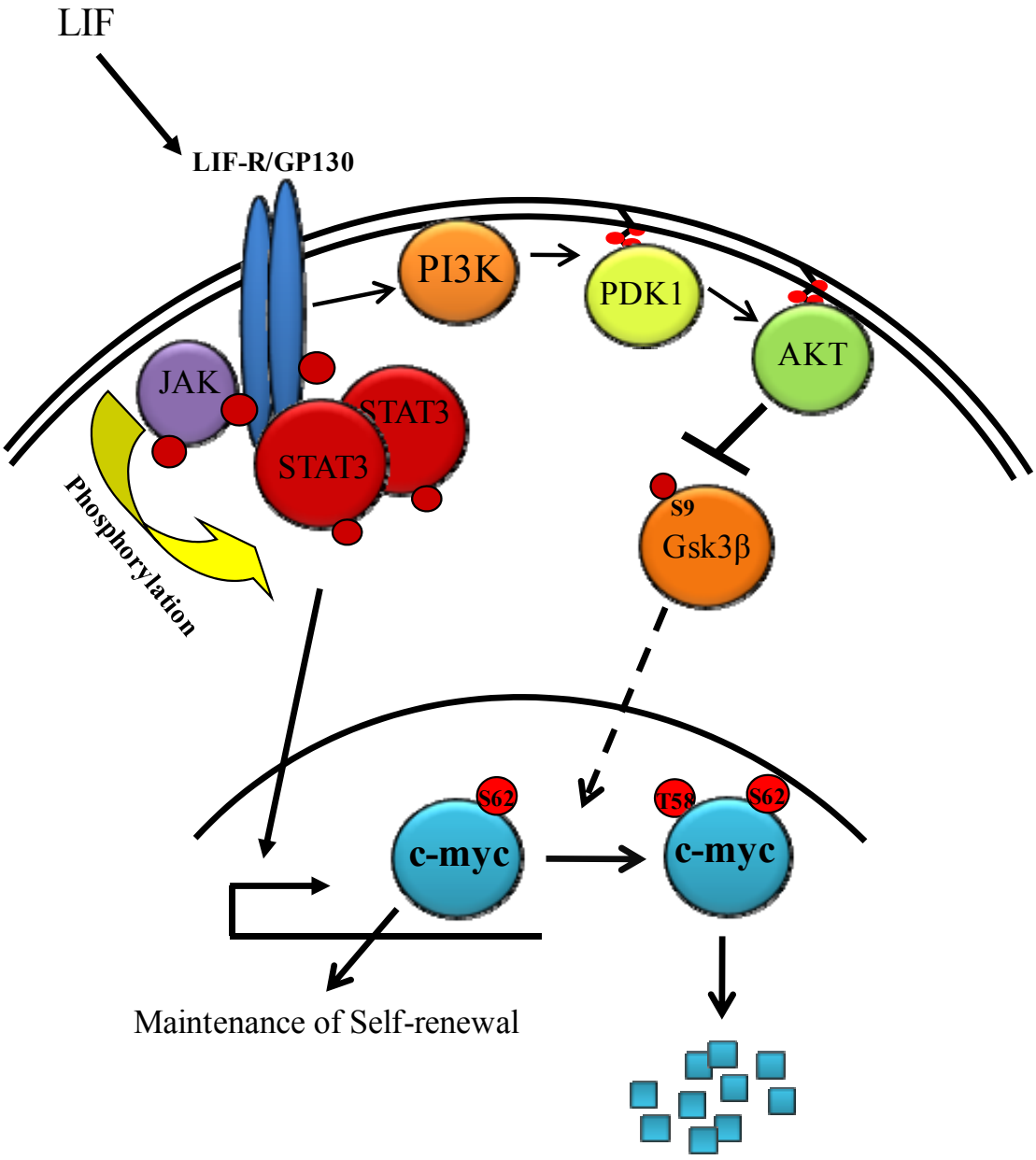

Figure 1.7. A role for Gsk3β in mESC maintenance. The above diagram depicts the proposed role for Gsk3β, its connection to the PI3K/Akt pathway and their convergence on the regulation of c-myc stability. Red circles denote phosphorylation events.

CHAPTER 2

Experimental Procedures

Cell Lines

The following mESC lines were used in these studies: R1 (75), D3 (30), E14Tg2a (50), EpiSCs (109), E14K, E14K Gsk3α/$\beta^{-/-}$ (28), murine iPSC (Dalton Lab).

Culture of mESCs and iPSCs

mESCs were cultured in the absence of feeders on culture grade plastic pre-coated with 0.2% gelatin-phosphate buffered saline (PBS), as previously described (102). Cells were maintained at 37°C, 10% CO_2 in Dulbecco's Modified Eagle Medium (DMEM) (Cellgro) supplemented with 10% fetal bovine serum (FBS) (Atlanta Biologicals), 10% knockout serum replacement (KSR) (Gibco), 2 mM L-glutamate (Cellgro), 1 mM sodium pyruvate (Cellgro), 0.1 mM β-mercaptoethanol (Gibco), 100 U/ml penicillin-streptomycin (Cellgro), and 1000 U/ml LIF (ESGRO, Chemicon). Cells were passaged every two to three days by adding 0.05% trypsin-EDTA (Invitrogen) to a plate of semi-confluent cells that have been washed with PBS. Following an incubation of 5 minutes at 37°C, cells were pipetted to obtain a single cell suspension and added to 8 ml of mESC media. Cells were centrifuged at 200 xg then resuspended at an appropriate volume of mESC media and reseeded at a density of approximately $1.5x10^4$ cells/cm^2.

Murine iPS cells, constructed by Dr. Amar Singh according to (108), were cultured, maintained and passaged as described above for mESCs.

Culture of EpiSCs

EpiSCs were cultured on culture grade plastic pre-seeded with a feeder layer of mouse embryonic fibroblasts (MEFs) (Millipore) at a density of $4.8x10^4$ cells/cm^2. EpiSCs were maintained at 37°C, 10% CO_2 in DMEM-F12 (Cellgro), 20% KSR (Gibco), 5 ng ml^{-1} FGF2 (R&D Systems), 0.1mM 2-mercaptoethanol (Gibco), 2mM L-glutamine (Cellgro), and 1x MEMs non-essential amino acids (Cellgro). Passaging was performed by incubating a plate of semi-confluent cells with 1.5 mg/ml collagenase type IV diluted in cell culture media for approximately 10 min at 37°C. Following the incubation, EpiSC colonies were dislodged and reduced in size by gentle pipetting, then added to an equal volume of EpiSC media. Cells were centrifuged at 200 xg then resuspended at an appropriate volume of mESC media and reseeded at a 1:5 or 1:6 dilution depending on cell density prior to passaging.

Differentiation of mESCs

Murine ESCs were differentiated by plating trypsinized cells onto culture grade plastic pre-coated with 0.2% gelatin-PBS for adherent differentiation, or onto bacteriological dishes for differentiation in suspension as embryoid bodies (EBs). Cells differentiated under both conditions were incubated at 37°C, 10% CO_2 in DMEM (Cellgro) supplemented with 10% FBS (Atlanta Biologicals), 2 mM L-glutamate (Cellgro), 1 mM sodium pyruvate (Cellgro), 0.1 mM β-mercaptoethanol (Gibco), and 100 U/ml penicillin-streptomycin (Cellgro).

Antibodies

Antibodies used in this study were as follows: mouse anti-Gsk3β (catalog no. 610202; BD Biosciences), rabbit anti-Gsk3β phospho-S9 (catalog no. 9336; Cell Signaling), anti-actin (catalog no. A2066; Sigma), Goat anti-Oct4 (catalog no. SC-8628; Santa Cruz), rabbit anti-c-myc (catalog no. 9402; Cell Signaling), rabbit anti-c-myc phospho-T58 (catalog no. 9401; Cell Signaling), rabbit anti-Akt (catalog no. 9272; Cell Signaling), rabbit anti-Akt phospho-S473 (catalog no. 9271; Cell Signaling), rabbit anti-Nanog (catalog no. RCBAB0002FF; Cosmo Bio), mouse anti-Cdk2 (catalog no. SC-6248; Santa Cruz), rabbit anti-HNF3β/FoxA2 (catalog no. 07-633; Upstate), mouse anti-HA (catalog no. 2367; Cell Signaling), rabbit anti-Axin (catalog no. SC-14029; Santa Cruz), rabbit anti-Flag (catalog no. F7425; Sigma), mouse anti-Flag (catalog no. F3165; Sigma), and anti-Fibrillarin (a gift from M. Terns, University of Georgia).

Reagents

The following materials were used in this study: (2'*Z*,3'*E*)-6-bromoindirubin-3'-oxime (BIO) (BIO/Gsk3 inhibitor IX, catalog no. 361552; Calbiochem), MeBIO (catalog no. 361556; Calbiochem), lithium chloride (catalog no. 7447-41-8; Fisher), Gsk3 inhibitor XV (catalog no. 361558; Calbiochem), CHIR 99021/CT 99021 (catalog no. 04-0004; Stemgent), Akt inhibitor V (AktV) (catalog no. 124012; Calbiochem), LY294002 (catalog no. ST-420; Biomol), PI-103 (catalog no. 528101; Calbiochem), leptomycin B (LB) (catalog no. 431050; Calbiochem), and 4-hydroxytamoxifen (4OHT) (catalog no. H6278; Sigma).

RNA isolation and quantitative RT-PCR analysis

Total RNA was isolated from cells using the RNeasy kit (QIAGEN) according to the manufacturer's instructions. cDNA was synthesized with approximately 1 μg RNA using iScript cDNA synthesis kit (BioRad) following the protocol recommended by the manufacturer. Real-time PCR was carried out using gene specific TaqMan Gene Expression Assays (Applied Biosystems), the Universal PCR Master Mix and 5 ng of cDNA. DNA was amplified in a 2-step amplification process consisting of an initial denaturation at 95°C for 3 min, followed by 40 cycles of 95°C for 15 sec and 60°C for 1 min. Cycling for all RT-PCR was carried out using the MyIQ Single-Color Real-Time PCR Detection System (BioRad). Analysis was carried out using BioRad iQ5 2.0 Standard Edition Optical System Software. Transcript levels of target genes were normalized to GAPDH.

Western Blot Analysis

To make whole cell extracts for Western blot analysis, mESCs grown as adherent colonies on tissue culture dishes were washed with ice cold PBS, then harvested using a cell scraper, into approximately 2 mls of PBS. Cells were then pelleted by centrifugation at 200 xg for 4 min at 4°C. mESCs differentiated in suspension as EBs were first centrifuged at 200 xg for 4 min at 4°C to remove culture media then washed in approximately 5 mls of PBS before being pelleted by an additional centrifugation step. Cell lysis was then carried out by resuspending cell pellets in approximately three to five pellet volumes of mammalian cell lysis buffer (50 mM HEPES pH 7.9, 250 mM KCl 0.1 mM EDTA, 10% glycerol, 0.1% NP40, 1 mM DTT) containing freshly added protease

(catalog no. 11697498001; Roche) and phosphatase inhibitor cocktails (catalog no. 524625; Calbiochem). Resuspended cell pellets were incubated on ice for 30 to 60 min, with occasional vortexing throughout. Following the incubation, cell lysate was centrifuged at 20,800xg for 10 min at 4°C and the supernatant. The supernatant or whole cell extract (WCE) was then transferred to a clean tube and the protein concentration determined using the Bradford Assay (catalog no. 500-0006; BioRad). Approximately 10-20 μg of protein per lane from WCE was loaded onto a 10% Tris-HCl polyacrylamide gel and subjected to SDS-PAGE at 90V for 90 min. Proteins were then electroblotted onto nitrocellulose membrane in western blot transfer buffer (25 mM Tris, 192 mM Glycine, 20% (v/v) methanol) at 250 mA for 60 min at 4°C. Membranes were blocked in 1% skim milk/TBST (Tris buffered saline with 0.05% tween 20) for 1 hour at room temperature with gently shaking. Primary antibody was added to the membranes at a dilution recommended by the manufacturer in 0.5% skim milk/TBST. After an overnight incubation at 4°C on a shaker, membranes were washed at room temperature three times in TBST for 10 min each. HRP-conjugated secondary antibody (DAKO) was then added to the membrane in 0.5% skim milk/TBST at a dilution of 1:2000 for 1 hour before washing an additional three times with TBST for 10 min each. Membranes were developed with the ECLPlus Western Blotting System Reagent (catalog no. RPN2106; GE Healthcare) and detected by chemiluminescence/autoradiography by exposure to X-ray film (GE Healthcare).

Immunofluorescence

Cells analyzed by Immunofluorescence were plated at a density of approximately $2.5x10^4$ cells per cm^2 onto gelantinized Lab-Tek chamber slides (catalog no. 177437;

Nunc) and cultured as previously described. Growth media was then aspirated and cells fixed for 5 min at room temperature with 4% paraformaldehyde in PBS. Cells were then washed with PBS and permeabilized for 5 min. at room temperature with 0.2% Triton X-100 in PBS. Cells were then incubated in blocking solution (10% goat or donkey serum, depending on species of antibody, in PBS) for 1 hour at room temperature. Primary antibody was incubated with the cells overnight at 4°C at a dilution of 1:100 in blocking solution. Cells were then washed three times with PBS and incubated with secondary antibody (AlexaFluor, Molecular Probes) at a dilution of 1:250 in blocking solution for 1 hour at 4°C before being washed an additional three times in PBS. Nuclei was stained with 4',6-diamidine-2-phenylidole dihydrochloride (DAPI) at a dilution of 1:250 in PBS or TO-PRO-3 at a dilution of 1:300 in PBS. Slides were mounted with Prolong Gold mounting media and immunofluorescence visualized on a Zeiss LSM 510 META Confocal microscope.

Immunoprecipitation

Proteins were immunoprecipitated from approximately 600 µg of WCE, prepared as described above, adjusted to a concentration of 1 mg per ml^{-1}. This was followed by a pre-clearing step that involved incubating the cell lysate with 40 µl of protein A/G PLUS-agarose (catalog no. SC-2003; Santa Cruz) at 4°C for 1 hour on an end-over-end shaker. After pre-clearing, beads were removed by centrifugation at 100 xg for 30 sec. Primary antibody was added to the pre-cleared lysate, at a dilution of 1:100, and then incubated overnight on an end-over-end shaker at 4°C. Approximately 40 µl of protein A/G PLUS-agarose was added and the samples incubated for a further four hours at 4°C on an end-over-end shaker. Samples were then centrifuged for 30 sec at 100 xg, the supernatant

removed and the remaining protein A/G PLUS-agarose subjected to four wash steps with 500 µl of mammalian cell lysis buffer. To detect immunoprecipitated proteins the washed protein A/G PLUS-agarose/antibody mix was boiled in 50 µl of SDS and analyzed by western blotting.

Cell Fractionation

Mouse ESCs were cultured, differentiated as embryoid bodies and then harvested as described above. Cell pellets from each sample were then separated into cytoplasmic and nuclear fractions using the celLytic NuCLEAR Extraction Kit (Sigma) according to manufacturer's instructions. Equal proportions of nuclear and cytoplasmic fractions from each sample were then subjected to western blotting.

Leishman Staining

Cells were first washed with PBS then Leishman's stain, consisting of 0.15% (w/v) Leishman powder (catalog no. L6254-25G; Sigma) in methanol, was added for approximately 10 min at room temperature. Leishman's stain was then removed and the cells washed three times with water before air drying for approximately 30 min. A positive score was assigned to colonies that were tightly packed, domed-shaped and had over >90% of colony staining brightly for Leishman stain. A negative score was given to colonies that had a more flattened morphology with less than 10% of the colony staining for Leishman Stain. A minimum of 100 colonies were scored, and the percentage of cells positive for Leishman staining calculated.

Alkaline Phosphatase Staining

Cells were washed with PBS then assayed for alkaline phosphatase using the Vector Red Alkaline Phosphatase Substrate Kit I (Vector Labs) according to manufacturer's instructions. A positive score was assigned to colonies that were tightly packed, domed-shaped and had over >90% of colony staining brightly Alkaline Phosphatase. A negative score was given to colonies that had a more flattened morphology with less than 10% of the colony staining for Alkaline Phosphatase. A minimum of 100 colonies were scored, and the percentage of Alkaline Phosphatase positive cells calculated.

Site-directed Mutagenesis

The site-directed mutagenesis of rat Gsk3β and mouse Frat1 was performed using the QuikChange II Site-Directed Mutagenesis Kit (Stratagene) according to manufacturer's instructions and verified by sequencing. All mutagenic primers were designed according to the primer design guidelines laid out specifically for the QuikChange II Site-Directed Mutagenesis Kit. Sequencing of DNA and synthesis of oligonucleotides were performed by the Georgia Genomics Facility. Mutation of the serine 9 residue in Gsk3β to an alanine was done using pBS-Gsk3β as a template with the following primers: S9A-forward primer 5'-CGA CCG AGA ACC ACC **GCC** TTT GCG GAG AGC TGC-3' and the S9A-reverse primer 5'- GCA GCT CTC CGC AAA **GGC** GGT GGT TCT CGG TCG-3'. Mutation of the lysine 85 residue in Gsk3β to a methionine was done using pBS-Gsk3β-HA as a template with the following primers: K85M-forward primer 5'-GGA GAA CTG GTG GCC ATC **ATG** AAA GTT CTT CAG

GAC AAG-3' and the K85M-reverse primer 5'-CTT GTC CTG AAG AAC TTT **CAT** GAT GGC CAC CAG TTC TCC-3'. Mutation of the glutamine 206 residue in Gsk3β to a glutamic acid was done using pBS-Gsk3β-HA as a template with the following primers: Q206E-forward primer 5'-GAC TTT GGA AGT GCA AAG **GAA** CTG GTC CGA GGA GAG CCC-3' and the Q206E-reverse primer 5'-GGG CTC TCC TCG GAC CAG **TTC** CTT TGC ACT TCC AAA GTC-3'. The S9A/Q206E Gsk3β double mutant was was done using pBS-Gsk3β^{S9A}-HA as a template with the Q206E forward and reverse primers. Mutation of the lysine 50 and 52 residues in mFrat1 to alanines was done using pBS-Flag-mFrat1 as a template with the following primers: NESala-forward primer 5'-G ATC GGC GAG ACG **GCG** CAG **GCG** GAC GCA GCG CAC-3' and the NESala-reverse primer 5'-GTG CGC TGC GTC **CGC** CTG **CGC** CGT CTC GCC GAT C-3'.

Molecular Cloning

The following vectors were used in this study: pBluescript KS^{+}-ampR (pBS), pCAG-IRES-puromycin, pCAG-IRES-neomycin, and pCAG-Floxed-GFP-IRES-PURO. Other previously constructed plasmids used in this study are as follows: pBS-Gsk3β (Dalton Lab), pCDNA-Flag-mFrat1 (gift from Dr. Trevor Dale), pBS-3xHA (Dalton Lab), pBS-Gsk3β$^{S9A.NLS}$-HA (Dalton Lab), pCAG-Cre (Dalton Lab), pCAG-c-myc^{T58A}-ER (19), pCAG-IRES-eGFP-myr-Akt-ER (118). The pCAG plasmid facilitated constitutive expression under the control of the cytomegalovirus enhancer, chicken β-actin promoter (CAG). The expression vector pCAG-Floxed-GFP-IRES-puromycin contained a cassette flanked by loxP sites that included the eGFP gene driven by the CAG promoter and an IRES linked to a puromycin resistance gene. Upon exposure to the enzyme Cre the eGFP/puroR cassette is excised resulting in the expression of

anything downstream of the cassette. pBS-3xHA contained three tandem copies of the HA epitope tag cloned into the NotI sites. pCDNA-Flag-mFrat1 contained an in-frame N-terminal Flag tag, while pBS-Gsk3β$^{S9A.NLS}$-HA has an in-frame 2x NLS followed by a 3x HA tag at the c-terminus of Gsk3β prior to the stop codon.

Restriction digests of plasmid DNA was carried out in a 100 µl volume consisting of 10 µg of DNA, 10-20 units of appropriate restriction enzyme (New England Biolabs), with BSA (if applicable) and the appropriate restriction enzyme buffer. Restriction enzyme reactions were typically incubated at 37°C for four hours. Following incubation digested DNA was purified by a PCR cleanup kit (Qiagen) according to manufacturer's instructions. Digested DNA fragments were then loaded onto a 0.8% agarose gel (0.8% agarose in 1x TAE (catalog no. 161-0743; Bio-Rad) with 10µg/ml ethidium bromide) and electrophoresed at 50 mA. The desired fragments were excised from the gel and purified using a Gel Extraction Kit (Stratagene).

Ligation reactions were carried out in a 10 µl volume consisting of Takara ligation mix with insert and vector DNA in an approximate 3:1 ratio. The reaction was incubated at 16°C overnight, after which 5 µl of the ligation reaction were transformed into chemically competent *E. coli* (One Shot Max Efficiency DH5α-T1, Invitrogen) according to manufacturer's instructions. Transformants were then plated onto LB plates containing ampicillin (100 µg/ml) and plasmid DNA extracted using the Qiagen Spin Miniprep or Midiprep kit (Qiagen) according to manufacturer's instructions. Insert integrity and orientation was verified by restriction digest analysis.

The plasmids pBS-Gsk3β-HA and pBS-Gsk3β^{S9A}-HA were constructed as follows: pBS-Gsk3β, previously constructed by insertion of the Gsk3β cDNA into the XbaI sites of pBS, was used as a template in a PCR to amplify a portion of the Gsk3β coding sequence from nucleotide 984 to the stop codon at nucleotide 1263. The PCR consisted of 100 ng DNA template, PCR reaction buffer (Invitrogen), 1 mM $MgCl_2$, 150 ng each of forward and reverse primer, 300 μM dNTPs, and 2.5 units of *Pfu* Turbo (Stratagene). DNA was amplified by 27 cycles of 94°C for 30 sec, 50°C for 30 sec and 72°C for 45 sec with a final extension of 72°C for 6 min. The following primers were used in this PCR: The forward primer, 5'-CAC ACA **CCG CGG CAA TTG TCT AGA** GCT AAC ACC ACT GG**A AGC TT**G-3' which engineered in the restriction sites *SacII*, *MfeI* and *XbaI* 14 nucleotides 5' to a native *HindIII* site. The reverse primer, 5'-CAC ACA **GGT ACC CAA TTG** *TCA* **GCG GCC GC**A GGT AGA GTT GGA GGC TGA TGC-3' which engineered in a *NotI* restriction site before the stop codon followed by an *MfeI* restriction site and a *KpnI* restrictions site. The Gsk3β fragment was digested with *KpnI* and *SacII*, purified and then ligated into a similarly digested pBS KS$^+$ cloning vector. The ligation reaction was then transformed into *E. coli* and the resulting plasmid pBS-Gsk3β$^{984\text{-}1263}$ purified and verified. pBS-Gsk3β$^{984\text{-}1263}$ and the plasmid pBS-3xHA were both digested with *NotI* and the resulting 3x HA tag purified and ligated into the *NotI* sites of pBS-Gsk3β$^{984\text{-}1263}$. Following transformation of the ligation reaction the resulting plasmid pBS-Gsk3β$^{984\text{-}1263}$-HA was purified and verified. The remaining portion of Gsk3β, nucleotides 1-983, was removed from pBS-Gsk3β by digestion with *XbaI* and *HindIII* and subsequently ligated into a similarly digested pBS-Gsk3β$^{984\text{-}1263}$-HA. The ligation reaction was then transformed into *E. coli* and the resulting pBS-

Gsk3β-HA plasmid purified and verified. In the same manner, pBS-Gsk3β^{S9A} was digested with *XbaI* and *HindIII* and the resulting Gsk3β^{S9A} fragment purified and ligated into a similarly digested pBS-Gsk3β$^{984\text{-}1263}$-HA resulting in pBS-Gsk3β^{S9A}-HA.

pCAGipuromycin expression plasmids containing Gsk3β^{K85M}-HA, Gsk3β^{Q206E}-HA, Gsk3β-HA, Gsk3β^{S9A}-HA, and Gsk3β$^{S9A.NLS}$-HA as well as pCAG-Floxed-eGFP-Gsk3β$^{S9A.NLS}$-HA were constructed as follows: Each of the various forms of HA tagged Gsk3β were removed from their corresponding pBS KS+ backbones by MfeI digestions, purified and subsequently ligated into the *EcoRI* sites of pCAGipuromycin. In addition MfeI digested Gsk3β$^{S9A.NLS}$-HA was ligated into the *MfeI* sites of pCAG-Floxed-eGFPipuromycin downstream of the floxed cassette. Ligation reactions were then transformed into *E. coli,* and the resulting pCAG expression plasmids purified and verified.

The expression constructs pCAG-Flag-Frat and pCAG-Flag-mFrat^{NESala} were constructed as follows: pCDNA-Flag-mFrat1 and pCAGineomycin were first digested separately with *NheI* and *XhoI*, respectively. In order to make the digested *NheI* site on pCDNA-Flag-mFrat1 compatible with the digested *XhoI* site on pCAG the two sites were made into blunt ends by an incubation at 25°C for 15 min. with DNA polymerase I (Klenow fragment; New England Biolabs), dNTPs and NEB buffer 2 (New England Biolabs). Following a purification step with a PCR cleanup kit (Qiagen), pCDNA-Flag-mFrat1 and pCAGipuromycin were both digested with NotI. The *NheI/NotI* digested Flag-mFrat1 was then ligated into the *XhoI/NotI* sites of pCAGineomycin. The ligation reactions were subsequently transformed into *E. coli* and the resulting pCAG-Flag-mFrat1 expression plasmid purified and verified. For the purposes of site-directed

mutagenesis Flag-mFrat1 was removed from pCAG-Flag-mFrat1 by digestion with *EcoRI* and *NotI*. The *EcoRI/NotI* digested Flag-mFrat1 was ligated into a similarly digested pBS KS^+. Following site-directed mutagenesis the resulting Flag-mFrat1 mutant was digested out of pBS KS^+ and ligated back into pCAGineomycin giving pCAG-Flag-mFrat1^{NESala}.

The expression construct pCAG-myr-Frat^{2xFlag} was constructed as follows: pCDNA-Flag-mFrat1 was used as a template in a PCR to amplify the coding sequence of mFrat1. The PCR reaction consisted of 500 ng of template, Pfx amplification buffer (Invitrogen), 1 mM $MgSO_4$, 100 nM of forward and reverse primers and 2.5 units of Pfx platinum (Invitrogen). DNA was amplified by 34 cycles of 94°C for 15 sec, 55°C for 30 sec and 68°C for 1 min. The following primers were used in this PCR: The forward primer, 5'-CAC ACA **GAA TTC** AGC CGC CAC C **ATG GGG AGC AGC AAG AGC AAG CCC AAG TCT AGA** CCC ATG CCT TGC CGG AGG GAG GAG-3' which engineering an EcoRI site followed by a Myristoylation sequence in its N-terminus. The reverse primer, 5'-GAC CTT CTT GTC CCT GGC AGC CCC **GAC TAC AAG GAC GAC GAT GAC AAG GAC TAC AAG GAC GAC GAT GAC AAG** *TAA* **GCG GCC GC** CAC ACA-3' which engineered a 2xFlag sequence followed by a NotI sequence in its C-terminus. The resulting PCR product was digested with EcoRI and NotI and ligated into a similarly digested pBS KS^+, transformed into E. coli and the resulting plasmid purified and verified. pBS-myr-Frat^{2xFlag} was then digested with XhoI and NotI and ligated into a similarly digested pCAGipuromycin expression vector. The ligation reaction was transformed into E. coli and resulting plasmid purified and verified giving pCAG-myr- Frat^{2xFlag}.

Transfection of Pluripotent Stem Cells

With the exception of R1 mESCs stably expressing c-myc^{T58A}-ER (19) and E14tg2a mESCs stably expressing myr-Akt-ER (118), all stably transfected clonal cell lines were generated as a result of this study using the procedure below.

mESCs were initially seeded at a density of 1 x 10^4 cells/cm^2 onto a tissue culture dish pre-coated with 0.2% gelatin-PBS. Transfection of mESCs with the expression plasmid of interest was carried out 24 hrs later using the Lipofectamine 2000 reagent (Invitrogen) according to manufacturer's instructions. The manufacturer's protocol was however modified, using 10 μg of DNA for transfections in a 6-well dish and 2 ug of DNA for transfections in a 4-well slide. To generate clonal cell lines stably expressing the gene of interest, transfected mESCs were passaged the following day onto a 10 cm gelatinized tissue culture dish and grown in the presence of puromycin (1 μg/ml) for ~7 days or neomycin (200 ug/ml) for ~14 days. After selection individual colonies were picked and sub-cultured further. For transient transfections mESCs were grown and transfected as described above and then either selected for only 4 days or not at all.

CHAPTER 3

A ROLE FOR GSK3β IN REGULATING MOUSE ESC SELF-RENEWAL[1]

[1] Copyright © American Society for Microbiology. Bechard, M., and Dalton, S. *Molecular and Cellular Biology*, 29, 2009, 2092-2104, doi:10.1128/MCB.01405-08.
Reprinted here with permission of publisher.

Background

The proto-oncogene c-*MYC* is a direct transcriptional target of LIF/STAT3 signaling and is essential for the maintenance of mESC self-renewal (19). Inactivation of Myc activity leads to differentiation, and its ectopic expression relieves the requirement for LIF/STAT3 signaling (19). Consistent with this, Myc levels are elevated in pluripotent mESCs but decline markedly during the initial stages of differentiation (19). Together, these findings establish Myc as a key regulator of mESC self-renewal. The importance of Myc activity in establishing and maintaining the pluripotent state is underscored by recent experiments showing that c-myc is important for the efficient generation of induced pluripotent stem (iPS) cells, in conjunction with other factors such as Oct4, Sox2, and Klf4 (84, 108, 119).

The transcriptional down-regulation of the *c-MYC* gene represents one of the first responses to the cessation of LIF signaling and the inactivation of STAT3 in mESCs (19). Besides being controlled by transcription, c-myc levels are primarily regulated by changes in protein stability. Although c-myc is an unstable protein in nontransformed cell lines, with a half-life ($t_{1/2}$) of ~10 to 15 min, it exhibits unusual stability in mESCs ($t_{1/2}$ of ~105 min) (19, 125). This is comparable to the stability of oncogenic forms of Myc expressed by transforming viruses (v-*myc*) or in tumors such as Burkett's lymphoma (125). Following the decline in PI3K/Akt activity that accompanies the loss of LIF signaling, c-myc turnover is accelerated by a mechanism requiring its phosphorylation on threonine 58 (T58) (19). Failure to phosphorylate c-myc on T58 following LIF withdrawal maintains it in a stable state, sustains elevated levels of c-myc protein, and supports LIF-independent self-renewal (19). Phosphorylation of c-myc on T58 and its

accelerated degradation is therefore a key event required for transition from the self-renewing state to commitment to differentiation.#

Aside from maintaining c-myc in an active stable state, another key aspect to maintaining mESC self-renewal is the inactivation of Gsk3β. Although inactive during self-renewal, as mESCs differentiate following LIF removal Gsk3β undergoes a significant activation event (19). Moreover, activation of Gsk3β precedes the T58 phosphorylation and subsequent degradation of c-myc following LIF removal (19). In other biological contexts it has been well-documented that the T58 dependent degradation of c-myc is catalyzed by Gsk3β (48, 63, 93). Therefore, it's plausible that the activations status of Gsk3β could regulate the self-renewal status of mESCs by controlling the stability of c-myc. However, this has not been formally demonstrated, and is therefore the focus of our initial investigations.

Results

Activation and nuclear localization of Gsk3β during early mESC differentiation.

While evaluating the regulation of Gsk3β in mESCs we observed that within 24 hours of LIF withdrawal its enzymatic activity increases over 15-fold (19). Upon further examination, a corresponding hypo-phosphorylation of Gsk3β was also shown to occur following LIF withdrawal (Fig 3.1). Surprisingly however, a re-localization from the cytoplasm to the nucleus was shown to occur along with its activation (Fig. 3.1). The significance of this re-localization was confirmed by subcellular fractionation which showed a complete accumulation of Gsk3β in the nucleus by day 2 of mESC differentiation (Fig. 3.2). These observations were seen whether mESC were

differentiated in adherent cultures or in suspension as EBs (EBs; Fig. 3.1 and 3.2). This indicates that the activation and nuclear localization of Gsk3β is a general phenomenon associated with early differentiation commitment.

Nuclear accumulation of hypo-phosphorylated Gsk3β also coincided with the decline of c-myc protein levels, increased c-myc T58 phosphorylation, and loss of Akt activity, as indicated by decreased phosphorylation on serine 473 (S473) (Fig. 3.3 and 3.4). In contrast to changes in levels of pluripotency markers, these events coincided with the loss of Nanog, but preceded the decline in Oct4 levels (Fig. 3.3 and 3.4). Furthermore, the addition of Gsk3 inhibitors such as BIO, lithium chloride, Gsk3 inhibitor XV, and CHIR 99021/CT 99021 to day 2 EBs blocked c-myc phosphorylation on T58, indicating that activation of Gsk3β is required for the accelerated turnover of c-myc, during early mESC differentiation (Fig 3.5). The inactive BIO analogue, MeBIO, had no effect under these conditions. These observations are consistent with our previous model (19) that activation of Gsk3β promotes mESC differentiation by promoting the degradation of c-myc through a T58-dependent mechanism. Although the accumulation of Gsk3β in the nucleus is specifically associated with its hypo-phosphorylation on S9, minor amounts of S9-phosphorylated Gsk3β were detected in differentiating cells, but only in the cytoplasm (Fig. 1A). The activation and nuclear accumulation of Gsk3β following LIF withdrawal was also observed in other mESC lines, including E14tg2a, and D3 (Fig. 3.6; McLean and Dalton unpublished data), indicating that these events are a general feature of early differentiation commitment.

One previous report showed that in L-cells and 10T1/2 cells, Gsk3β shuttles between the cytoplasm and nucleus even though it has a predominantly cytoplasmic

localization (38). However, it is unclear how general a phenomenon this is and moreover, the biological significance of Gsk3β shuttling and its mechanism of regulation have not been elucidated. To establish if Gsk3β nuclear-shuttling occurs in mESCs, they were treated with leptomycin B (LB), an inhibitor of CRM-mediated nuclear export. This resulted in the accumulation of S9-phosphorylated Gsk3β in the nucleus (Fig. 3.1 and 3.2), indicating that Gsk3β shuttles between the nucleus and cytoplasm in self-renewing mESCs. Similar experiments were performed in other pluripotent cell types of embryonic origin including, E14tg2a, epiblast stem cells (EpiSCs; (109)) and induced pluripotent stem cells (iPSCs; Fig. 3.7). In all cases, LB treatment resulted in the redistribution of Gsk3β from cytoplasm to the nucleus within 6 hours (Fig. 3.7), indicating that Gsk3β shuttling is a general attribute of pluripotent cells.

Gsk3β interferes with mESC maintenance by targeting c-myc. Although the accumulation of Gsk3β in the nucleus follows the withdrawal of LIF and results in increased phosphorylation of c-myc on T58, the biological consequences of this were not investigated. This was addressed by evaluating the effects of a nuclear localized, constitutively active mutant form of Gsk3β on self-renewal. We generated an R1 mESC cell line expressing a hemaglutinin (HA) tagged, constitutively active Gsk3β mutant (serine 9 to alanine substitution; S9A) with two SV40 nuclear localization signals ($Gsk3\beta^{S9A.NLS}$) under control of Cre recombinase (see Fig. 3.8A). Cre recombinase expression, following transient transfection, was monitored for loss of $eGFP^{+}$ fluorescence after 3 days, while Nanog expression was used to monitor mESC maintenance. In $eGFP^{+}$ $Nanog^{+}$ cells (-Cre), $Gsk3\beta^{S9A.NLS}$ was not expressed as indicated by the absence of HA immunostaining (Fig. 3.8A). However, Cre mediated excision, as

monitored by loss of eGFP fluorescence, established conditions where ~85% of eGFP$^-$ (+Cre) cells expressed nuclear Gsk3β$^{S9A.NLS}$. Only ~10% of eGFP$^-$ HA$^+$ cells retained Nanog expression, compared to 90% in eGFP$^+$ HA$^-$ cells (Fig. 3.8A, B). Under similar conditions, cells expressing vector alone (Fig. 3.8A, B) maintained levels of Nanog expression comparable to that in untransfected cells. These data indicate that enforced localization of constitutively active Gsk3β has a clear effect on mESC maintenance.

The previous observations suggested that nuclear Gsk3β interferes with mESC self-renewal and promotes differentiation. To test this hypothesis, R1 mESCs were either transfected with empty vector or Gsk3β$^{S9A.NLS}$ constructs and then selected with puromycin over 4 days. To assay what effect this had on self-renewal the cells were stained with Leishman reagent (97) (Fig. 3.9A, B). In addition, changes in general morphology were characterized by bright field microscopy (Fig. 3.9A). Cells transfected with empty vector generated colonies that were >80% positive in the Leishman stain assay and maintained a typical three dimensional domed-shaped colony morphology (Fig 3.9A, B). The remaining 20% of colonies were partially positive in the Leishman assay but did not completely stain and retained intermediate mESC colony morphology. However, only ~3% of colonies generated by transfection with Gsk3β$^{S9A.NLS}$ expression constructs scored positive in this assay. This also corresponded to a general disruption of colony architecture with most cells exhibiting a "flattened" morphology, reminiscent of differentiating primitive endoderm cells that form following LIF withdrawal and loss of Myc function (19, 79). The decrease in Leishman staining and disruption of colony architecture was, however, not observed in cells transfected with Gsk3β-HA or Gsk3β^{S9A}-HA expression constructs (Fig. 3.9B). Most of the colonies scoring negative in the

Leishman assay consisted of less than 5% positively stained cells. When BIO was added to Gsk3β$^{S9A.NLS}$-transfected cultures 24 hours post-transfection the percentage of Leishman-stained cells was restored to almost 90% and typical dome-shaped colony morphology was retained (Fig. 3.9A, B). Expression of Gsk3β$^{S9A.NLS}$ also caused a major decrease in Oct4 transcript levels (Fig. 3.9C) and increased T and Cdx2 transcript levels (Fig. 3.10A). In addition, ~50% of cells stained positive for the endoderm marker FoxA2 (Fig. 3.10A). Together, these data demonstrate that a biological consequence of active, nuclear-localized Gsk3β is the promotion of mESC differentiation.

To establish if nuclear Gsk3β triggers mESC differentiation by targeting c-myc, we repeated the previous experiment in a cell line expressing a stable, mutant form of c-myc (T58A) fused to the hormone-binding domain of the estrogen receptor (ER; Fig. 3.11A). Previously, we showed that this stable form of Myc (c-myc^{T58A}-ER) under control of 4OHT, can promote self-renewal in the absence of LIF (19). Critical to this was the ability of c-myc to avoid phosphorylation on T58, thereby retaining its comparatively long-half life (~105 minutes; (19). To address the possibility that Gsk3β antagonizes self-renewal by targeting Myc in this manner, we asked if ectopic c-myc activity could rescue the differentiation-promoting effects of Gsk3β$^{S9A.NLS}$. If c-myc is the main target for active, nuclear Gsk3β following LIF withdrawal or loss of PI3K/Akt signaling, ectopic expression of c-myc^{T58A}-ER should circumvent the effects of Gsk3β and cells should retain the capacity to self-renew, even over short periods of time. Transfection of vector alone, with or without 4OHT, was unable to block differentiation caused by Gsk3β$^{S9A.NLS}$ as determined by staining with Leishman reagent (<5% positive colonies) and colony morphology (Fig. 3.11B, C). As noted before, in the presence of

activated nuclear Gsk3β, cells adopt a morphology that is typical of primitive endoderm (Fig. 3.9A), similar to that seen following Myc inactivation or LIF withdrawal in mESCs (19). However, when the c-myc^{T58A}-ER fusion was activated by 4OHT, a typical dome-shaped colony morphology was maintained and cells retained uniform staining with Leishman reagent in the presence of Gsk3β$^{S9A.NLS}$ (Fig. 3.11B, C). These data show that if Myc activity is maintained in mESCs, the ability of Gsk3β to trigger differentiation is severely compromised. In conclusion, c-myc is a major target of Gsk3β when it enters the nucleus following removal of LIF during early mESC differentiation. The ability of c-myc to be targeted by Gsk3β following its accumulation in the nucleus is shown to be part of a pathway that impacts on mESC fate determination.

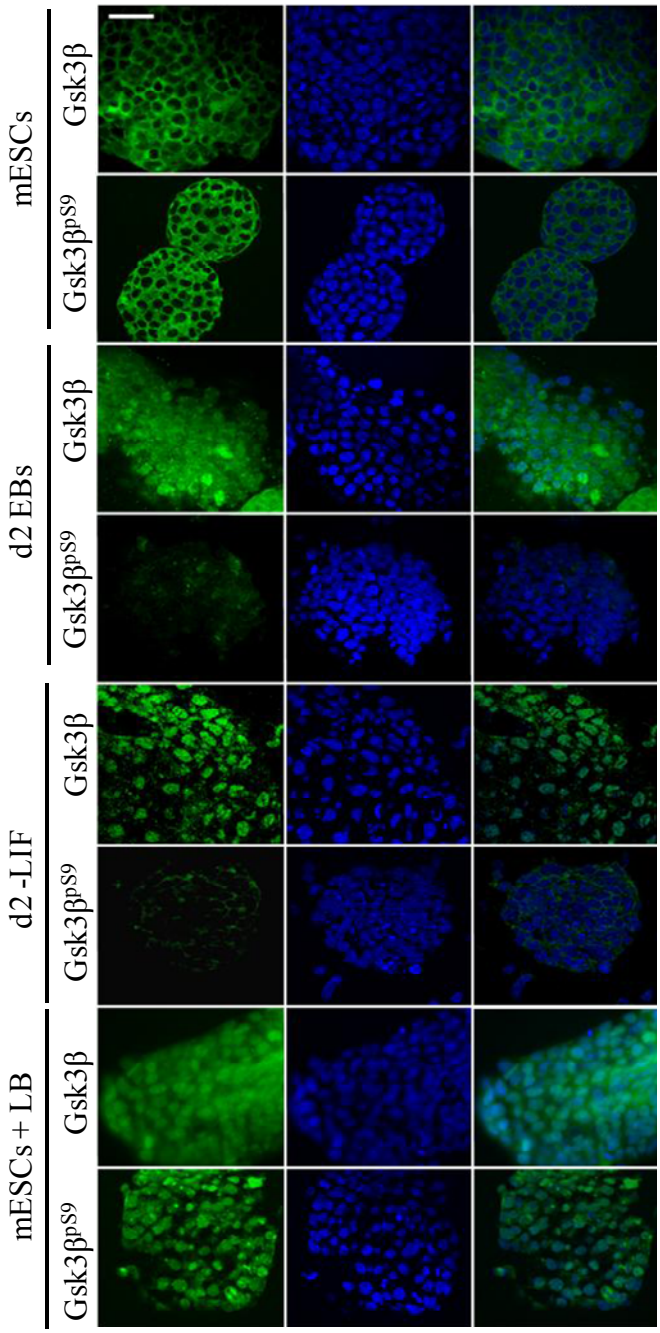

Figure 3.1. Gsk3β localization in mESCs and during early differentiation. R1 mESCs (plus LIF), day 2 (d2) EBs, R1 mESCs grown without LIF for 2 days (d2 LIF), and mESCs treated with LB (110 nM) for 6 hrs. were probed with antibodies as indicated. To-Pro-3 (blue) was used to visualize DNA. All staining was visualized by confocal microscopy. Scale bar, 50 μm.

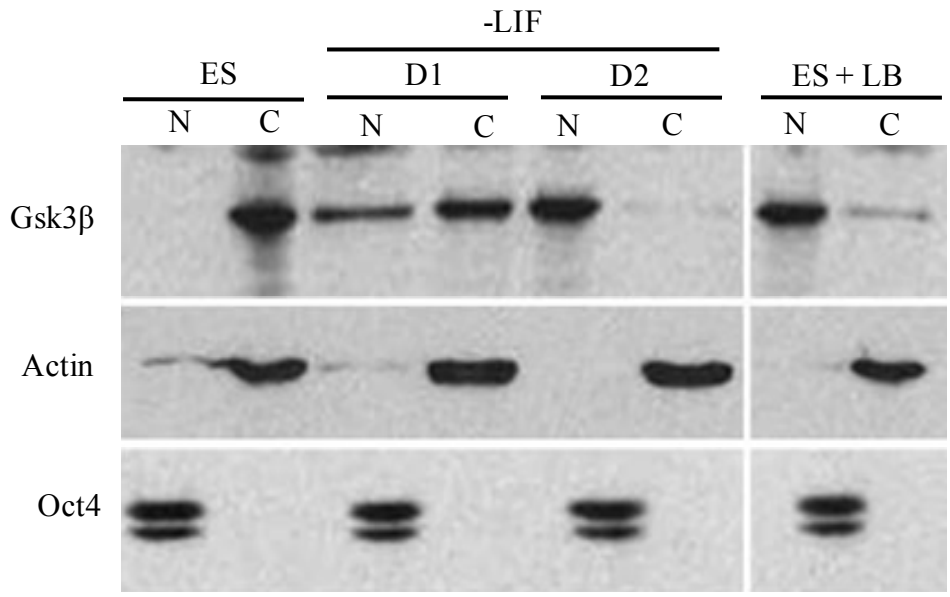

Figure 3.2. Analysis of Gsk3β localization during differentiation by subcellular fractionation. Nuclear (N) and cytoplasmic (C) extracts from R1 mESCs and mESCs grown in the absence of LIF for 1 day (D1) or 2 days (D2) were subjected to immunoblot analysis as indicated. Oct4 and actin were used as nuclear and cytoplasmic markers, respectively. Right panel: analysis of nuclear and cytoplasmic fractions from mESCs treated with LB (110 nM, 6 hrs.). Equal proportions of nuclear and cytoplasmic fractions were loaded for direct comparison.

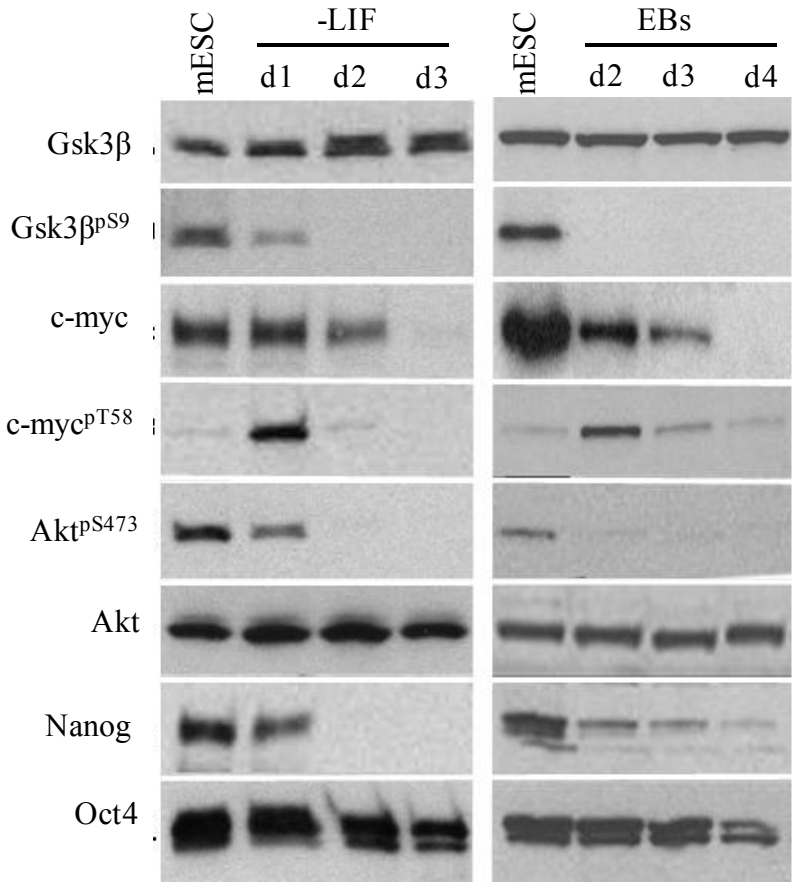

Figure 3.3. Western blot analysis of mESCs during early differentiation. Whole-cell lysates (20 μg) from R1 mESCs or mESCs grown in the absence of LIF for up to 3 days or as EBs over 4 days were immunoblotted as indicated.

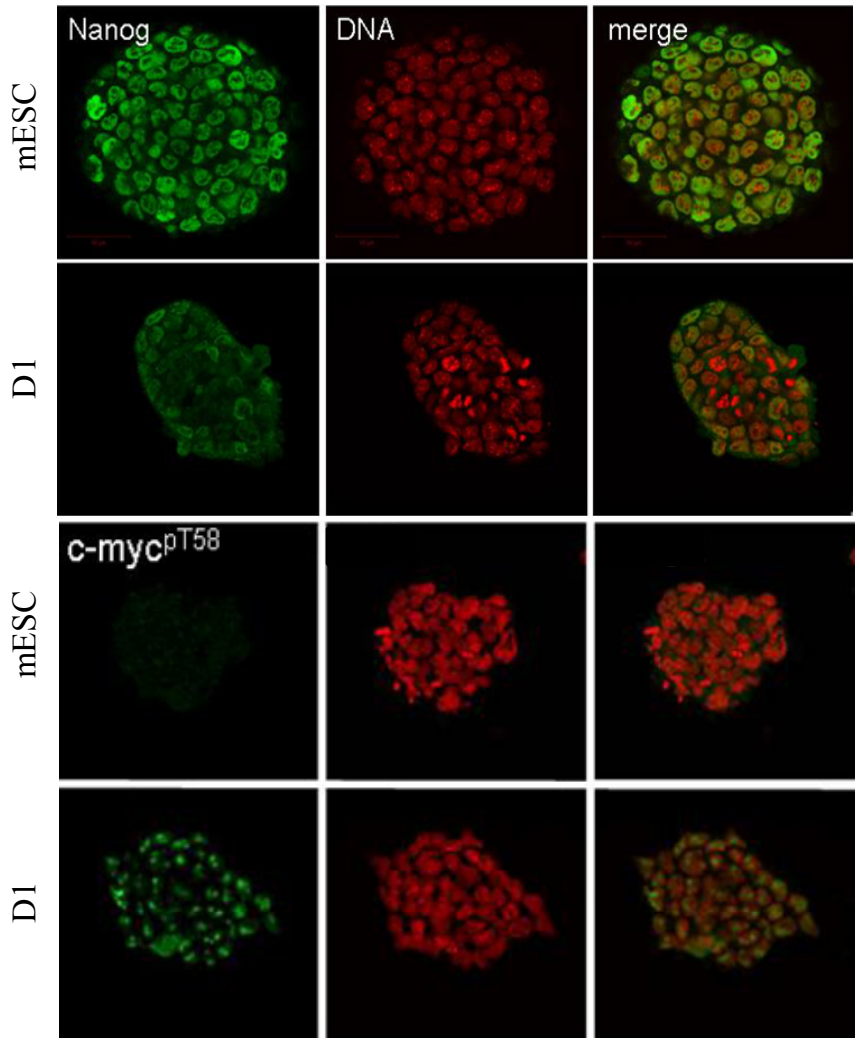

Figure 3.4. Immunostaining depicting changes in Nanog and c-myc phosphorylation following LIF removal. mESCs (plus LIF) or mESCs cultured for 1 day in the absence of LIF were immunostained for nanog and c-myc^{pT58}, images were generated by confocal microscopy.

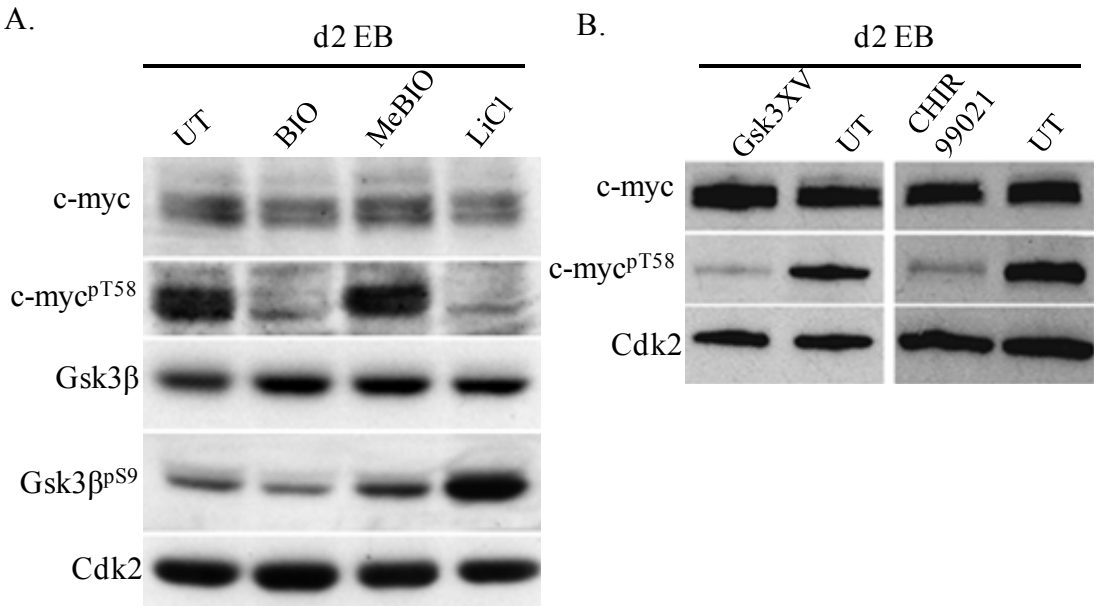

Figure 3.5. Small molecule inhibition of Gsk3β activity blocks c-myc phosphorylation during early mESC differentiation. (A). D3 mESCs were differentiated as embryoid bodies for 2 days in the absence of LIF (d2 EB) and treated with BIO (2 μM), MeBIO (2 μM) or LiCl (20 μM) 6 hours before harvesting. UT: untreated D3 mESCs. Cell lysates (20 μg total protein) were subjected to western blot analysis probing for antibodies as indicated. **(B).** R1 mESCs were differentiated as EBs for 2 days in the absence of LIF then treated with GSK3 inhibitor XV (10 nM) or CHIR 99021/CT99021 (3 μM) for 12 hours. Analysis of samples was as described in (A). Immunoblots were probed with antibodies as indicated.

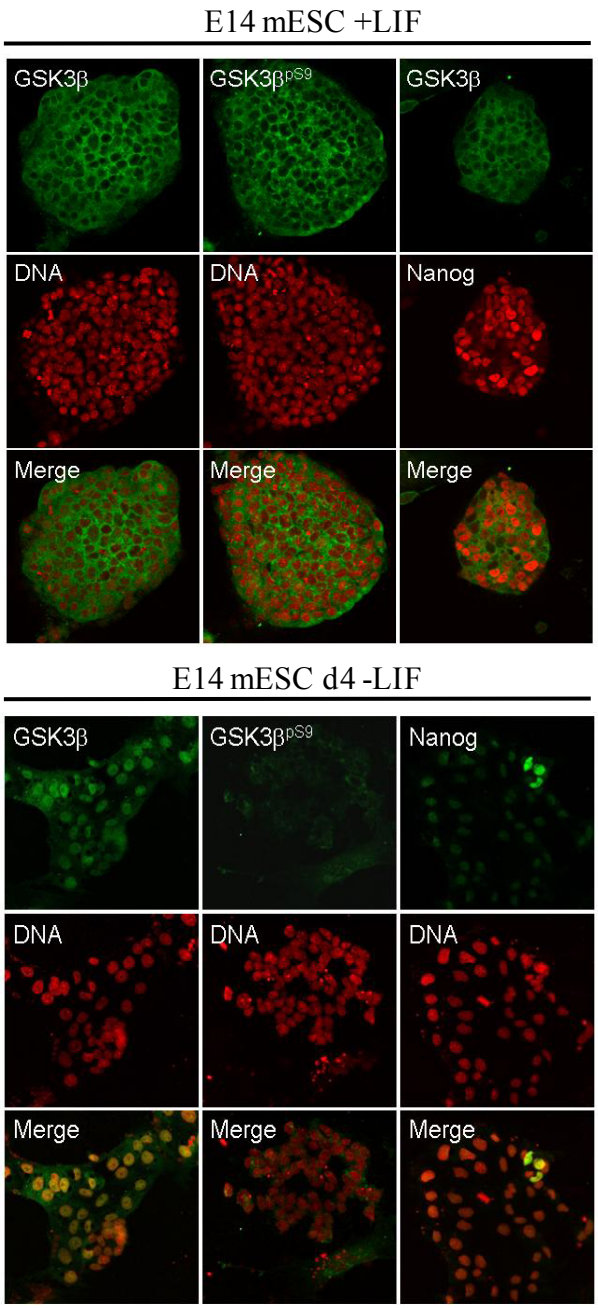

Figure 3.6. Gsk3β accumulates in the nucleus of differentiating E14 mESCs following LIF withdrawal. Top panel (left): E14 mESCs maintained in the presence of LIF were stained with antibodies for Gsk3β and Gsk3β^{pS9} and right, for Nanog and Gsk3β. DNA was detected by staining with TO-PRO-3. Bottom panel (left): analysis was as for (A), but were differentiated in the absence of LIF for 4 days.

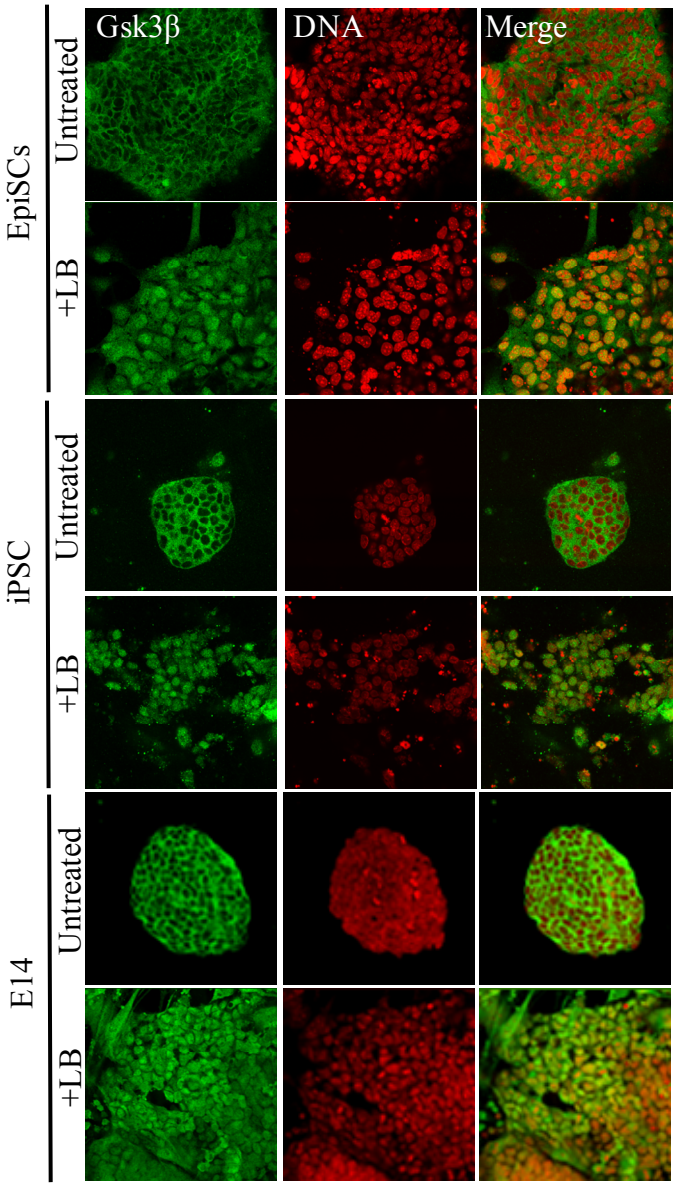

Figure 3.7. The cytoplasmic/nuclear shuttling of Gsk3β in other populations pluripotent stem cells. Confocal images of untreated (UT) and LB treated (6 hours; 110 nM) EpiSCs, iPSCs and E14 mESCs. Cells were fixed and stained with an antibody for Gsk3β. DNA visualized by staining with TO-PRO-3.

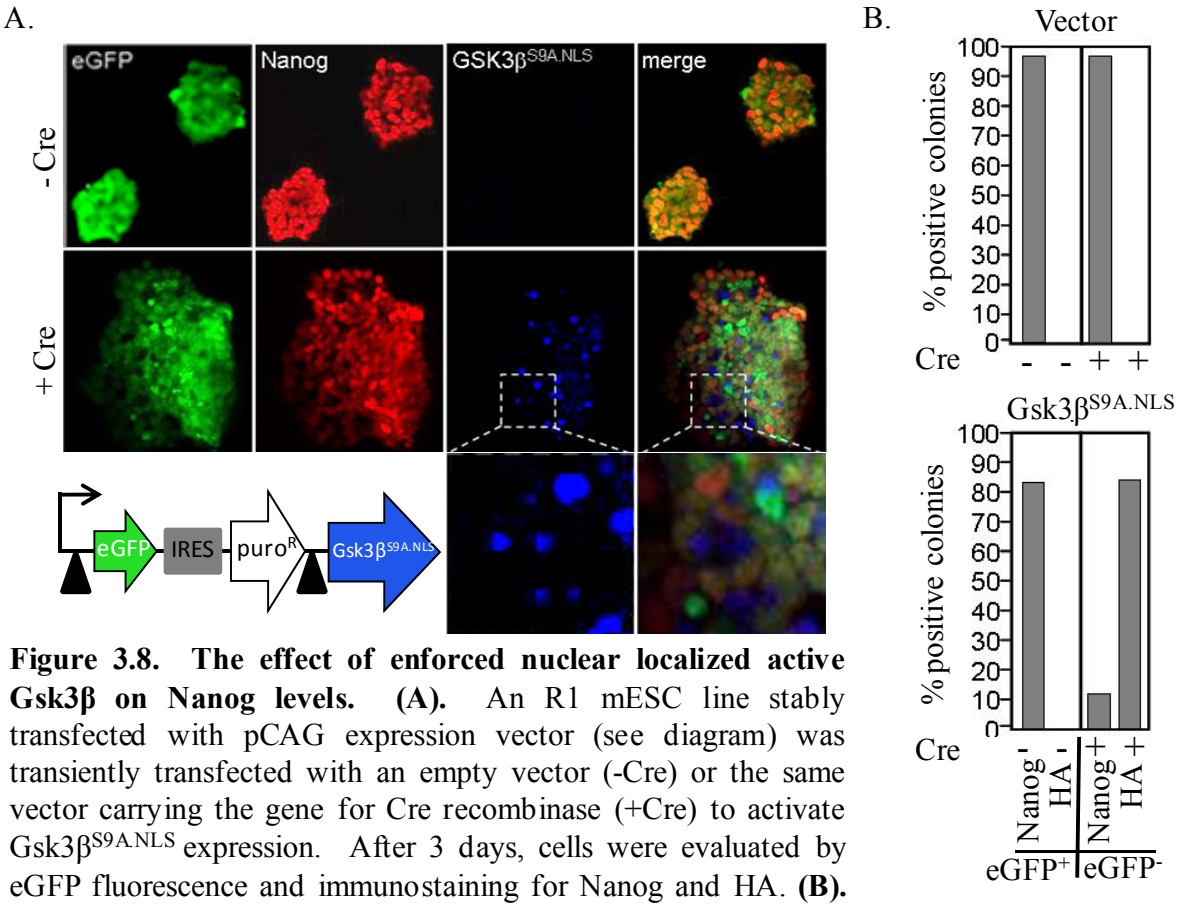

Figure 3.8. The effect of enforced nuclear localized active Gsk3β on Nanog levels. (A). An R1 mESC line stably transfected with pCAG expression vector (see diagram) was transiently transfected with an empty vector (-Cre) or the same vector carrying the gene for Cre recombinase (+Cre) to activate $Gsk3\beta^{S9A.NLS}$ expression. After 3 days, cells were evaluated by eGFP fluorescence and immunostaining for Nanog and HA. **(B).** Graphical representation of the percentages of Nanog- and HA-positive cells from panel A. At least 500 cells were scored under each of the experimental conditions.

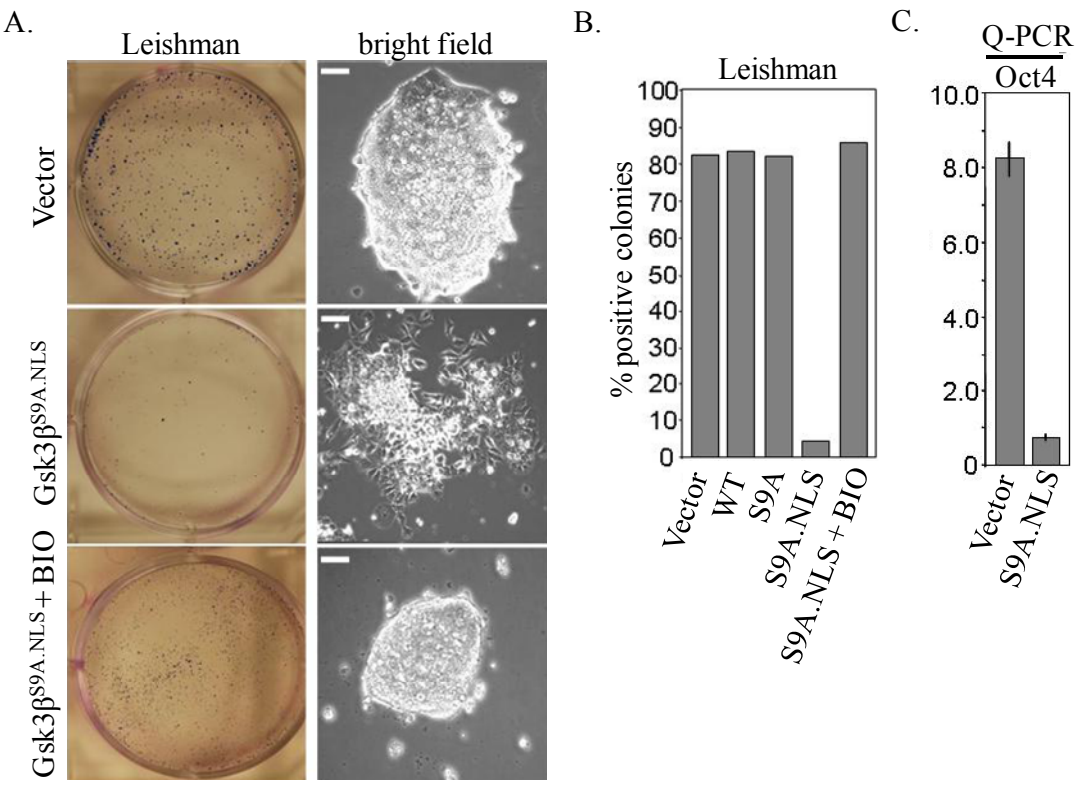

Figure 3.9. Enforced nuclear localization of active Gsk3β disrupts self-renewal of mESCs. (A). R1 mESCs were transiently transfected with vector alone (pCAGipuro) or the equivalent vector expressing Gsk3β$^{S9A.NLS}$ in the presence or absence of 2 μM BIO. 24 hours posttransfection, cells were selected with puromycin for 4 days. Self-renewal capacity was then analyzed by Leishman staining (Left) and bright field microscopy (right). Scale bar, 50 μm. **(B).** Graphical representation of the percentages of Leishman positive colonies from (A) in addition to R1 mESCs transfected with Gsk3β-HA (WT) and Gsk3β^{S9A}-HA constructs (S9A). **(C).** Q-PCR analysis of Oct4 transcript levels in R1 mESCs transfected with vector only or Gsk3β$^{S9A.NLS}$ (as in panel C) following 4 days of puromycin selection. Bars represent the standard errors of the means.

A.

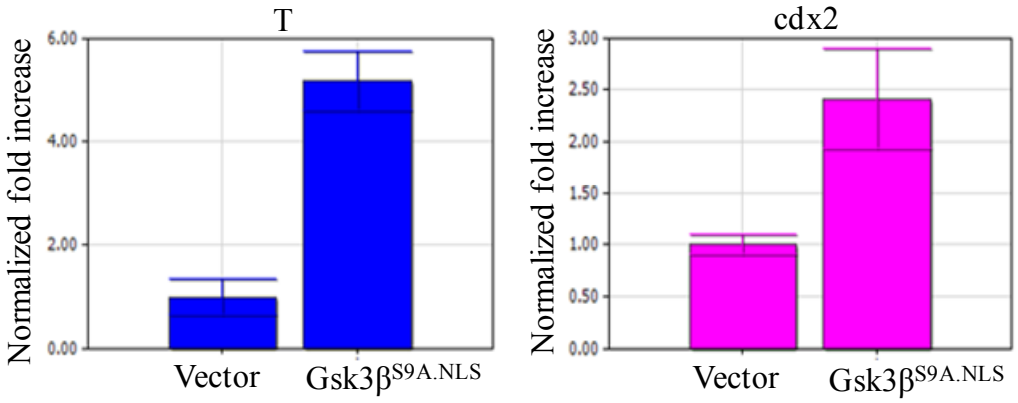

B.

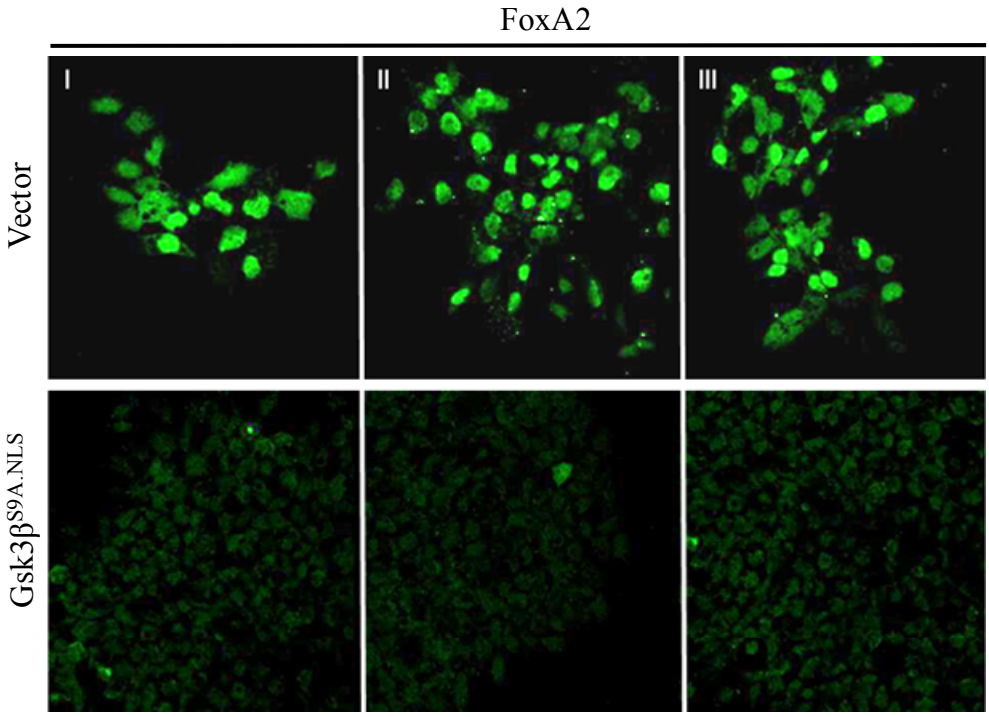

Figure 3.10. Enforced nuclear localization of active Gsk3β promotes differentiation of mESCs. (A). Q-PCR analysis of T/brachyury and Cdx2 transcript levels in R1 mESCs transfected with vector only or the equivalent vector expressing Gsk3β$^{S9A.NLS}$ as in Figure 3.9. Error bars represent +/- standard error of the mean. **(B).** Analysis of FoxA2 levels by immunofluorescence following transfection of empty vector and Gsk3β$^{S9A.NLS}$ as in **(A).** Three representative immuno-fluorescence panels are shown (I, II, III).

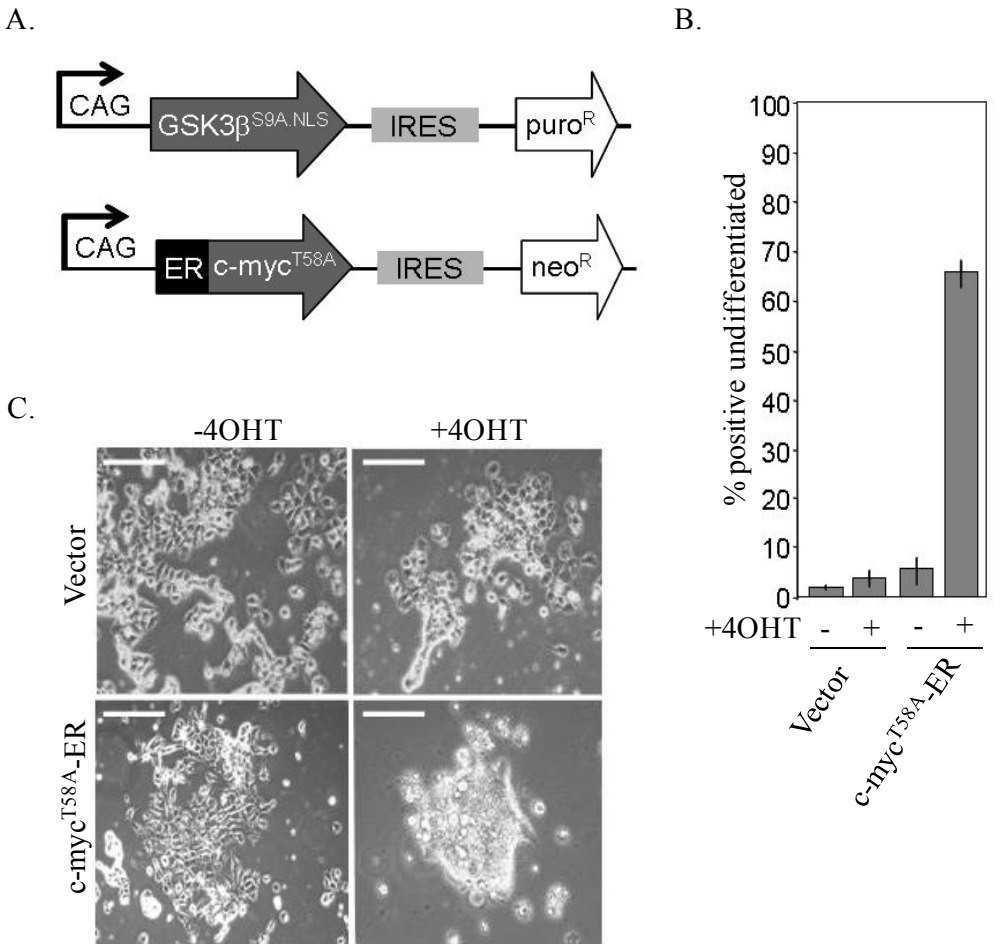

Figure 3.11. Effects of Gsk3β on mESC self-renewal can be blocked by enforced expression of a c-myc^{T58A} mutant. **(A).** Diagram depicting the pCAG expression constructs used in this experiment. neo^R, neomycin resistant; puro^R, puromycin resistant. **(B).** pCAG-c-myc^{T58A}-ER and its corresponding empty vector were used for the generation of two cell lines. These cell lines were transiently transfected with a Gsk3β$^{S9A.NLS}$ expression construct (see panel A) and selected for 4 days, as for Figure 3.9, in the presence (+4OHT) or absence (-4OHT) of 5 nM 4OHT. Colonies were then scored for Leishman staining. Error bars represent the standard errors of the means. **(C).** Morphology of transfected mESC colonies from panel B. Scale bar, 50 μm.

Discussion

Gsk3β is a shuttling protein. Although Gsk3β is generally considered to be a cytoplasmic protein, there are numerous examples where it has been shown to partially or transiently accumulate in the nucleus, for example, during apoptosis, replicative senescence, and during S phase of the cell cycle (10, 19, 26, 129). Once in the nucleus and depending on cell type, Gsk3β can phosphorylate substrates such as cyclin D, NFAT, and c-myc (8, 26, 125). However, very little is known in regards to the nuclear import/export mechanisms of Gsk3β and how it's regulated. One previously published report has however described that Gsk3β undergoes active nuclear-cytoplasmic shuttling in 10T1/2 fibroblasts and L cells (38). In corroboration of the previously described report, our results demonstrate that Gsk3β undergoes active nuclear-cytoplasmic shuttling in mESCs, despite its consistent cytoplasmic accumulation. However, given these observations we postulated that this could be a general feature of Gsk3β. We therefore investigated the shuttling capabilities of Gsk3β in 14 primary and transformed cell lines of murine and human origin. While relative distribution of Gsk3β between the nucleus and cytoplasm varied in different cell lines, its localization is dynamic in all cases, involving continual shuttling between the nucleus and cytoplasm (M. Bechard and S. Dalton, unpublished data). Nuclear-cytoplasmic shuttling of Gsk3β is therefore a general phenomenon that has major biological implications in a broad range of cell types.

Gsk3β disrupts mESC maintenance by targeting Myc. During self-renewal our results demonstrate that, despite its active shuttling to and from the nucleus, Gsk3β localizes to the cytoplasm in mESCs in an inactive state. The simplest interpretation of this is that during mESC self-renewal the rate by which Gsk3β is exported from the nucleus exceeds

that of its import resulting in its near exclusive accumulation in the cytoplasm. Interestingly, we demonstrate that following LIF withdrawal Gsk3β accumulates in the nucleus in an active state. Since Gsk3β actively shuttles to and from the nucleus under self-renewing conditions, it's reasonable to conclude that during mESC differentiation the nuclear accumulation of Gsk3β occurs as a result of a loss in its nuclear export capabilities. We also provide evidence that the accumulation of active Gsk3β in the nucleus disrupts self-renewal and promotes differentiation through the degradation of c-myc, a transcription factor that has a major role in maintaining and establishing the pluripotent state (19, 84, 108, 119). The connection between Gsk3β and c-myc was first suggested in a 2005 report from our lab, following observations that the c-myc^{T58A} mutant, which evades Gsk3β, sustains mESC self-renewal in the absence of LIF (19). Additional reports have highlighted the importance of suppressing Gsk3β activity in order to maintain ESC self-renewal and its requirement for normal differentiation (28, 92, 127). Altogether, the nuclear export of inactive Gsk3β in mESCs maintains the stability of c-myc, and thus self-renewal, by keeping it inaccessible to Gsk3β. Therefore, it's reasonable to conclude that the nuclear export of Gsk3β is a key regulatory step critical in the decision between self-renewal and differentiation.

Future directions. Several key questions remain unanswered in regards to the nuclear export of Gsk3β. Although, the nuclear import of Gsk3β is dependent upon a bipartite nuclear localization signal (NLS) (69), a valid nuclear export sequence has not yet been identified and therefore very little is known in regards to how Gsk3β exports from the nucleus. More importantly, despite an apparent inactivation of the nuclear export of Gsk3β during early mESC differentiation, the underlying mechanism responsible for this

is not understood. Since the nuclear localization of Gsk3β plays an important role in other biological contexts in addition to mESCs, it will be important to gain a better understanding of the underlying mechanism associated with its transport out of the nucleus.

CHAPTER 4

PI3K/AKT SIGNALING REGULATES THE NUCLEAR EXPORT OF GSK3β[2]

[2] Copyright © American Society for Microbiology. Bechard, M., and Dalton, S. *Molecular and Cellular Biology*, 29, 2009, 2092-2104, doi:10.1128/MCB.01405-08.
Reprinted here with permission of publisher.

Background

The PI3K pathway, which signals through Akt, has been demonstrated as a critical component in the maintenance of mESC self-renewal. Specifically, maintaining PI3K/Akt activity delays mESC differentiation, while interrupting it results in a loss of self-renewal (103, 118). PI3K signaling, in other biological contexts, is a well-established regulator of Gsk3β activity, inactivating the kinase through an Akt-dependent phosphorylation of S9 (29). Similarly, in mESCs, several observations strongly indicate that PI3K/Akt signaling regulates Gsk3β activity via S9 phosphorylation. First, inactivation of PI3K/Akt signaling under self-renewing conditions results in a significant decrease in S9 phosphorylation, indicating an activation of Gsk3β (87, 103). Second, our results demonstrate that upon LIF withdrawal Akt phosphorylation at serine 473 significantly decreases, indicating a loss in PI3K/Akt signaling (9). This is closely followed by the catalytic activation of Gsk3β, as seen by its hypo-phosphorylation at S9 (9, 19). Altogether, these observations strongly support the conclusion that in mESCs PI3K/Akt signaling is directly responsible for regulating the activity of Gsk3β.

During self-renewal when PI3K/Akt activity is high, Gsk3β activity shuttles to and from the nucleus in an inactive state. During differentiation, however, when PI3K/Akt activity is low Gsk3β accumulates in the nucleus due an apparent loss in its nuclear export capabilities. This correlation suggests that PI3K/Akt signaling may have a role in activating the nuclear export of Gsk3β, in addition to regulating its activity. Interestingly, several other reports have correlated the nuclear accumulation of Gsk3β to PI3K/Akt signaling as well. Most notably, Diehl and colleagues (1998) demonstrated that the nuclear accumulation of active Gsk3β, necessary for cyclin D1 degradation

during S-phase is due to a loss in PI3K/Akt signaling (26). The loss of PI3K/Akt signaling during S-phase was shown to trigger the degradation of c-myc as well, most likely through the nuclear accumulation of active Gsk3β (65). Finally, conditions which specifically inhibit PI3K/Akt signaling like serum withdrawal and wortmannin treatment (an inhibitor of PI3K) was shown to promote the nuclear accumulation of Gsk3β (10, 129). Despite these observations very little is understood in regards to the underlying mechanism linking PI3K/Akt signaling to the nuclear accumulation of Gsk3β. Since the nuclear exclusion of Gsk3β has a vital role in the maintenance of mESC self-renewal by preventing c-myc degradation, it was important to determine how the localization of Gsk3β is regulated. Therefore, the following investigations sought to shed some light on the potential involvement of PI3K/Akt signaling in regulating the nuclear export of Gsk3β in mESCs.

Results

Gsk3β accumulates in the nucleus of mESCs when PI3K is inhibited. The accumulation of active Gsk3β in the nucleus coincides with decreased Akt activity (Fig 3.1 through 3.3) and is possibly linked to loss of PI3K signaling following LIF withdrawal (87). Despite having well-defined roles in promoting self-renewal, a role for PI3K/Akt signaling in the regulation of Gsk3β sub-cellular localization, however, has not been previously proposed (68, 118). To evaluate the connection between PI3K/Akt signaling and Gsk3β sub-cellular localization further, we added inhibitors of PI3K (LY294002 and PI-103) and Akt (AktV) to mESCs cultured in the presence of LIF and asked if this was sufficient to re-localize Gsk3β to the nucleus. Treatment of mESCs with LY294002 promoted the nuclear accumulation of Gsk3β (Fig. 4.1), which coincided

with decreased c-myc levels and increased T58 phosphorylation (Fig. 4.2). T58-phosphorylated c-myc also co-localized with fibrillarin in nucleoli (Fig. 4.2A), the site where c-myc is targeted for ubiquitination and a key step required for its subsequent proteolysis (93). Nanog responded to LY294002 treatment in a similar manner to c-myc although Oct4 levels remained stable (Fig. 4.2B and Fig. 4.3). It is possible however, that the previously described results could be due to off-target effects of LY294002 instead of PI3K/Akt inhibition. Therefore, the effect of PI3K/Akt inhibition on Gsk3β activation and localization was evaluated by a more potent PI3K inhibitor (PI-103) and an Akt specific inhibitor (AktV). As seen with LY294002, addition of PI-103 and AktV both resulted in a re-localization of Gsk3β to the nucleus along with a corresponding increase in the phosphorylation of c-myc at T58 (Fig. 4.4 and 4.5). Inhibition of PI3K/Akt signaling therefore reproduces events associated with early differentiation with regards to Gsk3β activity status and sub-cellular localization.

Addition of BIO, but not its inactive analogue MeBIO, blocked down-regulation of c-myc levels and T58 phosphorylation following addition of LY294002, but had no impact on the nuclear accumulation of Gsk3β (Fig. 4.2 and data not shown). BIO also blocked the increase in T58 c-my phosphorylation following PI-103 and AktV treatment, while not effecting Gsk3β nuclear accumulation (data not shown). This indicates that although loss of PI3K/Akt signaling is required for Gsk3β nuclear accumulation, Gsk3β activity is not required. These results show that PI3K/Akt signaling is required to maintain Gsk3β in a cytoplasmic, inactive state in self-renewing mESCs, and implies a mechanism for how c-myc levels are regulated in mESCs and during early differentiation.

It is well established that Akt directly regulates Gsk3β activation through its phosphorylation of Gsk3β at S9. Therefore, an obvious explanation is that the nuclear localization of Gsk3β following decreased PI3K/Akt signaling could be due to the loss of S9 phosphorylation and its subsequent catalytic activation. However, the localization of an S9A mutated form of Gsk3β was indistinguishable from that of wild-type Gsk3β (Fig. 4.1 and Fig 4.6). Moreover, like wild-type Gsk3β, the $Gsk3\beta^{S9A}$ mutant still accumulated in the nucleus following LB treatment, indicating its shuttling capabilities were also unaffected (Fig. 4.6). In addition, inhibition of Gsk3β with BIO had no effect on its subcellular localization or its ability to shuttle (data not shown). The subcellular localization of Gsk3β, therefore, is controlled by Akt in a manner independent of its regulation through S9 (see Discussion).

Gsk3β regulates T58 phosphorylation of c-myc following loss of Akt activity. Next, we set out to formally establish if Gsk3β was required for degradation and phosphorylation of c-myc following the collapse of PI3K/Akt activity. This follows work presented earlier in this report where inhibition of PI3K/Akt signaling was shown to promote the accumulation of active, nuclear Gsk3β and to elevate c-myc phosphorylation on T58 (Fig. 4.1 and 4.2). Regulation of T58 phosphorylation was a focus since we previously showed that collapse of c-myc protein levels, during early differentiation, occurs through a T58-dependent mechanism and that a T58A mutant form of c-myc can maintain self-renewal in the absence of LIF (19). This question was addressed in wild-type and $Gsk3\alpha^{-/-}$ $Gsk3\beta^{-/-}$ (double knockout, DKO) E14 mESCs (28) by evaluating the T58 phosphorylation status of c-myc under conditions of high and low PI3K/Akt signaling. In unperturbed, wild-type E14 mESCs, Gsk3β is inactive in the cytoplasm and c-myc hypo-

phosphorylated on T58 (Fig. 4.7A). Upon treatment with LY294002, Gsk3β localizes to the nucleus, coinciding with elevation of c-myc T58 phosphorylation (Fig 4.7A). When BIO is added in combination with LY294002 however, Gsk3β still accumulates in the nucleus but c-myc T58 phosphorylation remains low (Fig. 4.7A). These data are consistent with earlier results obtained in R1 mESCs linking loss of Akt activity to Gsk3β nuclear localization and c-myc T58 phosphorylation (Fig. 4.1 through Fig. 4.5). When this experiment was repeated in an isogenic DKO E14 mESC line, c-myc was maintained in an unphosphorylated state, even in the presence of LY294002 (Fig. 4.7B). Transient expression of Gsk3β into DKO cells restored cytoplasmic staining and when treated with LY294002, Gsk3β localized to the nucleus (Fig. 4.7C). Increased T58 phosphorylation of c-myc accompanied the nuclear accumulation of Gsk3β in these experiments.

Immunoblot analysis was used to corroborate these observations (Fig. 4.8). As expected, inhibition of PI3K in WT E14 mESCs decreased S9 phosphorylation of Gsk3β but increased phosphorylation of c-myc on T58, the latter of which was blocked by the addition of BIO (Fig. 4.8). In the untreated E14 DKO line, Gsk3β levels were absent and c-myc T58 phosphorylation was low (Fig. 4.8). Restoration of Gsk3β activity following transfection re-established the sensitivity of S9 (Gsk3β) and T58 (c-myc) phosphorylation to LY294002, seen in WT E14 mESCs (Fig 4.8). Elevated c-myc T58 phosphorylation in the presence of LY294002 was once again blocked by BIO (Fig 4.8). In total, these results demonstrate that Gsk3β is responsible for c-myc phosphorylation in mESCs when PI3K/Akt signaling declines. Nuclear localization of Gsk3β and its ability to target Myc is therefore likely to be a critical determinant of differentiation commitment.

Akt controls nuclear export of Gsk3β in mESCs. Our results so far indicate that loss of PI3K/Akt activity is sufficient to promote the nuclear accumulation of active Gsk3β, elevate c-myc phosphorylation on T58 and for accelerated turnover of c-myc protein (also see (19)). Collectively, these events are sufficient to trigger mESC differentiation and their close temporal coordination suggests a mechanism where PI3K/Akt, Gsk3β and c-myc activities are linked by a common pathway. To further establish that Akt activity blocks nuclear accumulation of active Gsk3β, we employed a cell line expressing a constitutively active, myristoylated version of Akt fused to the steroid binding domain of the estrogen receptor (myr.Akt-ER). Addition of 4-hydroxytomoxifen (4OHT) to this cell line then allowed us to investigate the role of Akt in Gsk3β regulation. Previously, Watanabe and colleagues showed that when this cell line was treated with 4OHT, differentiation of mESCs was severely delayed following LIF withdrawal (118). The mechanism underpinning the ability of sustained Akt activity to maintain mESC self-renewal however was not addressed.

To investigate the link between Akt activity, Gsk3β sub-cellular localization and c-myc regulation, the status of Gsk3β and c-myc was evaluated in the absence of LIF, in the presence or absence of 4OHT (Fig. 4.9A). In the absence of 4OHT (myr.Akt-ER off), cells grown in the absence of LIF down-regulated c-myc protein and displayed a corresponding increase in T58 phosphorylation (Fig. 4.9B). Furthermore, Gsk3β accumulated in the nucleus in a S9 hypo-phosphorylated state, T58-phosphorylated c-myc accumulated in nucleolar speckles, and Nanog levels declined (Fig. 4.10 A-D). All of these are signatures of early mESC differentiation as observed previously in R1 mESCs (see Fig. 3.1 through 3.5). In the presence of 4OHT (myr.Akt-ER on) however,

cells failed to down-regulate c-myc, T58 phosphorylation remained low and Gsk3β S9-phosphorylation remained elevated (Fig. 4.9B). At the cellular level, Gsk3β remained in the cytosol in a S9-phosphorylated state, Nanog remained elevated in the nucleus but T58 staining of nucleolar speckles was absent (Fig. 4.9B and Fig. 4.10 A-D). Throughout these experiments eGFP fluorescence was used to confirm that cells were carrying the myr.Akt-ER construct, as previously described (118). These results demonstrate that in the absence of LIF, mESCs fail to differentiate normally when Akt activity is maintained and retain a domed-shaped colony morphology, elevated levels of Nanog, c-myc and low levels of c-myc T58 phosphorylation (Fig. 4.9B and Fig. 4.10A-D). Significantly, sustained Akt activity in the absence of LIF blocked the nuclear accumulation of active Gsk3β. Consequently, these cells maintain a large pool of stable Myc protein in the nucleus to support self-renewal.

One caveat to the interpretation of these results is that Gsk3β remained inactive in the cytoplasm because mESCs failed to differentiate due to maintained Akt activity. This would be consistent with Akt maintaining self-renewal but regulating Gsk3β localization indirectly. To address the question of whether Akt activity or differentiation per se was responsible for Gsk3β localization, a separate approach was taken. In the following experiments mESCs were allowed to differentiate for 3 days following withdrawal of LIF. Then, Akt was reactivated (myr.Akt-ER on) by addition of 4OHT and Gsk3β localization was assayed after a further 24 hours (Fig. 4.11A). As expected, Gsk3β accumulated in the nucleus in an active, S9-hypophosphorylated state following LIF withdrawal, with elevated levels of T58-phosphorylated c-myc (Fig. 4.11B-D). When myr.Akt-ER was reactivated by addition of 4OHT at day 3, Gsk3β re-localized to the

cytoplasm in a S9-phosphorylated, inactive state (Fig. 4.11B, C). Residual phosphorylation of c-myc on T58 was extinguished upon re-establishment of elevated Akt activity and reduced Gsk3β activity (Fig. 4.11D). To establish that cytoplasmic accumulation of Gsk3β under these conditions was due to nuclear export and not due to the accumulation of newly synthesized protein in the cytosol, LB was added to block the nuclear export pathway. This analysis unequivocally showed that LB treatment blocked the accumulation of Gsk3β in the cytoplasm, indicating that re-establishment of Akt activity in differentiating mESCs was sufficient for Gsk3β inactivation and for its nuclear export (Fig. 4.11E). Akt is therefore required for nuclear export of Gsk3β in mESCs and appears to promote self-renewal by regulating Gsk3β at multiple levels.

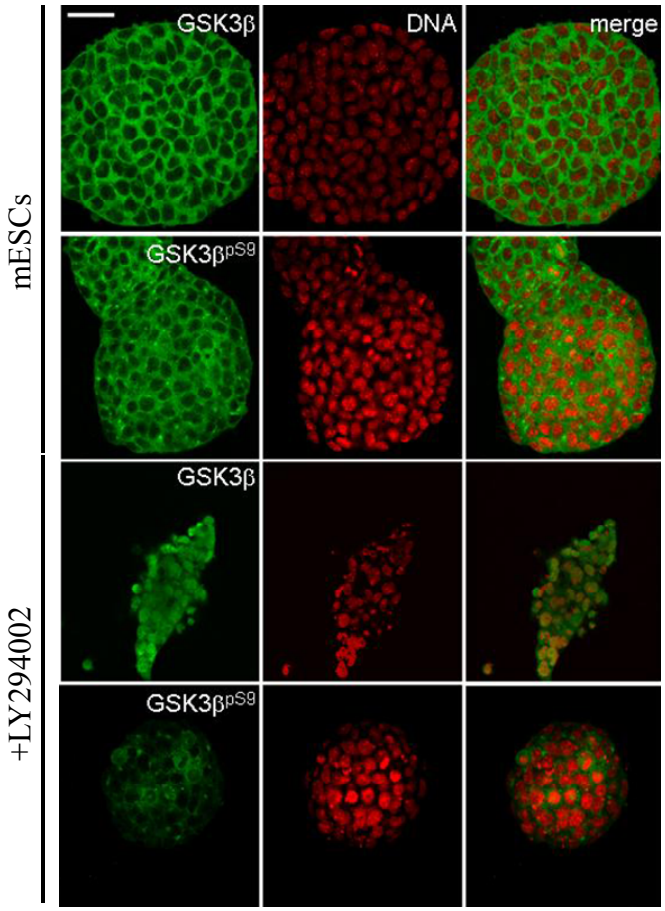

Figure 4.1. PI3K/Akt activity controls the cytoplasmic-nuclear distribution of Gsk3β in mESCs. R1 mESCs (plus LIF) were treated with vector alone or with LY294002 (40 μM, 24 hrs). Cells were then probed as indicated. To-Pro-3 (red) was used to visualize DNA. All staining was visualized by confocal microscopy. Scale bar, 50 μm.

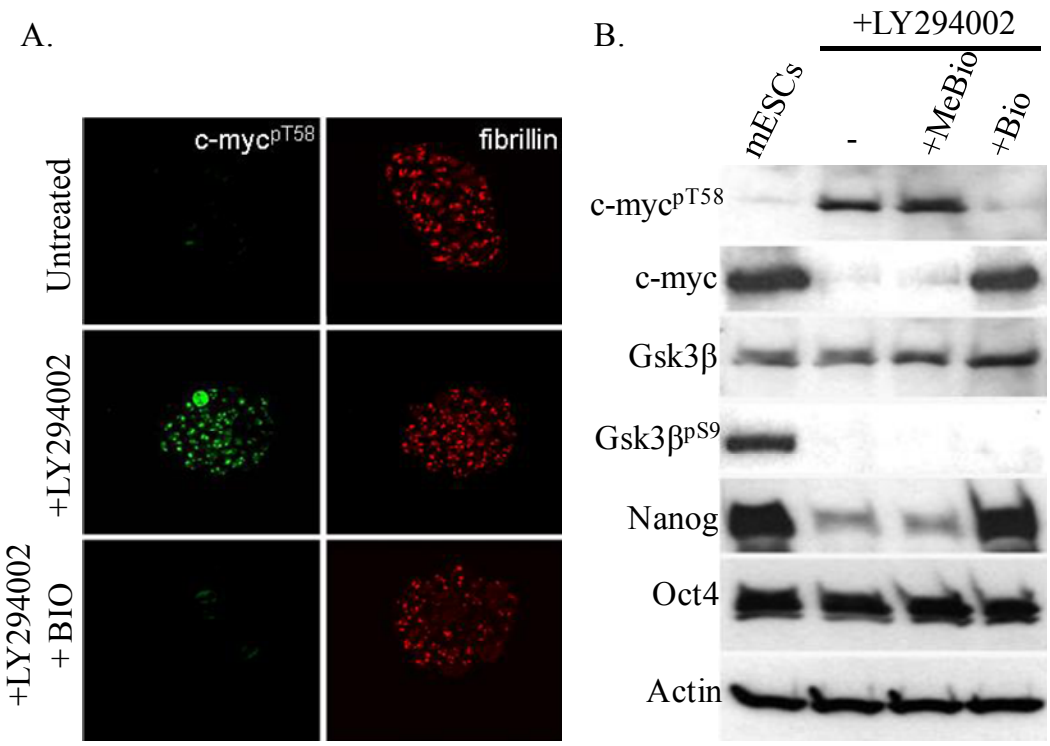

Figure 4.2. PI3K/Akt inactivation increases T58 phosphorylation of c-myc in a Gsk3β dependent manner. (A). mESCs treated for 24 hrs with LY294002 (40 μM) or LY294002 plus BIO (2 μM) and then probed with antibodies for c-myc^{pT58} or the nucleolar marker fibrillarin. **(B).** Immunoblot analysis of untreated mESCs or mESCs treated for 24 hrs with LY294002 (40 μM) and, where indicated, with MeBIO (2 μM) or BIO (2 μM). Whole-cell lysates (20 μg) were probed with antibodies as indicated.

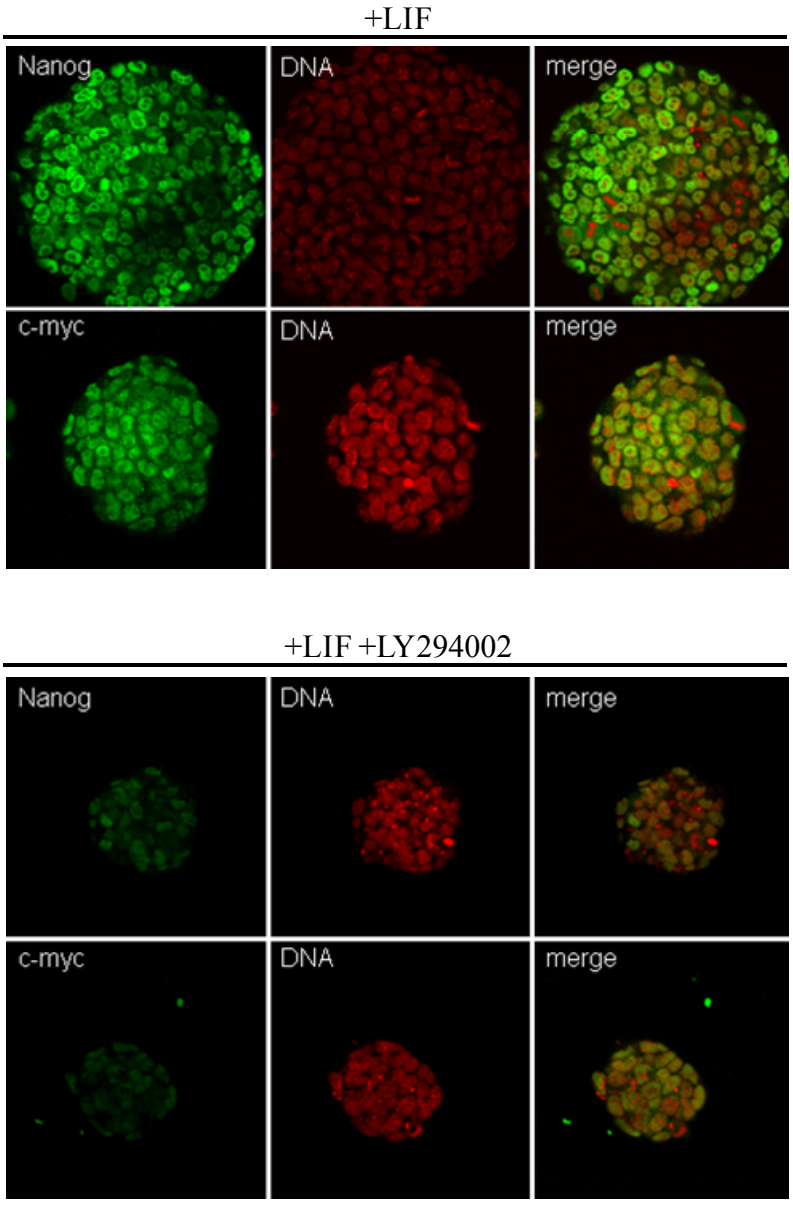

Figure 4.3. Inhibition of PI3K/Akt activity promotes loss of Nanog and c-myc. R1 mESCs were untreated (+LIF) or treated with LY294002 (40 μM) as in Figure 4.2. Cells were then fixed and stained with antibodies for Nanog, or c-myc. DNA was visualized by staining with TO-PRO-3, and images were generated by confocal microscopy.

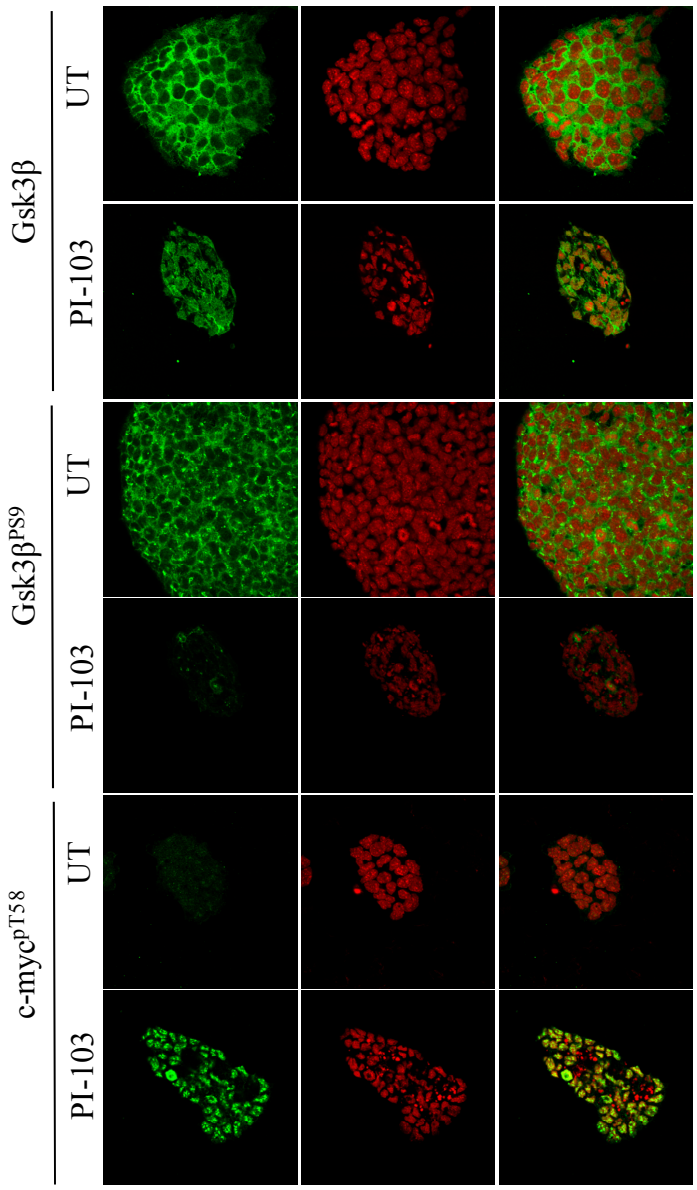

Figure 4.4. Inhibition of PI3K with the small molecule PI-103 causes Gsk3β to accumulate in the nucleus of mESCs. R1 mESCs were left untreated (UT) or treated with PI-103 (10 μM) for 12 hrs., then fixed and immunostained for antibodies as indicated. DNA was visualized with TO-PRO-3. Images were obtained by confocal microscopy.

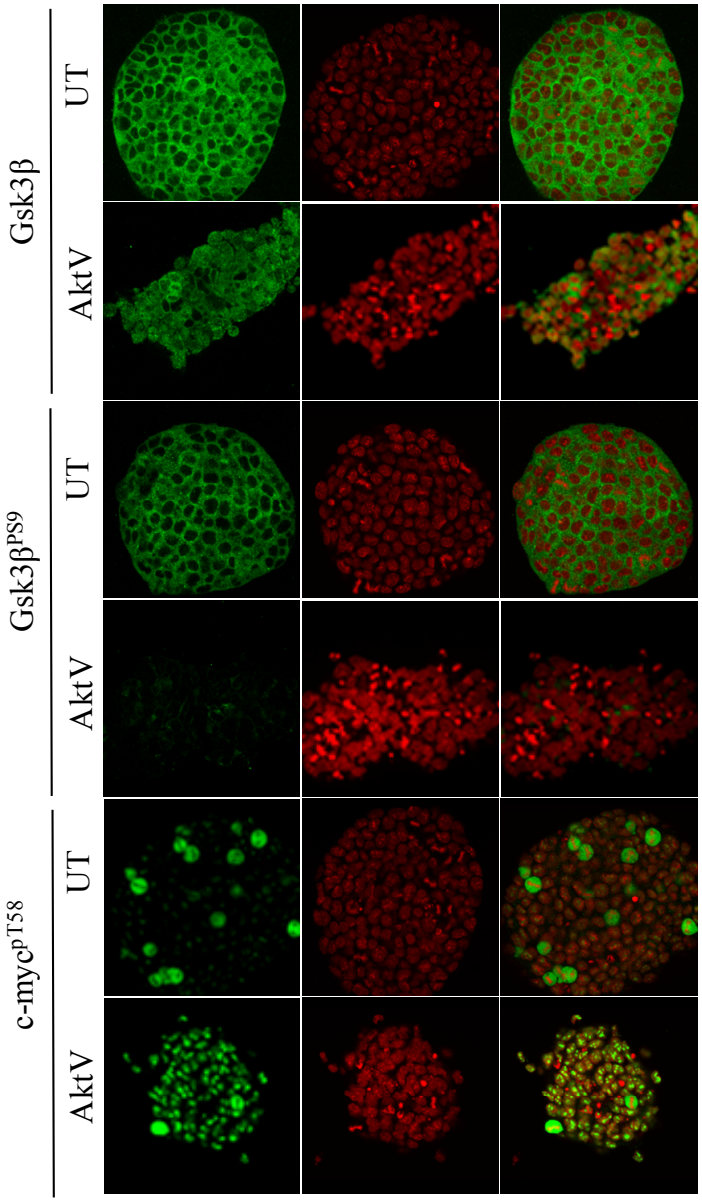

Figure 4.5. Inhibition of Akt with the small molecule AktV causes Gsk3β to accumulate in the nucleus of mESCs. R1 mESCs were left untreated (UT) or treated with AktV (5 μM) for 12 hours, then fixed and immunostained for antibodies as indicated. DNA was visualized with TO-PRO-3. Images were obtained by confocal microscopy.

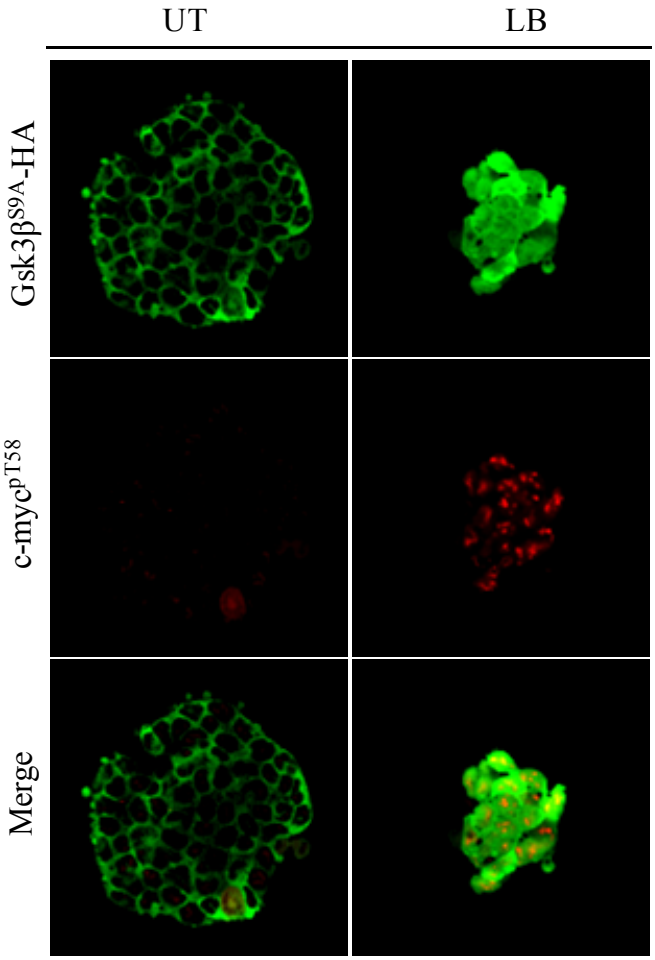

Figure 4.6. Gsk3β shuttling is independent of S9 phosphorylation. An R1 mESCs line stably transfected with pCAG-Gsk3β$^{S9A.HA}$ were either left untreated (UT) or treated with leptomycin B (+LB; 110 nM) for 6 hours. Cells were then fixed and immunostained with antibodies directed against the HA tag (Gsk3β$^{S9A.HA}$) or c-myc^{pT58}.

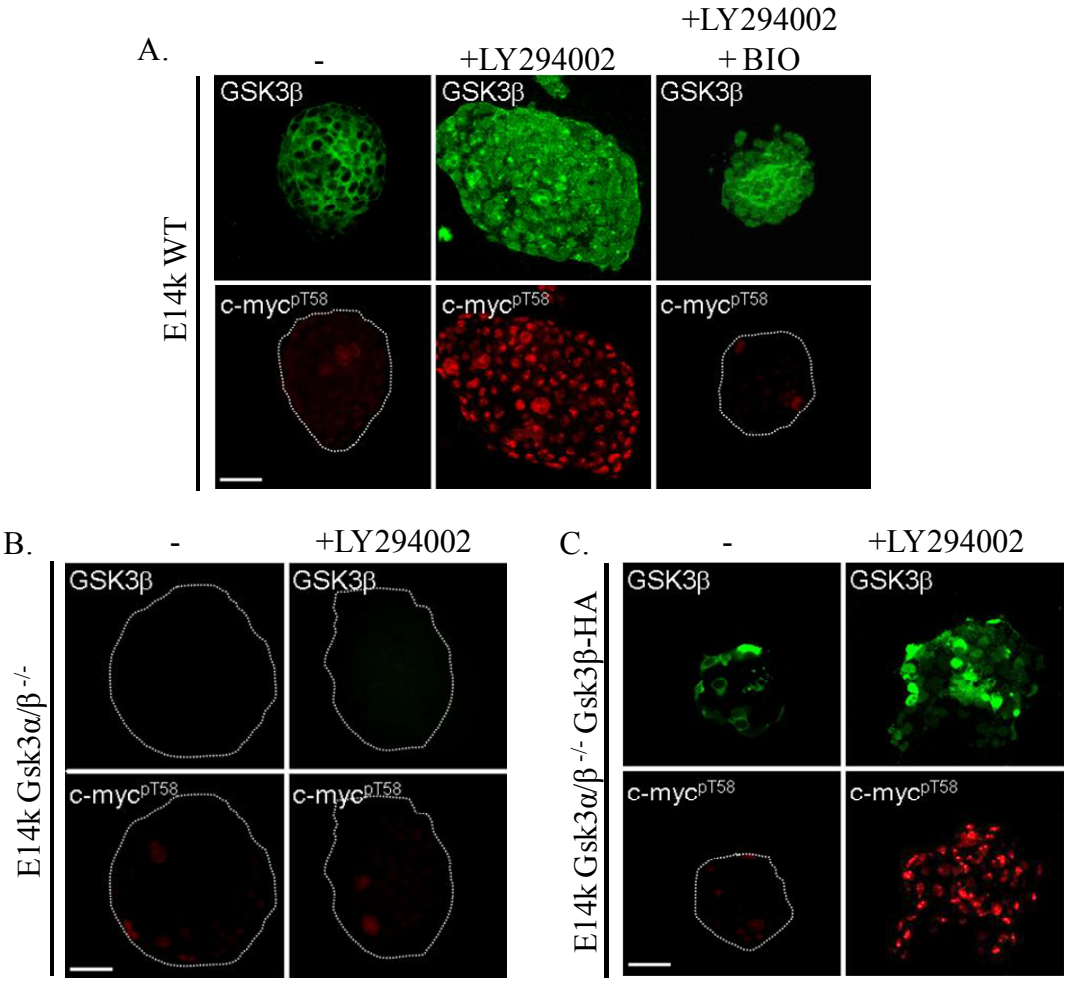

Figure 4.7. Nuclear accumulation of active Gsk3β via PI3K/Akt inhibition, is required for T58 phosphorylation of c-myc. (A). Untreated (UT) E14k mESCs (plus LIF) were treated with LY294002 (40 μM) or LY294002 (40 μM) plus BIO (2 μM) for 24 hrs. then subjected to immunostaining as indicated. Images were captured by confocal microscopy. Scale bar, 50 μm. (B). E14k Gsk3α$^{-/-}$ Gsk3β$^{-/-}$ DKO mESCs were treated as for panel A with LY294002 and were probed with antibodies as indicated. (C). E14k Gsk3α$^{-/-}$ Gsk3β$^{-/-}$ DKO mESCs (as for panel B) were transiently transfected with a Gsk3β-HA expression plasmid then treated with LY294002 (40 μM, 24 hrs; 2 days post-transfection). Three days post-transfection, cells were probed with antibodies for HA and c-myc^{pT58}. Images were generated by confocal microscopy. Scale bar, 50 μm.

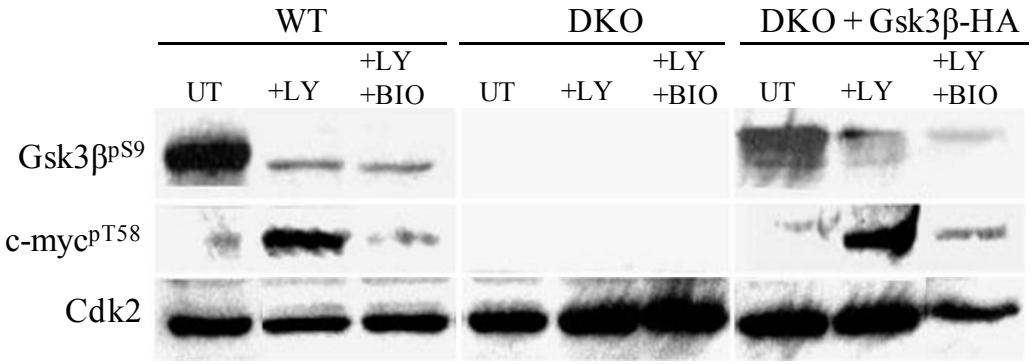

Figure 4.8. Gsk3β is required for phosphorylation of c-myc on T58. WT E14k mESCs, E14k Gsk3α$^{-/-}$ Gsk3β $^{-/-}$ DKO mESCs, and DKO mESCs transfected with a Gsk3β-HA expression plasmid were treated as indicated: untreated (UT), treated with 40 μM LY294002 (LY), or treated with 2 μM BIO (BIO). Inhibitors were added 2 days post-transfection. Cell lysates were analyzed by western blot probing with antibodies as indicated.

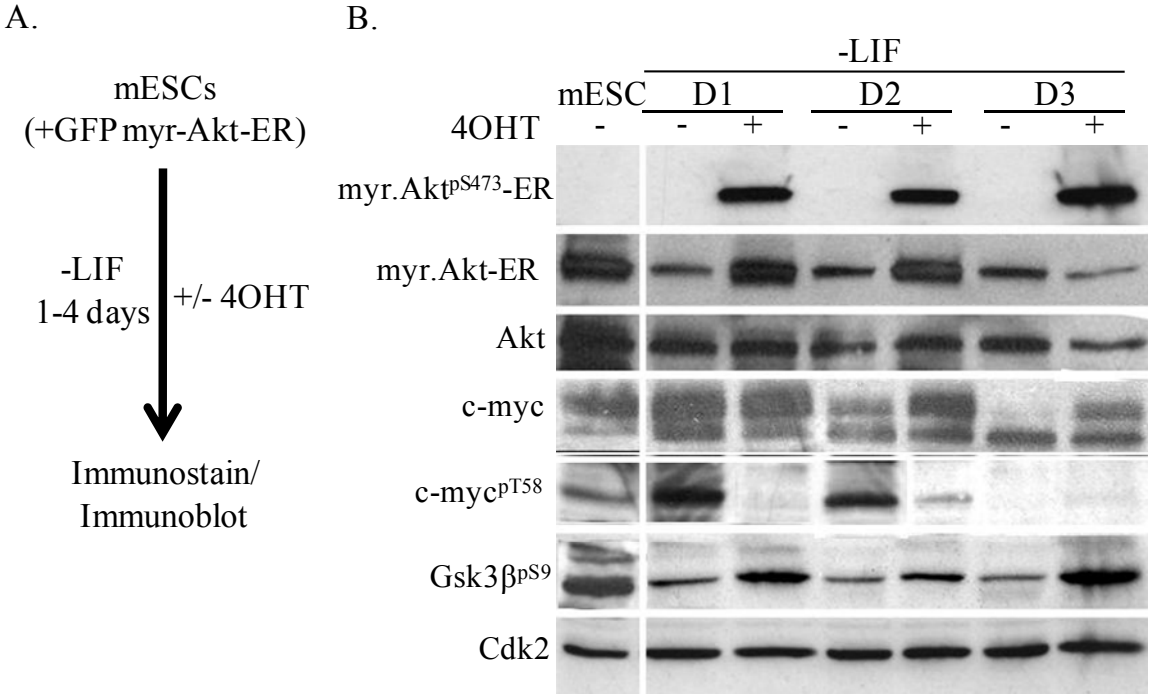

Figure 4.9. Ectopic Akt activation in the absence of LIF blocks Gsk3β activation and c-myc degradation. (A). Experimental scheme involving E14Tg2a mESCs expressing a myristoylated form of Akt fused to the steroid binding domain of the ER (myr.Akt-ER). The construct introduced expresses eGFP from an internal ribosome entry site (IRES) linked to the myr.Akt-ER cassette (28). **(B).** Cell lysates from mESCs (plus LIF) or cells cultured in the absence of LIF with (-) or without (+) 4OHT (1 μM) for 1 to 4 days (see panel A) were analyzed by western blot probing with antibodies as indicated.

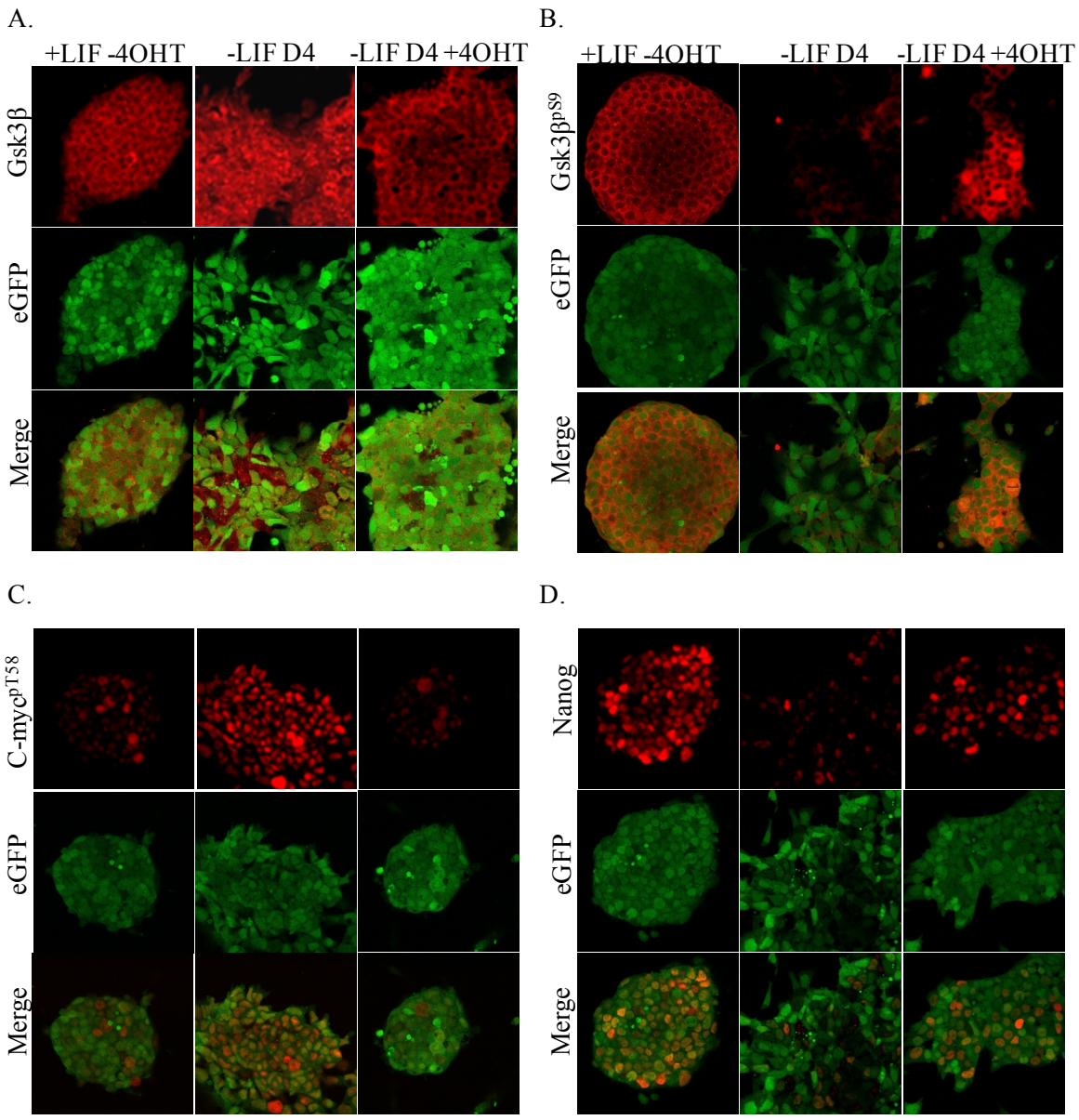

Figure 4.10. Ectopic Akt activation in the absence of LIF blocks nuclear accumulation of Gsk3β and subsequent c-myc T58 phosphorylation (A through D). mESCs from Fig 4.9 were grown with LIF and in the absence of LIF with or without 4OHT (as in Figure 4.9) . Cells were then probed with antibodies as indicated. Expression of myr.Akt-ER was established by eGFP fluorescence from a linked IRES.

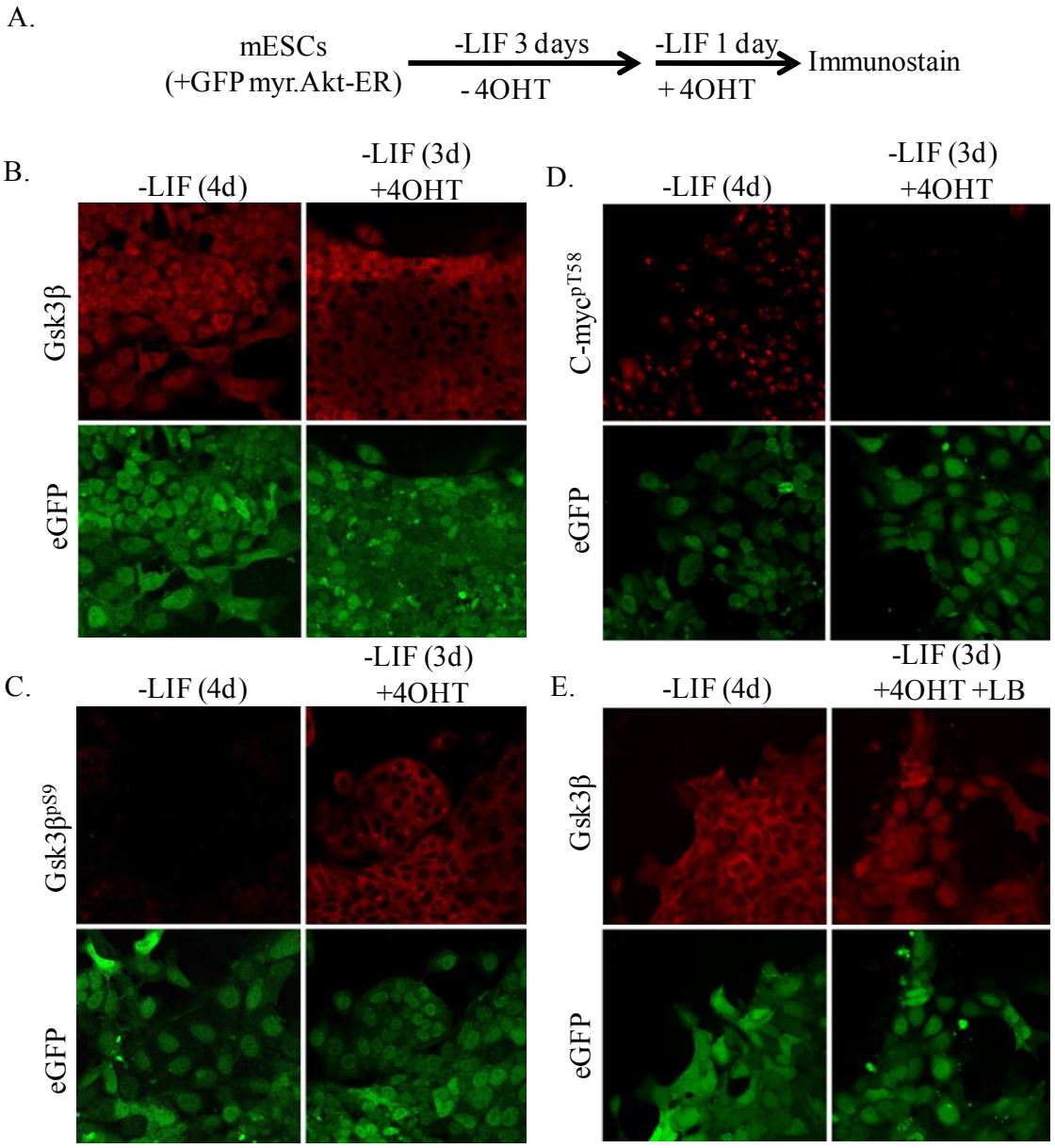

Figure 4.11. Nuclear Gsk3β can be redirected from the nucleus to the cytoplasm of differentiating mESCs by reactivation of Akt. (A). Experimental scheme for panels B through E, where myr.Akt-ER was activated in E14Tg2a mESCs by the addition of 4OHT (1 μM) for 24 hrs following 3 days of differentiation (-LIF) and re-localization of Gsk3β to the nucleus. **(B through D).** mESCs from Fig 4.9 were grown in the absence of LIF for 4 days (4d) with or without 4OHT and then probed as indicated. eGFP fluorescence (GFP) marks the positions of myr.Akt-ER-expressing cells. (E) mESCs expressing myr.Akt-ER were analyzed as for panel B except that LB was added 6 hrs. before fixation.

Discussion

Akt regulates the nuclear export of Gsk3β in mESCs. Regulation of Gsk3β activity has been demonstrated as a key factor in the maintenance of mESC self-renewal (9). Our results demonstrate that in addition to determining it activation status, Akt is the principal determinant of Gsk3β localization in mESCs as well. Under self-renewing conditions, when PI3K/Akt signaling is active, Gsk3β accumulates in the cytoplasm due to the Akt-dependent activation of its nuclear export. This finding is supported by several lines of evidence. First, inhibition of PI3K and Akt reproduces the nuclear accumulation of Gsk3β seen following the treatment of mESCs with LB. Second, under conditions where Gsk3β accumulates in the nucleus during differentiation, re-activation of Akt results in the re-localization of Gsk3β back to the cytoplasm. More importantly this Akt-dependent re-localization of Gsk3β restores its nuclear-cytoplasmic shuttling capabilities. In addition, we provide direct evidence that PI3K/Akt signaling mediates the phosphorylation-mediated degradation of c-myc, and thus its stability, through the regulation of Gsk3β activity and localization. Altogether these observations demonstrate that Akt has a vital role in regulating mESC self-renewal by preventing c-myc degradation through inactivation and nuclear exclusion of Gsk3β.

Akt regulates the nuclear export of Gsk3β independent of S9 phosphorylation. One obvious explanation is that the Akt-dependent phosphorylation of Gsk3β on S9 is also involved in the nuclear export of Gsk3β. However, mutation of the S9 residue to an alanine, preventing its Akt-mediated phosphorylation, had no effect on the localization of Gsk3β. Moreover, the S9A form of Gsk3β was still sensitive to LB, indicating it could still shuttle. The nuclear cytoplasmic shuttling of Gsk3β was also unaffected by the

Gsk3β specific inhibitor BIO. These observations prompted us to conclude that the nuclear export of Gsk3β in mESCs is not dependent upon its activation status or its S9 phosphorylation. These observations suggest that Akt regulates, either directly or indirectly, the efficient nuclear export of Gsk3β through an as yet to be identified Akt-dependent post-translational modification. Identification of this post-translation modification and its target will be the subject of further research, and should provide valuable knowledge in regards to this additional level of Gsk3β regulation.

Future directions. Previous work demonstrated that PI3K/Akt signaling is vital in the maintenance of murine, monkey, and more recently rabbit ESCs (87, 117, 118), but the mechanism for this has not been defined in any detail. Our work indicates that in ESCs, Akt signaling promotes self-renewal through the regulation of Gsk3β by at least two non-redundant mechanisms. First, Akt blocks the catalytic activation of Gsk3β through its phosphorylation of S9 in the N-terminus of Gsk3β. Second, Akt signaling is responsible for promoting the efficient nuclear export of Gsk3β, preventing it from accessing nuclear substrates like c-myc. In addition to Gsk3β, Akt promotes the efficient nuclear export of several other proteins through a variety of mechanisms, including the forkhead family of transcription factors (114), AHNAK (105), CDC25B (5), and LANA2 (72). The underlying mechanism by which Akt regulates the efficient nuclear export of Gsk3β in mESCs, however, is unknown. Since Gsk3β has no definable nuclear export signal it's likely that chaperone proteins are involved and are themselves subject to regulation by PI3K/Akt signaling. Two candidate proteins known to form complexes with Gsk3β that have been shown to shuttle in and out of the nucleus are Axin and Frat (22, 38, 120). The identity of the chaperone protein responsible for the nuclear export of Gsk3β and the

underlying mechanism connecting it to PI3K/Akt signaling will be the subject of further research. The involvement of PI3K/Akt/Gsk3 signaling in a wide range of biological processes suggests that these findings will have major implications for development, cell cycle control, apoptosis, replicative senescence, tissue homeostasis, and cancer.

CHAPTER 5

PI3K/AKT SIGNALING REGULATES GSK3β NUCLEAR EXPORT IN MOUSE ESCS VIA FRAT BINDING[3]

[3] Bechard, M., and Dalton, S. To be submitted to *Molecular and Cellular Biology*.

Background

In self-renewing mESCs, Gsk3β is inactivated and actively exported from the nucleus in an Akt-dependent manner (9). Following LIF withdrawal however Akt activity declines resulting in the activating hypo-phosphorylation of Gsk3β and its nuclear accumulation (9). Once in the nucleus, active Gsk3β promotes the phosphorylation mediated degradation of c-myc which in turn promotes mESC differentiation (9). The Akt-dependent export of Gsk3β out of the nucleus is therefore a key to the regulation of mESC self-renewal. Prior to this report however, there were major questions in regards to the nuclear export of Gsk3β and its connection to PI3K/Akt signaling.

A bipartite nuclear localization sequence (NLS) has been identified that is both necessary and sufficient to drive the nuclear localization of Gsk3β (69). In mESC as well as other cell types the nuclear export of Gsk3β is shown to be sensitive to LB, an inhibitor of Crm1-mediated nuclear export. This indicates that the nuclear export of Gsk3β is mediated by Crm1 through a leucine-rich nuclear export sequence (NES). To date however, there is no evidence for Gsk3β having a definable leucine-rich NES. We therefore hypothesize that the nuclear export of Gsk3β in mESCs is mediated through a binding partner. If so, identification of that binding partner will have important significance to understanding the regulation of Gsk3β in the regulation of mESC self-renewal. Two prime candidates with a Crm1-dependent NES that have been characterized as undergoing active nuclear-cytoplasmic shuttling are Axin and Frat (22, 38, 120). Moreover, the Axin and Frat binding sites on Gsk3β have been extensively characterized as well (38). As integral parts of the Wnt pathway Axin and Frat regulate

the stability of β-catenin through their differential binding to Gsk3β (122). Since a role for the WNT pathway in the maintenance of self-renewal has been described, it's likely that Gsk3β actively binds to Frat and Axin in mESCs. More importantly, Frat has been linked to the nuclear export of Gsk3β in other biological contexts (38). Together, these observations support the hypothesis that the nuclear export of Gsk3β in mESCs is mediated through a binding partner, possibly Axin or Frat.

Our observations indicate the efficient transport of Gsk3β out of the nucleus is dependent upon PI3K/Akt signaling (9). However, the underlying mechanism linking PI3K/Akt signaling to the nuclear export of Gsk3β remains unclear. Akt does however regulate the efficient nuclear export of several other proteins in addition to Gsk3β. Most notably, the Akt-dependent phosphorylation of FOXO1 promotes efficient nuclear export of these proteins by facilitating the binding of 14-3-3 (17). In the case of AHNAK, a neuroblast-associated differentiation protein, Akt promotes the nuclear export through an activating phosphorylation site within the NES (105). Interestingly, inhibition of PI3K/Akt signaling in both of these cases prevents the shuttling of these proteins, prompting their nuclear accumulation instead (17, 105). In light of this and the likely involvement of a Gsk3β binding partner, we postulate two mechanisms by which PI3K/Akt signaling could regulate the nuclear export of Gsk3β. First, PI3K/Akt signaling may regulate the nuclear export of the Gsk3β binding partner itself. Second, PI3K/Akt signaling may influence the complex formation of Gsk3β to its partner protein. Since the nuclear export of Gsk3β is required for promoting self-renewal, we sought to identify the potential binding partner and determine the mechanism of PI3K/Akt signaling in its regulation.

Results

Disruption of Frat binding causes the nuclear accumulation of Gsk3ß. To investigate if the nuclear export of Gsk3β in mESCs is dependent upon Frat or Axin we sought to disrupt their binding through the sited-directed mutagenesis of Gsk3β. Several reports have identified multiple residues in Gsk3β that when mutated disrupt Axin and/or Frat binding (Fig 5.1A) (38). Four mutations were of particular interest as they were characterized to disrupt Axin and Frat binding equally in the case of K85M and Q206E or differentially in the case of V267E/G268R (VEGR) and R180E (Fig 5.1A) (38, 40). We therefore generated these four mutant forms of Gsk3β by site-directed mutagenesis of a wild-type Gsk3β fused to a double HA tag (Fig. 5.1B). Although mRNA for Frat1 and Frat2 in mECS was readily detected by RT-PCR (data not shown), there are no antibodies commercially available that can reliably detect endogenous Frat protein levels (58). Therefore, we stably expressed wild-type Gsk3β^{2xHA} and the four Gsk3β^{2xHA} mutants in a mESC line expressing murine Frat1 with a double N-terminal Flag-tag (Flag-Frat) (A gift from Dr. Trevor Dale). Co-immunoprecipitations were used to determine if the Gsk3β mutations disrupted Frat or Axin binding. Using anti-HA antibodies and anti- Flag respectively, we first confirmed that Axin and Frat were able to bind wild-type HA-tagged Gsk3β by immunoprecipitation (Table 1, Fig. 5.2). Although we successfully pulled-down Gsk3β through the immunoprecipitation of Flag-tagged Frat, we were unable to pull-down Axin (data not shown, Fig. 5.2). This observation suggests that Axin and Frat do not bind Gsk3β at the same time (data not shown, Fig. 5.2). This is consistent with several reports that binding of Axin and Frat to Gsk3β is mutually exclusive and even competitive in nature (38, 40, 110). Upon examination of the Gsk3β

mutants it was discovered that three of these mutations (K85M, R180E, and VEGR) abolished both Axin and Frat binding (Table 1, Fig. 5.2). The other Gsk3β mutation (Q206E) however, abolished Frat binding while only slightly reducing Axin binding (Table 1, Fig. 5.2). Since the binding of Frat and Axin to Gsk3β has been described as competitive, an increase in Axin binding would have been expected instead of a slight reduction. Therefore, while the Gsk3β^{Q206E} mutation clearly blocks Frat binding, is also has an effect on Axin binding.

We next evaluated the localization of wild-type Gsk3β and the four Gsk3β mutants using immunofluorescence. As expected, the localization of the HA tagged wild-type Gsk3β, like the endogenous form, was almost exclusively cytoplasmic (Fig. 5.3). In contrast, Gsk3β^{K85M}, Gsk3β^{R180E}, and Gsk3β^{VEGR} all accumulated in the nucleus of mESCs (Table 1, Fig. 5.3). Although this strongly indicates an inactivation of Gsk3β nuclear export, we were unable to distinguish whether it was due to a disruption of Axin or Frat binding as they were both disrupted (Table 1, Fig. 5.2). Interestingly the remaining Gsk3β^{Q206E} mutant that preferentially disrupted Frat binding accumulated in the nucleus despite the binding of Axin, suggesting that Frat has a role in mediating the nuclear export of Gsk3β (Table 1, Fig 5.2-3). Although these results implicate Frat as the likely candidate for mediating the nuclear export of Gsk3β, a role for Axin cannot be discounted since this mutation did appear to have a slight effect on Axin binding.

Enforced expression of active Gsk3β in the nucleus of mESCs was recently shown to be sufficient to disrupt self-renewal (9). We therefore postulated that combining the constitutively nuclear localized Frat binding mutant (Gsk3β^{Q206E}) with its constitutive activation (S9A mutation) would have a negative impact on mESC self-

renewal. To test this, R1 mESCs were transfected with an empty vector, or the same vector carrying Gsk3β^{K85M}, Gsk3β^{Q206E}, or Gsk3β$^{S9A.Q206E}$ and then selected with puromycin for 4 days, as previously done. The self-renewing status of mESCs was then evaluated by alkaline phosphatase staining. As expected transfection of vector alone or Gsk3β^{K85M}, which in addition to constitutively localizing to the nucleus was also kinase dead (47, 52), resulted in >80% of the colonies staining positive for alkaline phosphatase (Fig 5.4A, B). Similar results were also obtained following the transfection of Gsk3β^{Q206E}, suggesting that it is inactive as well (Fig. 5.4A, B). Following the transfection of vector carrying Gsk3β$^{S9A.Q206E}$ however only ~20% of the colonies stained positive for alkaline phosphatase, indicating a significant disruption of mESC self-renewal (Fig. 5.4A, B). Taken together, this data demonstrates that disruption of Frat binding combined with the activation of Gsk3β is sufficient to disrupt mESC self-renewal. In addition, this result corroborates our previous observation that enforced expression of active Gsk3β in the nucleus negatively impacts self-renewal (9).

Frat mediates the localization of Gsk3β during self-renewal. Our results so far suggest that Frat binding is involved in the nuclear export of Gsk3β in mESCs. Therefore, we hypothesized that if the export of Gsk3β from the nucleus is directly dependent upon Frat, then inactivating the nuclear export of Frat should disrupt the nuclear export of Gsk3β. A previous report by Franca-Koh et al. (2002) demonstrated the mutation of two conserved leucine residues located in the NES of Frat was sufficient to inactivate its nuclear export (38). To test our hypothesis we constructed the same nuclear export deficient form of Frat (Flag-Frat^{NESala}), and transfected both Flag-Frat and Flag-Frat^{NESala} into R1 mESCs separately (Fig. 5.5A). Using immunofluorescence we characterized the

localization of endogenous Gsk3β in cells expressing these two forms of Frat. As expected, the localization of endogenous Gsk3β remained cytoplasmic in approximately 98% of cells expressing wild-type Flag-Frat, which also localized to the cytoplasm (Fig. 5.5B and 5.7). However, the localization of endogenous Gsk3β was nuclear in approximately 99% cells expressing the constitutively nuclear localized Flag-Frat1^{NESala} (Fig. 5.5B and 5.7). These observations demonstrate that the efficient export of Gsk3β out of the nucleus in mESCs is dependent upon the nuclear export of Frat.

To further investigate the relationship between Frat and Gsk3β, we sought to determine if anchoring Frat in the cytoplasm effects the nuclear/cytoplasmic shuttling of Gsk3β. To anchor Frat in the cytoplasm a myristoylation sequence was added to the N-terminus of a C-terminal Flag-tagged mFrat1 (myr-mFrat1^{2xFlag}). To evaluate the effect of myr-mFrat1^{2xFlag} on the shuttling of Gsk3β, LB was added to R1 mESCs 48 hours after its transfection. In the absence of LB both myr-mFrat1^{2xFlag} and endogenous Gsk3β were, as expected, localized to the cytoplasm (Fig. 5.6). In the presence of LB, however, the nuclear accumulation of Gsk3β was blocked in over 90% of the cells expressing myr-mFrat1^{2xFlag} (Fig. 5.6 and 5.7). This is in direct contrast to the nuclear accumulation of Gsk3β in untransfected cells as a result of LB treatment (Fig. 5.6). These observations demonstrate that anchoring Frat in the cytoplasm is sufficient to disrupt the nuclear-cytoplasmic shuttling of Gsk3β. Altogether these data indicate that Frat has a key role in regulating the localization of Gsk3β during self-renewal.

PI3K/Akt signaling regulates the binding of Gsk3β to Frat during self-renewal. Although our results clearly demonstrate a role for Frat in mediating the nuclear export of Gsk3β in mESCs, the mechanism by which PI3K/Akt signaling regulates its export is

unclear. Given the involvement of Frat we postulated that PI3K/Akt signaling could control the nuclear export of Gsk3β either by regulating the nuclear export capabilities of Frat or by modulating the binding of Frat to Gsk3β. Determining the effect that inhibition of PI3K/Akt signaling has on the localization of Frat would help distinguish between these mechanisms. The accumulation of Frat in the nucleus in response to low PI3K/Akt activity, as seen with Gsk3β, would indicate a negative impact on the nuclear export of Frat. This would suggest that PI3K/Akt signaling controls Gsk3β localization by regulating the nuclear export of Frat. However, if inhibition of PI3K/Akt signaling has no effect on the nuclear export of Frat, it is likely the nuclear export of Gsk3β is regulated through its binding to Frat. Frat has been previously described as actively shuttling in and out of the nucleus (38). To recapitulate this in our hands we treated R1 mESCs expressing Flag-mFrat1 with LB. As previously demonstrated with Gsk3β, LB treatment of mESCs resulted in the nuclear accumulation of Frat (Fig 3.1 and Fig. 5.8). To test if inhibition of PI3K/Akt signaling has an effect on the nuclear export of Frat, we treated mESCs expressing Flag-mFrat1 with PI-103. Unlike Gsk3β, the localization of Frat remained cytoplasmic following the treatment of mESCs with PI-103 (Fig. 4.4 and Fig. 5.8) (9). Therefore, under conditions in which PI3K/Akt activity is low, Gsk3β and Frat do not localize to the same compartment suggesting a role for PI3K/Akt signaling in modulating their binding to one another.

To elucidate whether inhibition of PI3K/Akt signaling affects the nuclear-cytoplasmic shuttling of Frat, LB was added to the culture following the addition of PI-103. This resulted in the nuclear accumulation of Frat and hence demonstrates that inhibition of PI3K/Akt signaling has no effect on the shuttling of Frat to and from the

nucleus (Fig 5.8). Therefore we predict that inhibition of PI3K/Akt signaling disrupts the nuclear export of Gsk3β by disrupting its binding to Frat. To test this prediction, we evaluated the binding of Frat to Gsk3β in the presence and absence of PI-103, through the immunoprecipitation of Flag-tagged mFrat1. In the absence of PI-103, Frat was able to pull-down endogenous Gsk3β (Fig. 5.9). However, in the presence of PI-103 the binding of Frat to Gsk3β was reduced, indicating PI3K/Akt signaling plays a role in modulating the binding of Frat to Gsk3β (Fig 5.9). These observations further support a role for Frat in mediating the nuclear export of Gsk3β in mESCs and indicate that the PI3K/Akt pathway regulates the nuclear export of Gsk3β by modulating its binding to Frat.

A.

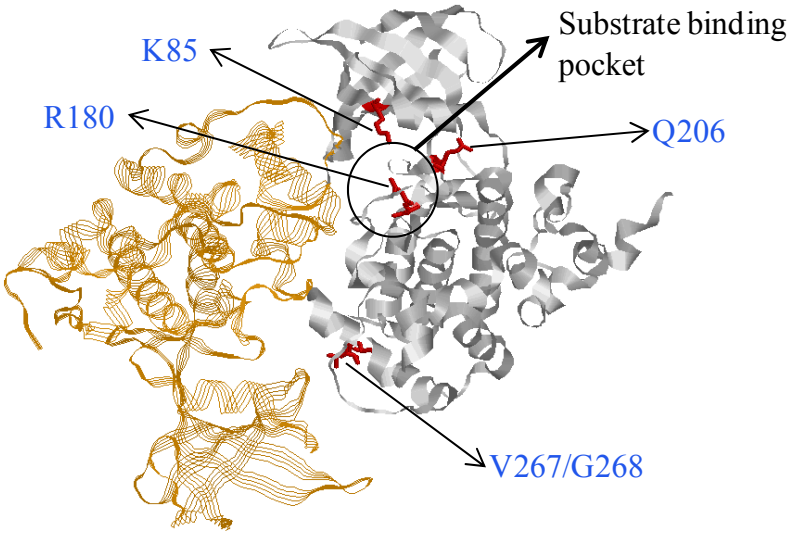

B.

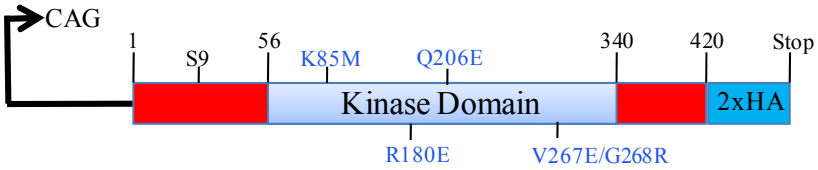

Figure 5.1. Diagram of residues important for the binding of Axin and Frat to Gsk3β. (A). Tertiary structure of a Gsk3β dimer depicting mutations used in this study (labeled arrows) to disrupt axin and/or frat binding. The molecular rendering of a dimer of Gsk3β was generated using the Rasmol software based on the protein data bank file 1H8F. **(B).** Schematic of HA tagged Gsk3β with mutations used to disrupt Axin and/or Frat binding. Mutations were made separately and each individual mutant form of HA tagged Gsk3β expressed under the control of the CAG1 promoter.

Table 1. Characterization of Gsk3β mutations designed to disrupt Axin and/or Frat binding.

Mutation	Axin Binding	Frat Binding	Gsk3β localization
Wild-type	Yes	Yes	C>N
K85M[a]	No	No	N>C
R180E	No	No	N>C
Q206E	Yes	No	N>C
V267E/G268R	No	No	N>C

[a] **Previously characterized as a kinase dead form of Gsk3β**

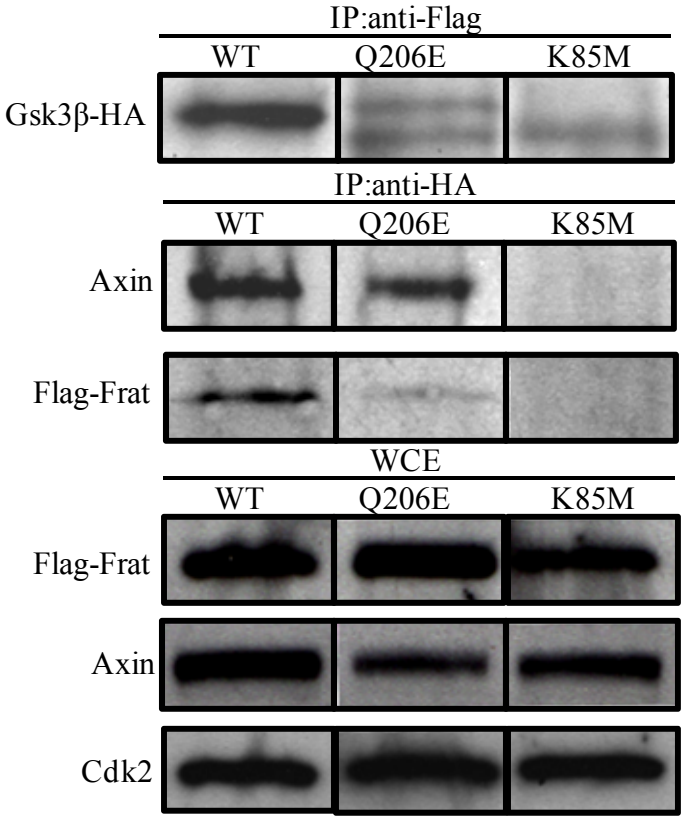

Figure 5.2. Disruption of Axin and Frat binding through Gsk3β mutations. (Upper panel) Cell lysate from mESCs stably expressing Gsk3β-HA^{Q206E}, Gsk3β-HA^{K85M}, or Wild-type (WT) Gsk3β-HA with Flag-Frat were subjected to immunoprecipitation using an anti-HA or anti-Flag antibody. Immunoprecipitates were analyzed by western blot probing for antibodies as indicated. (Lower panel) 20 μg of the whole cell extract (WCE) used in the immunoprecipitation reactions were subjected to western blot analysis probing with antibodies as indicated.

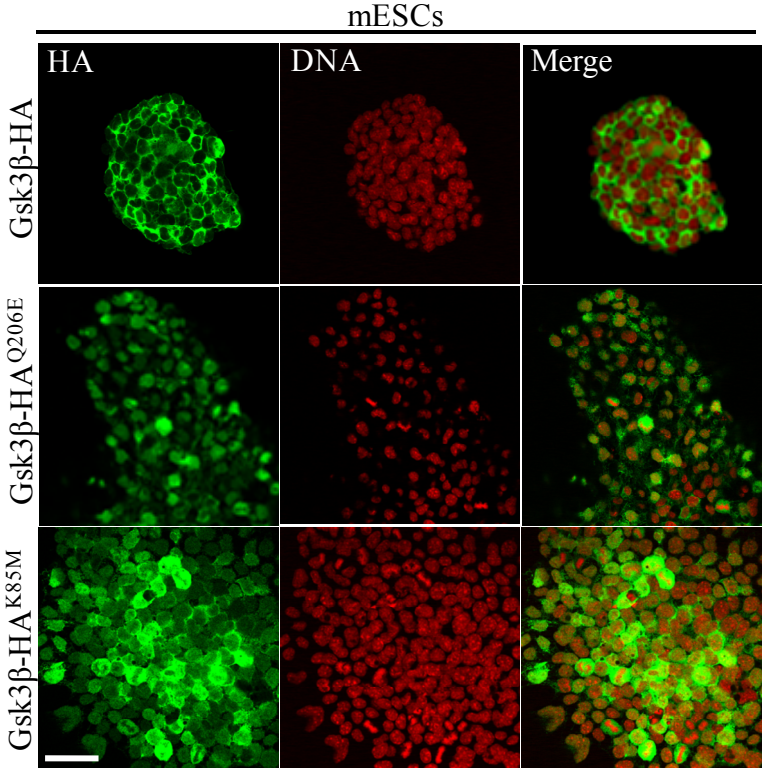

Figure 5.3. Disruption of Frat binding causes nuclear accumulation of Gsk3β. The stable mESC lines from Fig. 5.1 were subjected to immunostaining as indicated. DNA was visualized with TO-PRO-3. Images were obtained by confocal imaging. Scale bar, 50 μm.

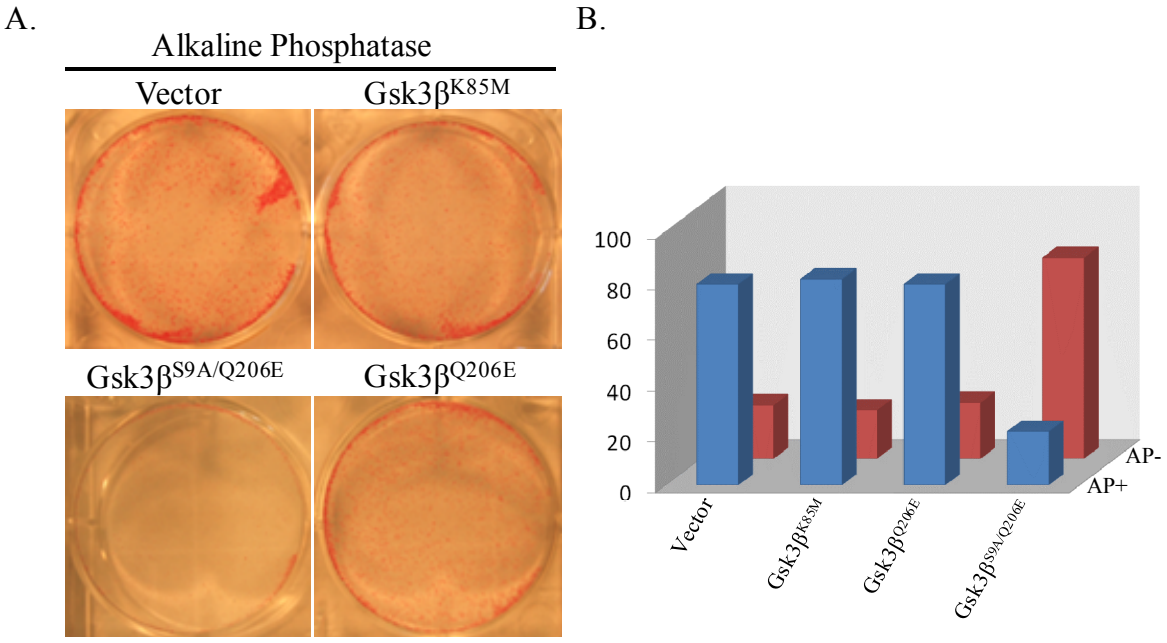

Figure 5.4. Enforced expression of an active form of Gsk3β incapable of binding Frat disrupts mESC self-renewal. (A). R1 mESCs were transiently transfected with vector alone (pCAGipuro) or the equivalent vector expressing Gsk3β^{K85M}, Gsk3β^{Q206E}, or Gsk3β$^{S9A.Q206E}$. 24 hours post-transfection, cells were selected with puromycin for 4 days, self-renewal capacity was then analyzed by alkaline phosphatase staining. **(B).** Graphical representation of the percentages of colonies positive (+) and negative (-) for Alkaline phosphatase (AP) staining.

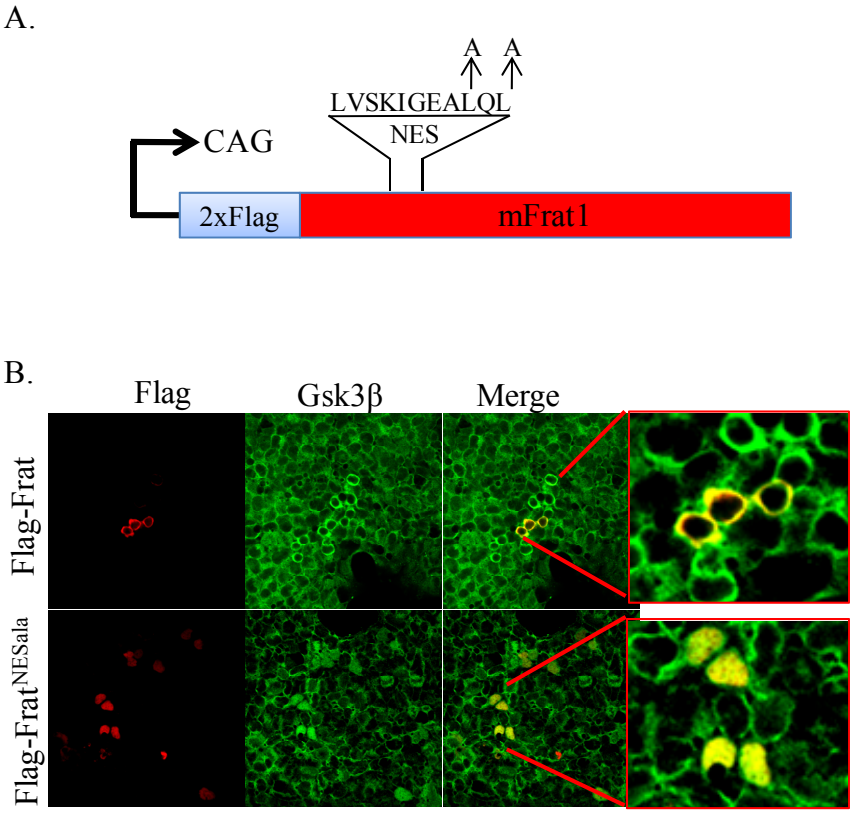

Figure 5.5. Disrupting the nuclear export of Frat causes the nuclear accumulaton endogenous Gsk3β in mESCs (A). Diagram of pCAGineo expression vector carrying Flag tagged murine Frat1 with the mutations used to disrupt the nuclear export sequence (NES). **(B).** R1 mESCs were transiently transfected either pCAGineo carrying wild-type Flag-Frat or Flag-Frat with its NES mutated (Flag-Frat^{NESala}), after 48 hours cells were immunostained with anti-Flag and anti-Gsk3β antibodies. Images were obtained by confocal imaging. Scale bar, 50 μm.

A.

B.

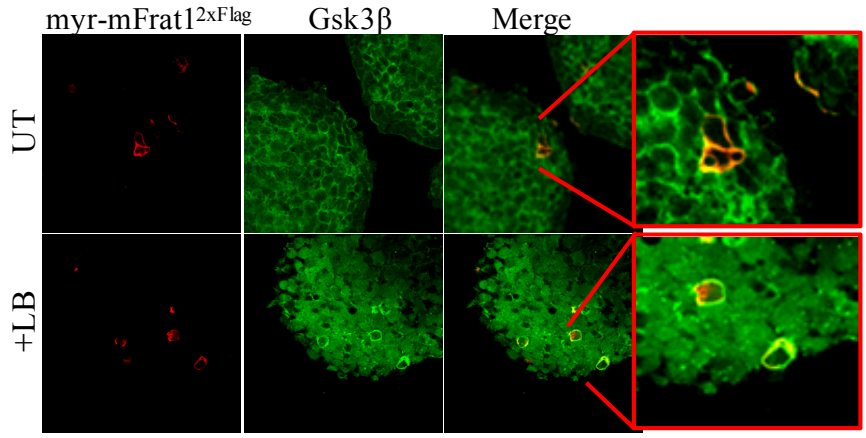

Figure 5.6. The cytoplasmic anchoring of Frat disrupts the nuclear-cytoplasmic shuttling of Gsk3β in mESCs (A). Diagram of pCAGipuro expression vector carrying the myristoylated Flag-tagged murine Frat1 (myr-mFrat1^{2xFlag}). **(B).** R1 mESCs were either left untreated or treated with LB (110 nM, 6hrs) 48 hrs after transiently transfecting with pCAGipuro carrying myr-mFrat1^{2xFlag}. Cells were then were then immunostained with anti-Flag and anti-Gsk3β antibodies. Images were obtained by confocal imaging. Scale bar, 50 µm.

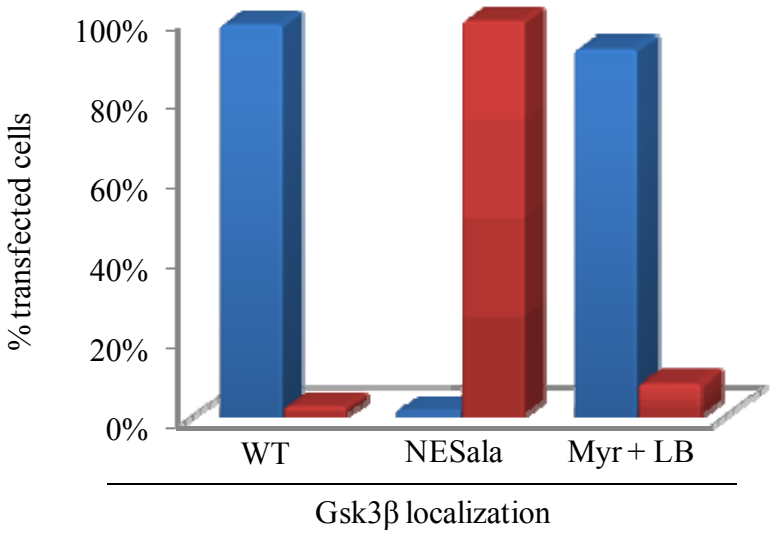

Figure 5.7. Diagram depicting correlation between the localization of Gsk3β and Frat. Graphical representation of the percentage of Gsk3β localized to the cytoplasm (■) or nucleus (■) of cells expressing either wild-type Frat (WT), $Frat^{NESala}$ (NESala), or myr-Frat (Myr). Cells transiently transfected with myr-$Frat^{2xflag}$ were additionally treated with LB (110 nM, 6 hrs) prior to their immunostaining. A minimum of 100 cells were counted for each condition.

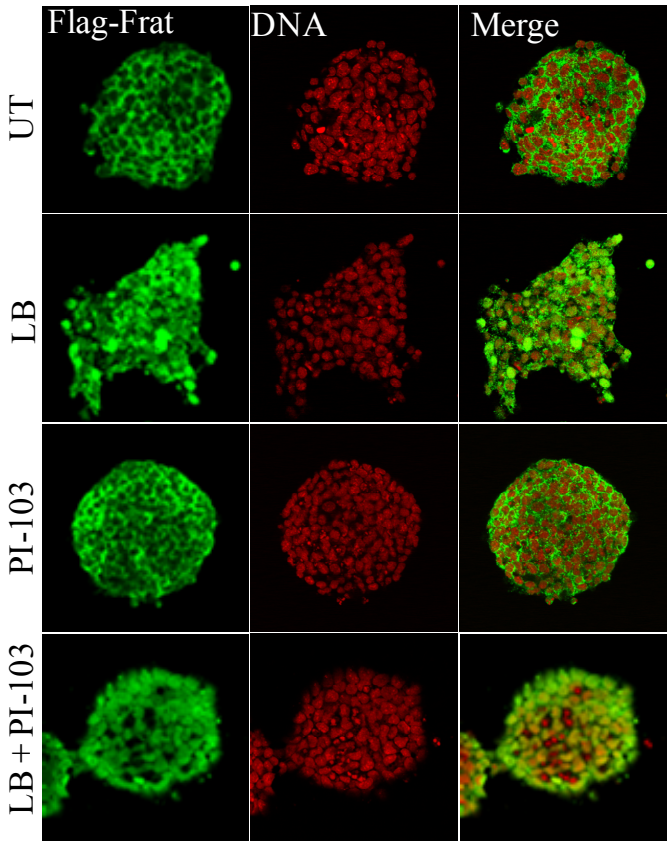

Figure 5.8. Inhibition of PI3K/Akt signaling has no effect on the nuclear/cytoplasmic shuttling of Frat. R1 mESCs stably expressing Flag-tagged Frat were untreated (UT) or treated with LB (110 nM for 6 hrs.), PI-103 (10 μm for 12 hrs.) or a combination of the two. Cells were then fixed and immunostained as indicated. DNA was visualized with To-Pro-3. Images were obtained by confocal imaging. Scale bar, 50 μm.

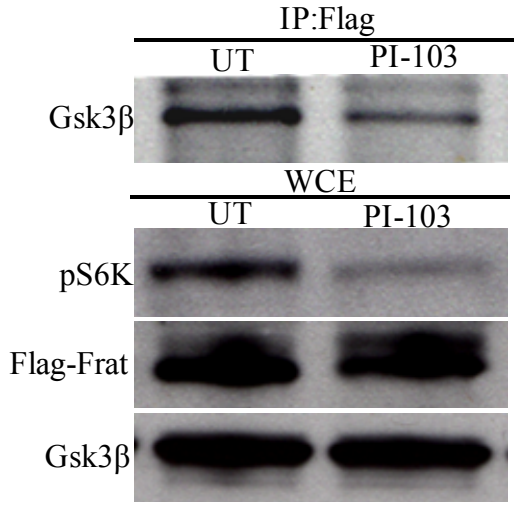

Figure 5.9. Inhibition of PI3K/Akt signaling decreases the binding of Frat to Gsk3β. WCE from R1 mESCs stably expressing Flag-Frat were subjected to immunoprecipitation using an anti-Flag antibody. Immunoprecipitates were then analyzed by western blot probing for antibodies as indicated. (Lower panel) 20 μg of the whole cell extract (WCE) used in the immunoprecipitation reactions were subjected to western blot analysis probing with antibodies as indicated.

Discussion

Frat mediates the nuclear export of Gsk3β in mESCs. The nuclear export of Gsk3β was previously shown to have a key role in the stabilization of c-myc in mESCs and is therefore important for mESC self-renewal and differentiation (9). The mechanism responsible for the nuclear export of Gsk3β in mESCs, however, was largely unknown. We have demonstrated that, under self-renewing conditions, Frat plays a key role in the localization of Gsk3β by mediating its nuclear export. This conclusion is supported by several lines of evidence. First, Gsk3β and Frat exist together as a complex in the cytoplasm of mESCs under self-renewing conditions. When mESCs are treated with LB, Gsk3β and Frat accumulate in the nucleus indicating they are actively undergoing nuclear/cytoplasmic shuttling. This corroborates other reports that Frat and Gsk3β are shuttling proteins whose nuclear export is Crm1 dependent (38, 69). Disruption of Frat binding by mutating Gsk3β was shown to result its nuclear accumulation, suggesting that the nuclear export of Gsk3β is reliant upon Frat. The constitutive localization of Frat to the nucleus, by inactivating its NES, was also shown to block the nuclear export of endogenous Gsk3β. In addition, anchoring Frat in the cytoplasm, anchors Gsk3β in the cytoplasm and disrupts its nuclear/cytoplasmic shuttling. Finally, expression of a constitutively active form of the Gsk3β mutant incapable of binding Frat was sufficient to disrupt mESC self-renewal.

PI3K/Akt signaling modulates Frat binding to Gsk3β. PI3K/Akt signaling has a well-established role in regulating Gsk3β activity through its phosphorylation at S9 (29). Independent of this, PI3K/Akt signaling has a role in regulating the nuclear export of Gsk3β in mESCs (9). In addition to this we have demonstrated a clear role for Frat in

mediating the nuclear export of Gsk3β. The underlying mechanism connecting these two components of the nuclear export of Gsk3β was unclear. We postulated however that PI3K/Akt signaling could regulate the nuclear export of Gsk3β one of two ways: by controlling the export of Frat, or by mediating the binding of Gsk3β to Frat. Our results have demonstrated that inhibition of the PI3K/Akt pathway, unlike Gsk3β, has no effect on the localization of Frat or its ability to actively shuttle in and out of the nucleus in mESCs. In addition, inhibition of PI3K/Akt signaling was shown to significantly disrupt the binding of Frat to endogenous Gsk3β. We conclude that under self-renewing conditions PI3K/Akt signaling keeps Gsk3β actively exporting from the nucleus by promoting its binding to Frat. To our knowledge this is the first evidence that the PI3K/Akt pathway is involved in regulating the binding of Frat to Gsk3β.

Future directions. Our work has provided strong evidence that under self-renewing conditions high PI3K/Akt signaling promotes the nuclear export of Gsk3β through the binding of Frat. More importantly, our results suggest that during differentiation, when PI3K/Akt signaling is low, Gsk3β has a decreased affinity for Frat and thus cannot export from the nucleus efficiently. Despite our observations connecting Frat binding to the PI3K/Akt-dependent nuclear export of Gsk3β several questions still remain. Specifically, our results do not completely discount Axin as having a role in the localization of Gsk3β. A recent paper however, has demonstrated that in other biological contexts Axin binding to Gsk3β facilitates its degradation of c-myc (1). Given these observations it's possible that Axin could serve a similar role in directing the Gsk3β-mediated degradation of c-myc during differentiation when PI3K/Akt activity is low and Gsk3β no longer binds to Frat. In addition, our previous results demonstrated a more direct role for Akt in

directing the nuclear export of Gsk3β. The precise underlying mechanism connecting Akt to the binding of Frat and Gsk3β however has not been defined. We postulate that Akt could modulate the binding of Frat to Gsk3β either directly or indirectly through an unidentified post-translational modification. Identification of this modification and determination of whether Akt is directly or indirectly responsible will require additional research. In addition to its role in mESCs, the PI3K/Akt/Gsk3β signaling network has important implications for other biological processes as well. Therefore a further understanding of the underlying mechanisms regulating these processes will impact multiple areas of biomedical research.

CHAPTER 6

Final Discussion and Conclusions[4]

[4] Copyright © American Society for Microbiology. Bechard, M., and Dalton, S. *Molecular and Cellular Biology*, 29, 2009, 2092-2104, doi:10.1128/MCB.01405-08.
Reprinted here with permission of publisher.

Implications

PI3K/Akt/Gsk3β signaling has well-established roles in many aspect of cell biology including, glucose metabolism, cell cycle regulation, apoptosis and proliferation (39). The dysregulation of this pathway is commonly associated with multiple forms of cancer and is central to the progression of diabetes (39). More recently, PI3K/Akt/Gsk3β signaling was shown to have a critical role in the maintenance of mESC self-renewal (19, 87, 103, 127). Prior to this report however, there were major gaps in our knowledge relating to the underlying mechanism linking PI3K/Akt signaling and Gsk3β to mechanisms underpinning pluripotency. Using mESCs as a model system, we sought to further investigate PI3K/Akt/Gsk3β signaling in the context of self-renewal. As a consequence of this research we have proposed a model defining novel roles for PI3K/Akt signaling through Gsk3β and its convergence on c-myc (Fig. 6.1). This has provided the mechanistic insight for several reports documenting the effects of PI3K/Akt/Gsk3β signaling on mESC self-renewal as well as other aspects of cell biology.

Our model demonstrates that inhibition and nuclear exclusion of Gsk3β is critical so that c-myc can be maintained at levels compatible with its role in self-renewal (Fig 6.1). The inability of Gsk3β to access nuclear substrates, like c-myc, also corroborates previous results demonstrating an unusually long $t_{1/2}$ in mESCs (~105 min) (19). Our results define a new level of control that restricts Gsk3β activity. Previously, AKT was known to restrict Gsk3β activity by inhibitory phosphorylation. Work presented in this dissertation provide additional mechanistic insight into how Gsk3β is controlled by defining a role for Akt in determining Gsk3β subcellular localization and thereby its access to substrates (Fig. 6.1). As such, the loss of PI3K/Akt signaling during early

mESC differentiation is directly responsible for the nuclear accumulation of Gsk3β and the ensuing degradation of c-myc (Fig 6.1). These observations offer an explanation as to why inhibition of Gsk3β improves the derivation of mESCs, is essential for the maintenance of self-renewal, and why its activation has a role in the differentiation of mESCs (28, 92, 111, 127). In addition, our model provides previously unknown mechanistic details associated with the role PI3K/Akt signaling has in maintaining mESC self-renewal (87, 103, 118).

In addition to regulating mESC self-renewal, Gsk3β localization also has a role in many important aspects of cell biology. One such example occurs during the S-phase of the cell cycle when cyclin D1 is degraded via the activation and nuclear accumulation of Gsk3β (26). Several studies have also demonstrated that the nuclear accumulation of Gsk3β occurs as a result of apoptosis as well (10, 31). In addition, accumulation of Gsk3β in the nucleus was shown to promote replicative senescence by targeting p53 (129). The striking commonality is that the nuclear accumulation of Gsk3β in all of these examples was correlated to the activation status of the PI3K/Akt pathway (10, 26, 129). Prior to this report it was unclear whether the loss of PI3K/Akt signaling was directly responsible for the nuclear accumulation of Gsk3β. Taking our results into consideration, it's likely that our model detailing the PI3K/Akt-dependent nuclear export of Gsk3β applies to the regulation of these important cellular processes as well (Fig 6.1).

Although PI3K/Akt is required for the nuclear export of Gsk3β, the underlying mechanism for this was at the time unclear. Data presented in chapter 5 demonstrates a key role for Frat in Gsk3β nuclear export. As part of this mechanism, PI3K/Akt is required to maintain interactions between Frat and Gsk3β (Fig. 6.1). This is consistent

with previous reports showing that Gsk3β becomes mislocalized to the nucleus when it cannot bind Frat (38). The three functionally redundant isoforms of Frat have a well-established role in regulating the Gsk3β-dependent degradation of β-catenin (112). Despite this however, mice lacking all isoforms of Frat show no gross abnormalities or any significant effect on Wnt signaling (113). Although Gsk3β localization was not examined, our results predict that its nuclear export will be less efficient in this Frat triple knockout mouse line. Our model therefore offers a plausible explanation for the lack of a phenotype associated with a Frat triple knockout mouse line, since loss of Frat would not affect the PI3K/Akt dependent regulation of Gsk3β activity. Originally Frat was identified as an oncogene whose enhanced expression provides an additional selective advantage in T-cell lymphomas already transformed by high levels of Myc (54). Given our observations it is likely that this selective advantage is conferred due to the role Frat has in mediating the stability of Myc by promoting the nuclear exclusion of Gsk3β.

Since PI3K/Akt signaling, in addition to mESC self-renewal, has a critical role in regulating proliferation and apoptosis, it is no surprise that dysregulation of PI3K/Akt signaling is a hallmark of several forms of cancer (39). Specifically, over-activation of PI3K/Akt signaling through the deregulation of PTEN was shown to be critical to the proliferation of medulloblastomas (46). The progression and survival of pancreatic cancer cells has also been demonstrated to depend upon elevated PI3K/Akt signaling (2). Interestingly, the over-activation of PI3K/Akt in pancreatic cancers was shown promote survival by increasing the stability of c-myc (2). Our observations show that PI3K/Akt signaling regulates the stability of c-myc by promoting the Frat-dependent nuclear exclusion of Gsk3β (Fig 6.1). Taking this into consideration it seems quite likely that our

model detailing the convergence of PI3K/Akt and Gsk3β on c-myc stability will also apply to tumor development.

Final Conclusions

In summary, we have established a mechanism to explain why PI3K/Akt signaling is important for mESC self-renewal, why and how Gsk3β activity is suppressed in mESCs, and why Gsk3β activation is a critical event during early differentiation. Finally, we have defined Myc as a nuclear target of this pathway and provided an explanation for how Myc is regulated in self-renewal and early differentiation. We believe that control of Gsk3β localization and enzymatic activity in mESCs, each controlled independently by PI3K/Akt, is likely to reflect a general mechanism applicable to the regulation of Gsk3β and Myc in a wide range of biological contexts. This research has profound implications for development, cancer, and the regulation of other stem cell compartments in vivo where Myc has well-defined roles (86).

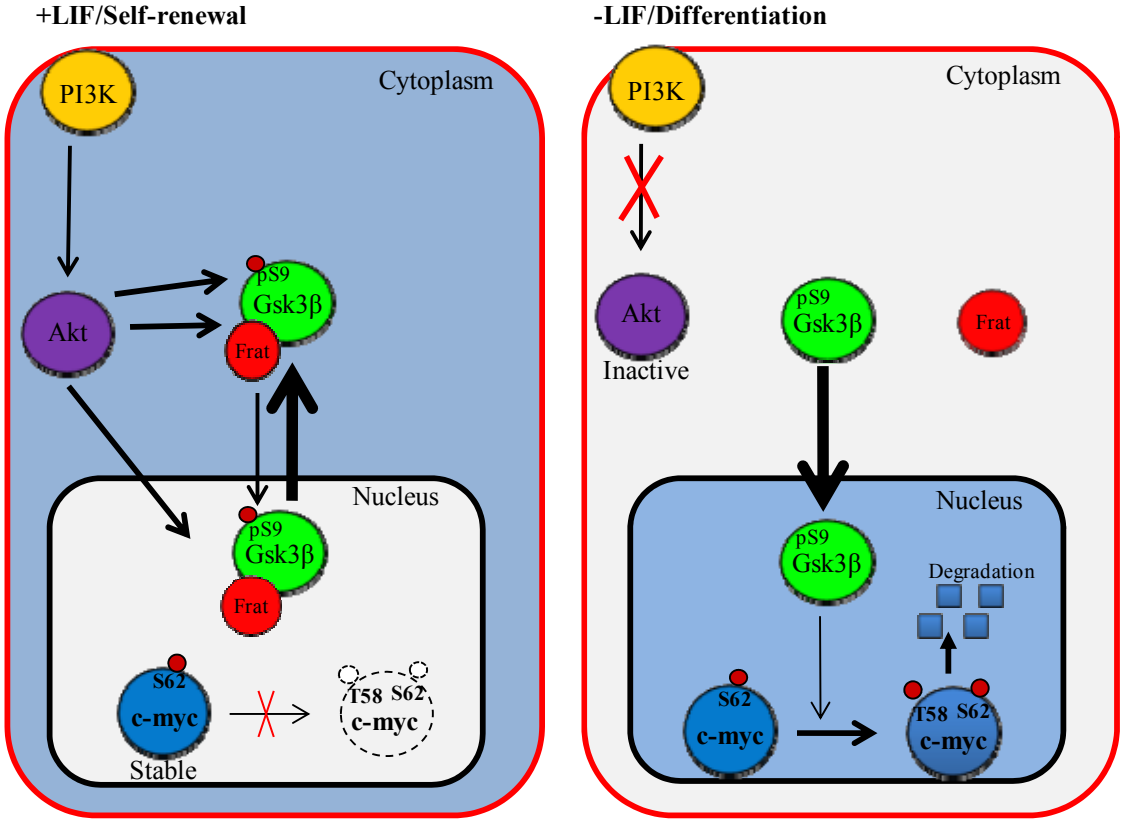

Figure 6.1. Model illustrating the role of the PI3K/Akt/Gsk3β signaling axis in mESC self-renewal and differentiation.

REFERENCES

1. **Arnold, H. K., X. Zhang, C. J. Daniel, D. Tibbitts, J. Escamilla-Powers, A. Farrell, S. Tokarz, C. Morgan, and R. C. Sears.** 2009. The Axin1 scaffold protein promotes formation of a degradation complex for c-Myc. Embo J **28:**500-12.

2. **Asano, T., Y. Yao, J. Zhu, D. Li, J. L. Abbruzzese, and S. A. Reddy.** 2004. The PI 3-kinase/Akt signaling pathway is activated due to aberrant Pten expression and targets transcription factors NF-kappaB and c-Myc in pancreatic cancer cells. Oncogene **23:**8571-80.

3. **Aubert, J., H. Dunstan, I. Chambers, and A. Smith.** 2002. Functional gene screening in embryonic stem cells implicates Wnt antagonism in neural differentiation. Nat Biotechnol **20:**1240-5.

4. **Avilion, A. A., S. K. Nicolis, L. H. Pevny, L. Perez, N. Vivian, and R. Lovell-Badge.** 2003. Multipotent cell lineages in early mouse development depend on SOX2 function. Genes Dev **17:**126-40.

5. **Baldin, V., N. Theis-Febvre, C. Benne, C. Froment, M. Cazales, O. Burlet-Schiltz, and B. Ducommun.** 2003. PKB/Akt phosphorylates the CDC25B phosphatase and regulates its intracellular localisation. Biol Cell **95:**547-54.

6. **Baudino, T. A., C. McKay, H. Pendeville-Samain, J. A. Nilsson, K. H. Maclean, E. L. White, A. C. Davis, J. N. Ihle, and J. L. Cleveland.** 2002. c-Myc is essential for vasculogenesis and angiogenesis during development and tumor progression. Genes Dev **16:**2530-43.

7. **Bax, B., P. S. Carter, C. Lewis, A. R. Guy, A. Bridges, R. Tanner, G. Pettman, C. Mannix, A. A. Culbert, M. J. Brown, D. G. Smith, and A. D. Reith.** 2001. The structure of phosphorylated GSK-3beta complexed with a peptide, FRATtide, that inhibits beta-catenin phosphorylation. Structure **9:**1143-52.

8. **Beals, C. R., C. M. Sheridan, C. W. Turck, P. Gardner, and G. R. Crabtree.** 1997. Nuclear export of NF-ATc enhanced by glycogen synthase kinase-3. Science **275:**1930-4.

9. **Bechard, M., and S. Dalton.** 2009. Subcellular localization of glycogen synthase kinase 3beta controls embryonic stem cell self-renewal. Mol Cell Biol **29:**2092-104.

10. **Bijur, G. N., and R. S. Jope.** 2001. Proapoptotic stimuli induce nuclear accumulation of glycogen synthase kinase-3 beta. J Biol Chem **276:**37436-42.

11. **Boulton, T. G., N. Stahl, and G. D. Yancopoulos.** 1994. Ciliary neurotrophic factor/leukemia inhibitory factor/interleukin 6/oncostatin M family of cytokines induces tyrosine phosphorylation of a common set of proteins overlapping those induced by other cytokines and growth factors. J Biol Chem **269:**11648-55.

12. **Boyer, L. A., T. I. Lee, M. F. Cole, S. E. Johnstone, S. S. Levine, J. P. Zucker, M. G. Guenther, R. M. Kumar, H. L. Murray, R. G. Jenner, D. K. Gifford, D. A. Melton, R. Jaenisch, and R. A. Young.** 2005. Core transcriptional regulatory circuitry in human embryonic stem cells. Cell **122:**947-56.

13. **Boyer, L. A., K. Plath, J. Zeitlinger, T. Brambrink, L. A. Medeiros, T. I. Lee, S. S. Levine, M. Wernig, A. Tajonar, M. K. Ray, G. W. Bell, A. P. Otte, M. Vidal, D. K. Gifford, R. A. Young, and R. Jaenisch.** 2006. Polycomb complexes repress developmental regulators in murine embryonic stem cells. Nature **441:**349-53.

14. **Bradley, A., M. Evans, M. H. Kaufman, and E. Robertson.** 1984. Formation of germ-line chimaeras from embryo-derived teratocarcinoma cell lines. Nature **309:**255-6.

15. **Brazil, D. P., Z. Z. Yang, and B. A. Hemmings.** 2004. Advances in protein kinase B signalling: AKTion on multiple fronts. Trends Biochem Sci **29:**233-42.

16. **Brons, I. G., L. E. Smithers, M. W. Trotter, P. Rugg-Gunn, B. Sun, S. M. Chuva de Sousa Lopes, S. K. Howlett, A. Clarkson, L. Ahrlund-Richter, R. A. Pedersen, and L. Vallier.** 2007. Derivation of pluripotent epiblast stem cells from mammalian embryos. Nature **448:**191-5.

17. **Brunet, A., A. Bonni, M. J. Zigmond, M. Z. Lin, P. Juo, L. S. Hu, M. J. Anderson, K. C. Arden, J. Blenis, and M. E. Greenberg.** 1999. Akt promotes cell survival by phosphorylating and inhibiting a Forkhead transcription factor. Cell **96:**857-68.

18. **Canelles, M., M. D. Delgado, K. M. Hyland, A. Lerga, C. Richard, C. V. Dang, and J. Leon.** 1997. Max and inhibitory c-Myc mutants induce erythroid differentiation and resistance to apoptosis in human myeloid leukemia cells. Oncogene **14:**1315-27.

19. **Cartwright, P., C. McLean, A. Sheppard, D. Rivett, K. Jones, and S. Dalton.** 2005. LIF/STAT3 controls ES cell self-renewal and pluripotency by a Myc-dependent mechanism. Development **132:**885-96.

20. **Chambers, I., D. Colby, M. Robertson, J. Nichols, S. Lee, S. Tweedie, and A. Smith.** 2003. Functional expression cloning of Nanog, a pluripotency sustaining factor in embryonic stem cells. Cell **113:**643-55.

21. **Chambers, I., and A. Smith.** 2004. Self-renewal of teratocarcinoma and embryonic stem cells. Oncogene **23:**7150-60.

22. **Cong, F., and H. Varmus.** 2004. Nuclear-cytoplasmic shuttling of Axin regulates subcellular localization of beta-catenin. Proc Natl Acad Sci U S A **101:**2882-7.

23. **Cross, D. A., D. R. Alessi, P. Cohen, M. Andjelkovich, and B. A. Hemmings.** 1995. Inhibition of glycogen synthase kinase-3 by insulin mediated by protein kinase B. Nature **378:**785-9.

24. **Dajani, R., E. Fraser, S. M. Roe, N. Young, V. Good, T. C. Dale, and L. H. Pearl.** 2001. Crystal structure of glycogen synthase kinase 3 beta: structural basis for phosphate-primed substrate specificity and autoinhibition. Cell **105:**721-32.

25. **Davis, A. C., M. Wims, G. D. Spotts, S. R. Hann, and A. Bradley.** 1993. A null c-myc mutation causes lethality before 10.5 days of gestation in homozygotes and reduced fertility in heterozygous female mice. Genes Dev **7:**671-82.

26. **Diehl, J. A., M. Cheng, M. F. Roussel, and C. J. Sherr.** 1998. Glycogen synthase kinase-3beta regulates cyclin D1 proteolysis and subcellular localization. Genes Dev **12:**3499-511.

27. **Ding, V. W., R. H. Chen, and F. McCormick.** 2000. Differential regulation of glycogen synthase kinase 3beta by insulin and Wnt signaling. J Biol Chem **275:**32475-81.

28. **Doble, B. W., S. Patel, G. A. Wood, L. K. Kockeritz, and J. R. Woodgett.** 2007. Functional redundancy of GSK-3alpha and GSK-3beta in Wnt/beta-catenin signaling shown by using an allelic series of embryonic stem cell lines. Dev Cell **12:**957-71.

29. **Doble, B. W., and J. R. Woodgett.** 2003. GSK-3: tricks of the trade for a multi-tasking kinase. J Cell Sci **116:**1175-86.

30. **Doetschman, T. C., H. Eistetter, M. Katz, W. Schmidt, and R. Kemler.** 1985. The in vitro development of blastocyst-derived embryonic stem cell lines: formation of visceral yolk sac, blood islands and myocardium. J Embryol Exp Morphol **87:**27-45.

31. **Elyaman, W., F. Terro, N. S. Wong, and J. Hugon.** 2002. In vivo activation and nuclear translocation of phosphorylated glycogen synthase kinase-3beta in neuronal apoptosis: links to tau phosphorylation. Eur J Neurosci **15:**651-60.

32. **Ernst, M., A. Oates, and A. R. Dunn.** 1996. Gp130-mediated signal transduction in embryonic stem cells involves activation of Jak and Ras/mitogen-activated protein kinase pathways. J Biol Chem **271:**30136-43.

33. **Evans, M. J., and M. H. Kaufman.** 1981. Establishment in culture of pluripotential cells from mouse embryos. Nature **292:**154-6.

34. **Ferkey, D. M., and D. Kimelman.** 2002. Glycogen synthase kinase-3 beta mutagenesis identifies a common binding domain for GBP and Axin. J Biol Chem **277:**16147-52.

35. **Flach, G., M. H. Johnson, P. R. Braude, R. A. Taylor, and V. N. Bolton.** 1982. The transition from maternal to embryonic control in the 2-cell mouse embryo. Embo J **1:**681-6.

36. **Frame, S., and P. Cohen.** 2001. GSK3 takes centre stage more than 20 years after its discovery. Biochem J **359:**1-16.

37. **Frame, S., P. Cohen, and R. M. Biondi.** 2001. A common phosphate binding site explains the unique substrate specificity of GSK3 and its inactivation by phosphorylation. Mol Cell **7:**1321-7.

38. **Franca-Koh, J., M. Yeo, E. Fraser, N. Young, and T. C. Dale.** 2002. The regulation of glycogen synthase kinase-3 nuclear export by Frat/GBP. J Biol Chem **277:**43844-8.

39. **Franke, T. F.** 2008. PI3K/Akt: getting it right matters. Oncogene **27:**6473-88.

40. **Fraser, E., N. Young, R. Dajani, J. Franca-Koh, J. Ryves, R. S. Williams, M. Yeo, M. T. Webster, C. Richardson, M. J. Smalley, L. H. Pearl, A. Harwood, and T. C. Dale.** 2002. Identification of the Axin and Frat binding region of glycogen synthase kinase-3. J Biol Chem **277:**2176-85.

41. **Funayama, N., F. Fagotto, P. McCrea, and B. M. Gumbiner.** 1995. Embryonic axis induction by the armadillo repeat domain of beta-catenin: evidence for intracellular signaling. J Cell Biol **128:**959-68.

42. **Gardner, R. L., and J. Rossant.** 1979. Investigation of the fate of 4-5 day post-coitum mouse inner cell mass cells by blastocyst injection. J Embryol Exp Morphol **52:**141-52.

43. **Grimes, C. A., and R. S. Jope.** 2001. The multifaceted roles of glycogen synthase kinase 3beta in cellular signaling. Prog Neurobiol **65:**391-426.

44. **Haegele, L., B. Ingold, H. Naumann, G. Tabatabai, B. Ledermann, and S. Brandner.** 2003. Wnt signalling inhibits neural differentiation of embryonic stem cells by controlling bone morphogenetic protein expression. Mol Cell Neurosci **24:**696-708.

45. **Hart, M. J., R. de los Santos, I. N. Albert, B. Rubinfeld, and P. Polakis.** 1998. Downregulation of beta-catenin by human Axin and its association with the APC tumor suppressor, beta-catenin and GSK3 beta. Curr Biol **8:**573-81.

46. **Hartmann, W., B. Digon-Sontgerath, A. Koch, A. Waha, E. Endl, I. Dani, D. Denkhaus, C. G. Goodyer, N. Sorensen, O. D. Wiestler, and T. Pietsch.** 2006. Phosphatidylinositol 3'-kinase/AKT signaling is activated in medulloblastoma cell proliferation and is associated with reduced expression of PTEN. Clin Cancer Res **12:**3019-27.

47. **He, X., J. P. Saint-Jeannet, J. R. Woodgett, H. E. Varmus, and I. B. Dawid.** 1995. Glycogen synthase kinase-3 and dorsoventral patterning in Xenopus embryos. Nature **374:**617-22.

48. **Henriksson, M., A. Bakardjiev, G. Klein, and B. Luscher.** 1993. Phosphorylation sites mapping in the N-terminal domain of c-myc modulate its transforming potential. Oncogene **8:**3199-209.

49. **Hoeflich, K. P., J. Luo, E. A. Rubie, M. S. Tsao, O. Jin, and J. R. Woodgett.** 2000. Requirement for glycogen synthase kinase-3beta in cell survival and NF-kappaB activation. Nature **406:**86-90.

50. **Hooper, M., K. Hardy, A. Handyside, S. Hunter, and M. Monk.** 1987. HPRT-deficient (Lesch-Nyhan) mouse embryos derived from germline colonization by cultured cells. Nature **326:**292-5.

51. **Huang, M., U. Kamasani, and G. C. Prendergast.** 2006. RhoB facilitates c-Myc turnover by supporting efficient nuclear accumulation of GSK-3. Oncogene **25:**1281-9.

52. **Ikeda, S., S. Kishida, H. Yamamoto, H. Murai, S. Koyama, and A. Kikuchi.** 1998. Axin, a negative regulator of the Wnt signaling pathway, forms a complex with GSK-3beta and beta-catenin and promotes GSK-3beta-dependent phosphorylation of beta-catenin. Embo J **17:**1371-84.

53. **Johansson, B. M., and M. V. Wiles.** 1995. Evidence for involvement of activin A and bone morphogenetic protein 4 in mammalian mesoderm and hematopoietic development. Mol Cell Biol **15:**141-51.

54. **Jonkers, J., H. C. Korswagen, D. Acton, M. Breuer, and A. Berns.** 1997. Activation of a novel proto-oncogene, Frat1, contributes to progression of mouse T-cell lymphomas. Embo J **16:**441-50.

55. **Kelly, D. L., and A. Rizzino.** 2000. DNA microarray analyses of genes regulated during the differentiation of embryonic stem cells. Mol Reprod Dev **56:**113-23.

56. **Kelly, O. G., K. I. Pinson, and W. C. Skarnes.** 2004. The Wnt co-receptors Lrp5 and Lrp6 are essential for gastrulation in mice. Development **131:**2803-15.

57. **Kelly, S. J.** 1977. Studies of the developmental potential of 4- and 8-cell stage mouse blastomeres. J Exp Zool **200:**365-76.

58. **Kimelman, D.** 2005. Frat1. UCSD-Nature Molecule Pages **1**.

59. **Kishida, S., H. Yamamoto, S. Ikeda, M. Kishida, I. Sakamoto, S. Koyama, and A. Kikuchi.** 1998. Axin, a negative regulator of the wnt signaling pathway, directly interacts with adenomatous polyposis coli and regulates the stabilization of beta-catenin. J Biol Chem **273:**10823-6.

60. **Kiuchi, N., K. Nakajima, M. Ichiba, T. Fukada, M. Narimatsu, K. Mizuno, M. Hibi, and T. Hirano.** 1999. STAT3 is required for the gp130-mediated full activation of the c-myc gene. J Exp Med **189:**63-73.

61. **Kopp, J. L., B. D. Ormsbee, M. Desler, and A. Rizzino.** 2008. Small Increases in the Level of Sox2 Trigger the Differentiation of Mouse Embryonic Stem Cells. Stem Cells.

62. **Logan, C. Y., and R. Nusse.** 2004. The Wnt signaling pathway in development and disease. Annu Rev Cell Dev Biol **20:**781-810.

63. **Lutterbach, B., and S. R. Hann.** 1994. Hierarchical phosphorylation at N-terminal transformation-sensitive sites in c-Myc protein is regulated by mitogens and in mitosis. Mol Cell Biol **14:**5510-22.

64. **Malynn, B. A., I. M. de Alboran, R. C. O'Hagan, R. Bronson, L. Davidson, R. A. DePinho, and F. W. Alt.** 2000. N-myc can functionally replace c-myc in murine development, cellular growth, and differentiation. Genes Dev **14:**1390-9.

65. **Marques, M., A. Kumar, I. Cortes, A. Gonzalez-Garcia, C. Hernandez, M. C. Moreno-Ortiz, and A. C. Carrera.** 2008. Phosphoinositide 3-kinases p110alpha and p110beta regulate cell cycle entry, exhibiting distinct activation kinetics in G1 phase. Mol Cell Biol **28:**2803-14.

66. **Martin, G. R.** 1981. Isolation of a pluripotent cell line from early mouse embryos cultured in medium conditioned by teratocarcinoma stem cells. Proc Natl Acad Sci U S A **78:**7634-8.

67. **Matsuda, T., T. Nakamura, K. Nakao, T. Arai, M. Katsuki, T. Heike, and T. Yokota.** 1999. STAT3 activation is sufficient to maintain an undifferentiated state of mouse embryonic stem cells. Embo J **18:**4261-9.

68. **McLean, A. B., K. A. D'Amour, K. L. Jones, M. Krishnamoorthy, M. J. Kulik, D. M. Reynolds, A. M. Sheppard, H. Liu, Y. Xu, E. E. Baetge, and S. Dalton.** 2007. Activin a efficiently specifies definitive endoderm from human embryonic stem cells only when phosphatidylinositol 3-kinase signaling is suppressed. Stem Cells **25:**29-38.

69. **Meares, G. P., and R. S. Jope.** 2007. Resolution of the nuclear localization mechanism of glycogen synthase kinase-3: functional effects in apoptosis. J Biol Chem **282:**16989-7001.

70. **Meissner, A., M. Wernig, and R. Jaenisch.** 2007. Direct reprogramming of genetically unmodified fibroblasts into pluripotent stem cells. Nat Biotechnol **25:**1177-81.

71. **Mitsui, K., Y. Tokuzawa, H. Itoh, K. Segawa, M. Murakami, K. Takahashi, M. Maruyama, M. Maeda, and S. Yamanaka.** 2003. The homeoprotein Nanog is required for maintenance of pluripotency in mouse epiblast and ES cells. Cell **113:**631-42.

72. **Munoz-Fontela, C., M. Collado, E. Rodriguez, M. A. Garcia, A. Alvarez-Barrientos, J. Arroyo, C. Nombela, and C. Rivas.** 2005. Identification of a nuclear export signal in the KSHV latent protein LANA2 mediating its export from the nucleus. Exp Cell Res **311:**96-105.

73. **Murphy, M. J., A. Wilson, and A. Trumpp.** 2005. More than just proliferation: Myc function in stem cells. Trends Cell Biol **15:**128-37.

74. **Nagy, A.** 2003. Manipulating the mouse embryo : a laboratory manual, 3rd ed. Cold Spring Harbor Laboratory Press, Cold Spring Harbor, N.Y.

75. **Nagy, A., J. Rossant, R. Nagy, W. Abramow-Newerly, and J. C. Roder.** 1993. Derivation of completely cell culture-derived mice from early-passage embryonic stem cells. Proc Natl Acad Sci U S A **90:**8424-8.

76. **Nichols, J., B. Zevnik, K. Anastassiadis, H. Niwa, D. Klewe-Nebenius, I. Chambers, H. Scholer, and A. Smith.** 1998. Formation of pluripotent stem cells in the mammalian embryo depends on the POU transcription factor Oct4. Cell **95:**379-91.

77. **Nishimoto, M., A. Fukushima, A. Okuda, and M. Muramatsu.** 1999. The gene for the embryonic stem cell coactivator UTF1 carries a regulatory element which selectively interacts with a complex composed of Oct-3/4 and Sox-2. Mol Cell Biol **19:**5453-65.

78. **Niwa, H., T. Burdon, I. Chambers, and A. Smith.** 1998. Self-renewal of pluripotent embryonic stem cells is mediated via activation of STAT3. Genes Dev **12:**2048-60.

79. **Niwa, H., J. Miyazaki, and A. G. Smith.** 2000. Quantitative expression of Oct-3/4 defines differentiation, dedifferentiation or self-renewal of ES cells. Nat Genet **24:**372-6.

80. **Ogawa, K., H. Matsui, S. Ohtsuka, and H. Niwa.** 2004. A novel mechanism for regulating clonal propagation of mouse ES cells. Genes Cells **9:**471-7.

81. **Ogawa, K., R. Nishinakamura, Y. Iwamatsu, D. Shimosato, and H. Niwa.** 2006. Synergistic action of Wnt and LIF in maintaining pluripotency of mouse ES cells. Biochem Biophys Res Commun **343:**159-66.

82. **Okamoto, K., H. Okazawa, A. Okuda, M. Sakai, M. Muramatsu, and H. Hamada.** 1990. A novel octamer binding transcription factor is differentially expressed in mouse embryonic cells. Cell **60:**461-72.

83. **Okita, K., H. Hong, K. Takahashi, and S. Yamanaka.** 2010. Generation of mouse-induced pluripotent stem cells with plasmid vectors. Nat Protoc **5:**418-28.

84. **Okita, K., T. Ichisaka, and S. Yamanaka.** 2007. Generation of germline-competent induced pluripotent stem cells. Nature **448:**313-7.

85. **Okita, K., M. Nakagawa, H. Hyenjong, T. Ichisaka, and S. Yamanaka.** 2008. Generation of mouse induced pluripotent stem cells without viral vectors. Science **322:**949-53.

86. **Oster, S. K., C. S. Ho, E. L. Soucie, and L. Z. Penn.** 2002. The myc oncogene: MarvelouslY Complex. Adv Cancer Res **84:**81-154.

87. **Paling, N. R., H. Wheadon, H. K. Bone, and M. J. Welham.** 2004. Regulation of embryonic stem cell self-renewal by phosphoinositide 3-kinase-dependent signaling. J Biol Chem **279:**48063-70.

88. **Pan, G. J., Z. Y. Chang, H. R. Scholer, and D. Pei.** 2002. Stem cell pluripotency and transcription factor Oct4. Cell Res **12:**321-9.

89. **Polakis, P.** 2000. Wnt signaling and cancer. Genes Dev **14:**1837-51.

90. **Qi, X., T. G. Li, J. Hao, J. Hu, J. Wang, H. Simmons, S. Miura, Y. Mishina, and G. Q. Zhao.** 2004. BMP4 supports self-renewal of embryonic stem cells by inhibiting mitogen-activated protein kinase pathways. Proc Natl Acad Sci U S A **101:**6027-32.

91. **Rodda, D. J., J. L. Chew, L. H. Lim, Y. H. Loh, B. Wang, H. H. Ng, and P. Robson.** 2005. Transcriptional regulation of nanog by OCT4 and SOX2. J Biol Chem **280:**24731-7.

92. **Sato, N., L. Meijer, L. Skaltsounis, P. Greengard, and A. H. Brivanlou.** 2004. Maintenance of pluripotency in human and mouse embryonic stem cells through activation of Wnt signaling by a pharmacological GSK-3-specific inhibitor. Nat Med **10:**55-63.

93. **Sears, R. C.** 2004. The life cycle of C-myc: from synthesis to degradation. Cell Cycle **3:**1133-7.

94. **Selvakumaran, M., D. Liebermann, and B. Hoffman.** 1996. The proto-oncogene c-myc blocks myeloid differentiation independently of its target gene ornithine decarboxylase. Blood **88:**1248-55.

95. **Shirogane, T., T. Fukada, J. M. Muller, D. T. Shima, M. Hibi, and T. Hirano.** 1999. Synergistic roles for Pim-1 and c-Myc in STAT3-mediated cell cycle progression and antiapoptosis. Immunity **11:**709-19.

96. **Silva, J., O. Barrandon, J. Nichols, J. Kawaguchi, T. W. Theunissen, and A. Smith.** 2008. Promotion of reprogramming to ground state pluripotency by signal inhibition. PLoS Biol **6:**e253.

97. **Smith, A. G.** 1991. Culture and Differentiation of Embryonic Stem Cells. Methods in Cell Science **13:**89-94.

98. **Smith, A. G.** 2001. Embryo-derived stem cells: of mice and men. Annu Rev Cell Dev Biol **17:**435-62.

99. **Smith, A. G., J. K. Heath, D. D. Donaldson, G. G. Wong, J. Moreau, M. Stahl, and D. Rogers.** 1988. Inhibition of pluripotential embryonic stem cell differentiation by purified polypeptides. Nature **336:**688-90.

100. **Smith, A. G., and M. L. Hooper.** 1987. Buffalo rat liver cells produce a diffusible activity which inhibits the differentiation of murine embryonal carcinoma and embryonic stem cells. Dev Biol **121:**1-9.

101. **Stadtfeld, M., M. Nagaya, J. Utikal, G. Weir, and K. Hochedlinger.** 2008. Induced pluripotent stem cells generated without viral integration. Science **322:**945-9.

102. **Stead, E., J. White, R. Faast, S. Conn, S. Goldstone, J. Rathjen, U. Dhingra, P. Rathjen, D. Walker, and S. Dalton.** 2002. Pluripotent cell division cycles are driven by ectopic Cdk2, cyclin A/E and E2F activities. Oncogene **21:**8320-33.

103. **Storm, M. P., H. K. Bone, C. G. Beck, P. Y. Bourillot, V. Schreiber, T. Damiano, A. Nelson, P. Savatier, and M. J. Welham.** 2007. Regulation of Nanog expression by phosphoinositide 3-kinase-dependent signaling in murine embryonic stem cells. J Biol Chem **282:**6265-73.

104. **Sun, H., R. Lesche, D. M. Li, J. Liliental, H. Zhang, J. Gao, N. Gavrilova, B. Mueller, X. Liu, and H. Wu.** 1999. PTEN modulates cell cycle progression and cell survival by regulating phosphatidylinositol 3,4,5,-trisphosphate and Akt/protein kinase B signaling pathway. Proc Natl Acad Sci U S A **96:**6199-204.

105. **Sussman, J., D. Stokoe, N. Ossina, and E. Shtivelman.** 2001. Protein kinase B phosphorylates AHNAK and regulates its subcellular localization. J Cell Biol **154:**1019-30.

106. **Takada, S., K. L. Stark, M. J. Shea, G. Vassileva, J. A. McMahon, and A. P. McMahon.** 1994. Wnt-3a regulates somite and tailbud formation in the mouse embryo. Genes Dev **8:**174-89.

107. **Takahashi-Tezuka, M., Y. Yoshida, T. Fukada, T. Ohtani, Y. Yamanaka, K. Nishida, K. Nakajima, M. Hibi, and T. Hirano.** 1998. Gab1 acts as an adapter molecule linking the cytokine receptor gp130 to ERK mitogen-activated protein kinase. Mol Cell Biol **18:**4109-17.

108. **Takahashi, K., and S. Yamanaka.** 2006. Induction of pluripotent stem cells from mouse embryonic and adult fibroblast cultures by defined factors. Cell **126:**663-76.

109. **Tesar, P. J., J. G. Chenoweth, F. A. Brook, T. J. Davies, E. P. Evans, D. L. Mack, R. L. Gardner, and R. D. McKay.** 2007. New cell lines from mouse epiblast share defining features with human embryonic stem cells. Nature **448:**196-9.

110. **Thomas, G. M., S. Frame, M. Goedert, I. Nathke, P. Polakis, and P. Cohen.** 1999. A GSK3-binding peptide from FRAT1 selectively inhibits the GSK3-catalysed phosphorylation of axin and beta-catenin. FEBS Lett **458:**247-51.

111. **Umehara, H., T. Kimura, S. Ohtsuka, T. Nakamura, K. Kitajima, M. Ikawa, M. Okabe, H. Niwa, and T. Nakano.** 2007. Efficient derivation of embryonic stem cells by inhibition of glycogen synthase kinase-3. Stem Cells **25:**2705-11.

112. **van Amerongen, R., and A. Berns.** 2005. Re-evaluating the role of Frat in Wnt-signal transduction. Cell Cycle **4:**1065-72.

113. **van Amerongen, R., M. Nawijn, J. Franca-Koh, J. Zevenhoven, H. van der Gulden, J. Jonkers, and A. Berns.** 2005. Frat is dispensable for canonical Wnt signaling in mammals. Genes Dev **19:**425-30.

114. **Van Der Heide, L. P., M. F. Hoekman, and M. P. Smidt.** 2004. The ins and outs of FoxO shuttling: mechanisms of FoxO translocation and transcriptional regulation. Biochem J **380:**297-309.

115. **Vanhaesebroeck, B., S. J. Leevers, K. Ahmadi, J. Timms, R. Katso, P. C. Driscoll, R. Woscholski, P. J. Parker, and M. D. Waterfield.** 2001. Synthesis and function of 3-phosphorylated inositol lipids. Annu Rev Biochem **70:**535-602.

116. **Vanhaesebroeck, B., and M. D. Waterfield.** 1999. Signaling by distinct classes of phosphoinositide 3-kinases. Exp Cell Res **253:**239-54.

117. **Wang, S., Y. Shen, X. Yuan, K. Chen, X. Guo, Y. Chen, Y. Niu, J. Li, R. H. Xu, X. Yan, Q. Zhou, and W. Ji.** 2008. Dissecting signaling pathways that govern self-renewal of rabbit embryonic stem cells. J Biol Chem **283:**35929-40.

118. **Watanabe, S., H. Umehara, K. Murayama, M. Okabe, T. Kimura, and T. Nakano.** 2006. Activation of Akt signaling is sufficient to maintain pluripotency in mouse and primate embryonic stem cells. Oncogene **25:**2697-707.

119. **Wernig, M., A. Meissner, R. Foreman, T. Brambrink, M. Ku, K. Hochedlinger, B. E. Bernstein, and R. Jaenisch.** 2007. In vitro reprogramming of fibroblasts into a pluripotent ES-cell-like state. Nature **448:**318-24.

120. **Wiechens, N., K. Heinle, L. Englmeier, A. Schohl, and F. Fagotto.** 2004. Nucleo-cytoplasmic shuttling of Axin, a negative regulator of the Wnt-beta-catenin Pathway. J Biol Chem **279:**5263-7.

121. **Williams, R. L., D. J. Hilton, S. Pease, T. A. Willson, C. L. Stewart, D. P. Gearing, E. F. Wagner, D. Metcalf, N. A. Nicola, and N. M. Gough.** 1988. Myeloid leukaemia inhibitory factor maintains the developmental potential of embryonic stem cells. Nature **336:**684-7.

122. **Wodarz, A., and R. Nusse.** 1998. Mechanisms of Wnt signaling in development. Annu Rev Cell Dev Biol **14:**59-88.

123. **Woodgett, J. R.** 1990. Molecular cloning and expression of glycogen synthase kinase-3/factor A. Embo J **9:**2431-8.

124. **Woodgett, J. R., and P. Cohen.** 1984. Multisite phosphorylation of glycogen synthase. Molecular basis for the substrate specificity of glycogen synthase kinase-3 and casein kinase-II (glycogen synthase kinase-5). Biochim Biophys Acta **788:**339-47.

125. **Yeh, E., M. Cunningham, H. Arnold, D. Chasse, T. Monteith, G. Ivaldi, W. C. Hahn, P. T. Stukenberg, S. Shenolikar, T. Uchida, C. M. Counter, J. R. Nevins, A. R. Means, and R. Sears.** 2004. A signalling pathway controlling c-Myc degradation that impacts oncogenic transformation of human cells. Nat Cell Biol **6:**308-18.

126. **Ying, Q. L., J. Nichols, I. Chambers, and A. Smith.** 2003. BMP induction of Id proteins suppresses differentiation and sustains embryonic stem cell self-renewal in collaboration with STAT3. Cell **115:**281-92.

127. **Ying, Q. L., J. Wray, J. Nichols, L. Batlle-Morera, B. Doble, J. Woodgett, P. Cohen, and A. Smith.** 2008. The ground state of embryonic stem cell self-renewal. Nature **453:**519-23.

128. **Yoshikawa, Y., T. Fujimori, A. P. McMahon, and S. Takada.** 1997. Evidence that absence of Wnt-3a signaling promotes neuralization instead of paraxial mesoderm development in the mouse. Dev Biol **183:**234-42.

129. **Zmijewski, J. W., and R. S. Jope.** 2004. Nuclear accumulation of glycogen synthase kinase-3 during replicative senescence of human fibroblasts. Aging Cell **3:**309-17.